

INTERNATIONAL INSTITUTE FOR HYDRAULIC
AND ENVIRONMENTAL ENGINEERING

LECTURE NOTES ON
LOCAL SCOUR

BY
H.N.C. BREUSERS

DELFT

1979

INTERNATIONAL INSTITUTE FOR HYDRAULIC
AND ENVIRONMENTAL ENGINEERING

LECTURE NOTES ON
LOCAL SCOUR

BY
H.N.C. BREUSERS

DELFT

1979

LOCAL SCOUR

CONTENT

1. INTRODUCTION
2. SCOUR AROUND BRIDGE PIERS
3. SCOUR DOWNSTREAM OF CONSTRUCTIONS
 - 3.1 Relations for the equilibrium scour depth downstream of weirs
 - 3.2 Relations for rivers with fine sand bed, based on regime theory
 - 3.3 Time-dependent relations for scour in fine-sand estuaries
4. SCOUR AROUND ABUTMENTS AND SPUR DIKES
5. MODEL INVESTIGATIONS
6. PROTECTION AGAINST SCOUR

APPENDICES

1. Local scour around cylindrical piers
2. Closure of estuarine channels in tidal regions
3. Three-dimensional local scour in non-cohesive sediments.

1. INTRODUCTION

Local scour is caused by local disturbances of the flow and sediment transport field. Examples are: scour around (bridge)piers and abutments and scour downstream of dams. In all these cases a local increase in mean velocity and/or turbulence intensity gives an increase in local transport capacity. From the equation of continuity:

$$\frac{\partial h}{\partial t} = \frac{\partial S}{\partial x} \quad (h = \text{depth}, S = \text{transport})$$

it follows that scour will occur. The scouring continues until the local depth has increased so much that the velocities are reduced sufficiently to bring

$$\frac{\partial S}{\partial x} \text{ to zero.}$$

S can remain positive of course so that a dynamic equilibrium is obtained, for example for a pile in a sediment transporting river.

There are too many examples of failure of constructions due to local scour to neglect the phenomenon. The effects of local scour can be overcome by an increase in construction depth (bridge piers) or diminished by a bottom protection.

The following subjects will be discussed:

- scour around (bridge) piers,
- scour downstream of constructions (dams, weirs),
- scour around abutments and spur dikes,
- model investigations,
- protection.

2. SCOUR AROUND BRIDGE PIERS

Scour around bridge piers is due to a combination of three effects:

- local scour near the bridge pier caused by the disturbance of the flow field around the pier,
- a lowering of the river bed in the cross section of the bridge due to the contraction of the river profile at that section,
- a general lowering of the river bed in the river around the bridge site due to degradation or non-uniform river bed changes during floods.

These last two aspects, together with practical experience for the situation of a bridge in the flood plain, are discussed in an excellent way by C.R. Neill [1].

The local scour near the bridge pier is discussed in detail in a review article by Breusers, Nicollet and Shen [2], which is given as appendix 1.

An analysis of existing data shows that the scour depth could be expressed as:

$$\frac{d_s}{b} = f_1\left(\frac{\bar{U}}{\bar{U}_c}\right) \cdot f_2\left(\frac{d_o}{b}\right) \cdot f_3(\text{shape}) \cdot f_y\left(\alpha \cdot \frac{l}{b}\right)$$

d_s = scour depth (below original river bed)

b = width of pier

\bar{U} = mean velocity

\bar{U}_c = critical mean velocity for beginning of motion

d_o = water depth

α = angle of attack

l = length of pier

For most practical situations: $\bar{U}/\bar{U}_c > 1.0$ so that $f_1(\bar{U}/\bar{U}_c) = 1.0$ (see Appendix 1).

$f_2(d_o/b)$ is given as:

$$f_2(d_o/b) = 2.0 \tanh(d_o/b)$$

in which

$$\tanh(x) = \frac{e^x - e^{-x}}{e^x + e^{-x}}$$

For large $d_o/b: f_2 \approx 2$

$f_3(\text{shape}) = 1.0$ for circular and round-nosed piers
= 0.75 for stream-lined piers
= 1.3 for rectangular piers

For $f_y(\alpha, l/b)$, see Figure 32 of Appendix 1.

If the river bed around the pier is protected with a revetment, then it should be placed at or below the lowest river bed level to avoid an extra obstruction. The stone size should be designed for a velocity 2.0 times the approach velocity \bar{U} (see further par. 6) to account for the increase in velocities near the pier.

REFERENCES

- [1] C.R. NEILL (ed.). A guide to bridge hydraulics.
University of Toronto Press, 1973
- [2] H.N.C. BREUSERS, G. NICOLLET, H.W. SHEN. Local scour around cylindrical piers.
Journal of Hydraulic Research 15 (3), p. 211-252, 1977

3. SCOUR DOWNSTREAM OF CONSTRUCTIONS

The construction of a dam or a weir in a river changes the transport conditions and causes local scour. In literature several approaches can be found:

3.1 Relations for the equilibrium scour depth downstream of weirs etc.

These relations were derived mainly for coarse material ($d > 1 \text{ mm}$).

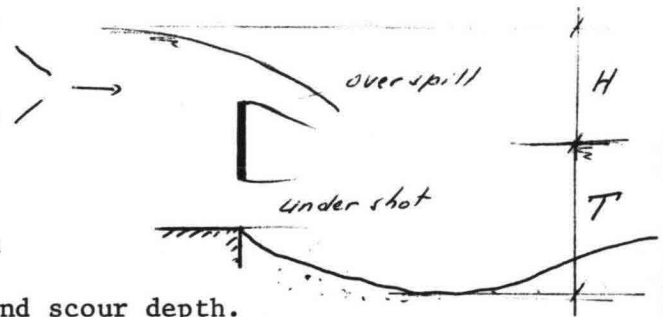
Examples are the relations given by Eggenberger and Müller [1]

overspill: $T = 22.8H^{0.5} q^{0.6} D_{90}^{-0.4}$

undershot: $T = 10H^{0.5} q^{0.6} D_{50}^{-0.4}$

T and H in m, q in m^2/s , D_{90} in mm

T = sum of downstream waterdepth and scour depth.



or by Kotoulas [2]

$$T = 1.9g^{-0.35} H^{0.35} q^{0.7} D_{95}^{-0.4}$$



3.2 Relations for rivers with fine sand bed, based on the regime theory [3]

The starting point is the regime depth d_r for example the Lacey expression:

$$d_{r,3} = 0.473 (Q/f)^{1/3} \quad (\text{m or ft-units})$$

Q = total discharge

or if the flow is limited in width:

$$d_{r,2} = 1.34 q^{2/3} . f^{-1/3} \quad (\text{m-units})$$

q = discharge per m'

f = siltfactor, sometimes given as $1.76D^{0.5}$ D in mm

The total scoured depth T (sum of original waterdepth and scoured depth) is than taken as a multiple of the regime depth:

for scour near bridge piers	$T = 2 d_r$
for scour at nose of spur dikes and guide banks	$T = 2 \text{ to } 2.75 d_r$
for flow perpendicular to banks	$T = 2.25 d_r$
downstream of barrages with hydraulic jump on the stilling-basin floor	$T = 1.75 \text{ to } 2.25 d_r$

3.3 Time-dependent relations for scour in fine-sand estuaries

For several practical problems, the equilibrium scour depth is not of interest because the situation in which scour occurs is only of a temporary character. Examples are closure works in tidal channels in which scour has to be considered only during the construction phases.

Interpretation of model tests requires in this case the knowledge of the time scale of the scouring process. The Delft Hydraulics Laboratory developed relations based on a large number of tests (see the articles by Breusers, van der Meulen and Vinjé). (Appendices 2 and 3).

During the closing of an estuary situations will occur with a greatly reduced cross section whereas the tidal discharges remain very large. This means that the mean velocity in the closing gap and the turbulence strongly increase which gives an increase in scour depth. Especially methods in which an estuary is closed from the sides (for example with caissons) will have an enormous scouring potential (see for example Figure 5 on page 4 and Figure 4 on page 19 of Appendix 2). The scour depths can be reduced by making bottom protections on both sides of the closing gap but scour will always occur.

The most general conclusion of the studies by the Delft Hydraulics Laboratory on local scour was that for a given flow field, independent of the bed material the scour could be expressed as a unique function of time :

$$\frac{h_{\max}}{h_0} = f\left(\frac{t}{t_1}\right)$$

h_{\max} = scour depth (measured from the original bed level)

h_0 = original water depth

t_1 = time to reach $h_{\max} = h_0$

For two-dimensional scour it was found that (see page 11 of Appendix 2)

$$\frac{h_{\max}}{h_0} = \left(\frac{t}{t_1}\right)^{0.38}$$

but for other (three-dimensional) situations other relations apply (see for example Figure 3 of Appendix 3). This figure also shows that the relationship is independent of bed material and waterdepth for a given geometry.

Important is the time scale of the process, or the scale of t_1 . For all tests, both two and three-dimensional, the following relation is valid:

$$\eta_{t_1} = \eta_{\Delta}^{1.7} \cdot \eta_h^2 \cdot \eta_{(\alpha\bar{U} - \bar{U}_{cr})}^{-4.3}$$

η = scale factor (prototype/model)

Δ = $(\rho_s - \rho_w)/\rho_w$

h = waterdepth

α = factor, depending on flow field and turbulence. For uniform, two-dimensional flow $\alpha = 1.5$, whereas for very turbulent three-dimensional flow situations α can be as high as 6 - 8 (see Appendix 3).

\bar{U} = mean velocity at the end of the bed protection

\bar{U}_{cr} = critical mean velocity for beginning of motion

The time scale η_{t_1} for the scouring process is of course different from the hydraulic time scale $\eta_t = \eta_L \cdot \eta_U^{-1}$.

All relations given above were for cohesionless materials. In fact only a limited number of experiments have been performed for cohesive soils. The scouring resistance of clay is of course larger than for sand. No general relations can be given however. For an example see [4].

REFERENCES

- [1] W. EGGENBERGER, R. MULLER. Experimentelle und theoretische Untersuchungen über das Kolkproblem.
Mitt. Versuchsanstalt für Wasserbau. E.T.H. Zürich, no. 5, 1944.
- [2] M. KOTOULAS. Das Kolkproblem unter besonderen Berücksichtigung der Faktoren Zeit und Geschiebemischung.
Diss. Braunschweig, 1967.
- [3] T. BLENCH. Regime behaviour of canals and rivers.
Butterworths, London.
- [4] A.A. KRUCHININA. Investigation findings on scouring process in cohesive soils.
Comm. All. Union Scient. Res. Inst. B.E. Vedenev 88, p. 72/79, 1969

4. SCOUR AROUND ABUTMENTS AND SPUR DIKES

For these types of constructions no general design rules may be given, except the general relations of the regime theory. The actual scour depends too much on the geometry of the construction and the flow field. Some references are given below:

B.P. DAS. Bed scour at end-dump channel constructions.
Proc. ASCE 99 (HY12), 1973.

C.R. NEILL (ed.). Guide to bridge hydraulics.
Ontario, University of Toronto Press, 1973.

M.A. GILL. Erosion of sand beds around spur dikes.
Proc. ASCE 98 (HY9), p. 1587/1602, 1972.

L. VEIGA DA CUNHA. Erosões localizadas junto de obstáculos salientes de margens.
Diss. Lisboa, 1971.

5. MODEL INVESTIGATIONS

For model studies on the equilibrium scour depth the following scale laws have to be considered:

- a. undistorted model $N_L = N_h$
- b. Froude law $N_{\bar{U}} = N_h^{\frac{1}{2}}$ in view of the necessary reproduction of the free surface.
- c. $N_{u_x} = N_{u_{xcr}}$ to obtain a correct reproduction of the equilibrium conditions in the scour hole.

The third law reduces to the simple law:

$$N_D = N_L$$

if the bed material in the prototype is so coarse that the model material is larger than 1 mm. If the model material becomes finer, deviations from this simple relation occur due to the influence of viscosity (Shields curve).

If the material in the prototype is already fine, one cannot fulfill all scale relations using sand in the model, so that materials with a lower density have to be used. In that case also the time scale of local scour can be of importance (see par. 3.3).

6. PROTECTION AGAINST SCOUR

Scour can be reduced by streamlining the construction (bridge piers), making guide walls (abutments) or by stilling basins (spillways). If the resulting scour is not acceptable a bottom protection has to be constructed. Except for the circular bridge piers no general design rules can be given because the necessary protection depends too much on the actual geometry, the composition of the bed etc. A minimum requirement is of course that the upper part of the protection is stable against the flow and that the filter construction is sufficient to prevent leaking of sand through the protection. Special care has to be given to the end of the protection where undermining has to be avoided.

Both stability and filter construction are discussed in the lecture notes on "Revetments" by A. Zanen. For uniform flow a stability criterion may be derived by taking a Shields ψ -value of 0.03:

$$\psi = \frac{U_{cr}^2}{\Delta g D}$$

with:

$$\frac{\bar{U}}{U_{cr}} = 5.75 \log \frac{12h}{k_s}$$

This leads to:

$$\bar{U}_{cr} = 0.7\sqrt{2g\Delta D} \log \frac{12h}{k_s}$$

For D the nominal diameter D_n can be taken defined by:

$$\text{Volume} = \frac{\pi}{6} \cdot D_n^3$$

For $k_s = D$ and $h/D = 4$ one finds:

$$\bar{U}_{cr} = 1.2\sqrt{2g\Delta D}$$

which is the well-known Isbash formula for the stability of a stone in a bed.

If the flow is turbulent due to a construction (spillway, stilling basin etc.) one has to reduce the permissible value of U_{cr} with a factor:

$$\frac{\bar{U}_{cr}(r)}{\bar{U}_{cr}} = \frac{1.45}{1+3r}$$

where r is the relative turbulence intensity (r.m.s. value divided by mean value). For uniform flow r is taken as 0.15. In very turbulent situations r can reach values of 0.3 to 0.4. In actual situations model tests will be necessary.

LOCAL SCOUR AROUND CYLINDRICAL PIERS

EROSION LOCALE AUTOUR DES PILES CYLINDRIQUES

by/par

H. N. C. BREUSERS

Delft Hydraulics Laboratory, Delft, The Netherlands

G. NICOLLET

Laboratoire National d'Hydraulique, Chatou, France

H. W. SHEN

Colorado State University, Fort Collins, U.S.A.

(IAHR Task Force on Local Scour around Piers)

Summary A "state of the art" report on the subject of local scour around cylindrical piers is given here. After a description of the scouring process, a critical review of literature on model and field data is presented, and the empirical data are compared with theoretical considerations. The final result is a set of design suggestions together with possibilities for protection against scour.

Sommaire Ce rapport donne le point des connaissances dans le domaine de l'érosion locale en autour des piles cylindriques: analyse du processus d'érosion, étude critique des résultats expérimentaux modèle et nature disponibles dans la littérature, confrontation des résultats aux schémas théoriques. En conclusion est proposée une loi pour la prévision de la profondeur d'affouillement, ainsi que des dispositifs de protection.

1 Introduction

At the request of the IAHR Section on Fluvial Hydraulics a task force was formed to prepare a state of the art report on local scour near piers. The present Report is the result of individual contributions but has been critically reviewed by all members.

The Report is principally restricted to the following conditions:

- cylindrical piers (all shapes),
- non-cohesive granular bed material, and
- one-way current (no tidal influence and waves).

The following aspects are presented:

- the description of the scouring process and an analysis of relevant parameters;
- a description of model and field data;
- a comparison of data with theoretical work and a discussion on the influence of various parameters; and
- the protection against scour and the development of suggestions for design relations.

Received June 28, 1977

It will be clear that, as in many other fields of sediment transport, upto now no entirely satisfactory theoretical and experimental results have been obtained, because the processes involved of water and sediment movement are too complicated and experimental data are incomplete and sometimes conflicting. It has seemed possible however, to give a reasonable description of the scouring process and to make suggestions for design relations on local scour near piers.

2 Description of the flow field around a pier and the scour process

2.1 Flow field

The dominant feature of the flow near a pier is the large-scale eddy structure, or the system of vortices which develop about the pier. These vortex systems are the basic mechanism of local scour, which has long been recognized by investigators (see TISON (1940), KEUTNER (1932), POSEY (1949), LAURSEN and TOCH (1956), NEILL (1964), BATA (1960), ROPER, SCHNEIDER and SHEN (1967), Highway Research Board (1970) and MELVILLE (1975)).

It has been described by ROPER, SCHNEIDER and SHEN that, depending on the type of pier and free-stream conditions, the eddy structure can be composed of any, all, or none of three basic systems: the horseshoe-vortex system, the wake-vortex system, and/or the trailing-vortex system. The vortex systems are an integral part of the flow structure and strongly affect the vertical component of the velocity in the neighbourhood of the pier.

The vortex filaments, transverse to the flow in a two-dimensional undisturbed velocity field, are concentrated by the presence of a blunt-nosed pier to form the horseshoe-vortex system. The mechanism by which the concentration is accomplished is the pressure field induced by the pier. If the pressure field is sufficiently strong, it causes a three-dimensional separation of the boundary layers which, in turn, rolls up ahead of the pier to form the horseshoe-vortex system.

A blunt-nosed pier is one which induces a sufficiently large pressure gradient to initiate the process just described. All other piers are referred to as sharp nosed, and it is important to know that, at least conceptually, no vorticity is created at the nose of such piers, although actually some vortex systems always evolve around any bridge piers. The blunt-nosed pier serves as a focusing or concentrating device for the vorticity already present in the undisturbed stream. For a three-dimensional pier, as shown in Fig. 1, the ends of the vortex filaments, composing the horseshoe-vortex, stretch downstream toward infinity, increasing the rotational velocities in the vortex core in accordance with the kinematic laws of vortex behaviour. Clearly, the geometry of the pier

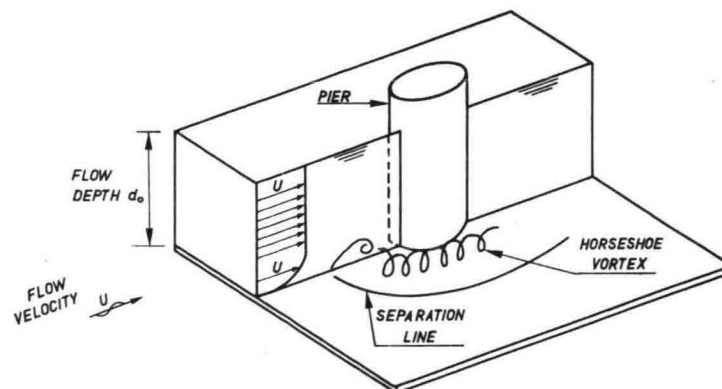


Fig. 1.

is important in determining the strength of the horseshoe-vortex, although this system is not steady for all flow conditions studied. SCHWIND (1962) noted that for some Reynolds numbers the horseshoe-vortex is shed periodically, while SHEN, SCHNEIDER and KARAKI (1969) and MELVILLE (1975) noticed that the shedding is observable during scour as slugs of sediment being pulsed around the pier.

Some pier shapes, such as wedge or lenticular, may be either blunt-nosed or sharp-nosed, depending on the wedge angle and the angle of attack of the undisturbed flow. SHEN and SCHNEIDER (1970) found in the limited number of experiments they conducted that a wedge-shaped pier with a wedge angle of 30° in a plane bed may be considered to be sharp-nosed. However, an asymmetrical dune moving past this pier can change the local angle of attack so that the pier acts as a blunt-nosed pier. In this case a large scour hole develops at the nose of the pier.

MELVILLE (1975) measured mean flow directions, mean flow magnitude, turbulent flow fluctuations, turbulent power spectra and shear stresses around a circular pier (5.08 cm in diameter) for flat-bed, intermediate and equilibrium scour holes, in a 45.6 cm wide laboratory flume. He found that a strong vertically downward flow developed ahead of the cylinder as the scour hole enlarged. The size and the circulation of the horseshoe-vortex increased rapidly, and the velocity near the bottom of the hole decreased as the scour hole was enlarged. The magnitude of the down-flow appeared to be directly associated with the rate of scour. The rate of increase of circulation fell off as the scour hole developed and reached a constant value at the equilibrium stage. Spectra of turbulent velocity fluctuations near the bed of the scour hole indicated a greater energy content in the 1 to 10 Hz range than that of the approached flow and a corresponding lesser energy content at higher frequencies. The combination of temporal mean bed shear and turbulent agitation at the bed tended to decrease as the scour hole enlarged until equilibrium was reached.

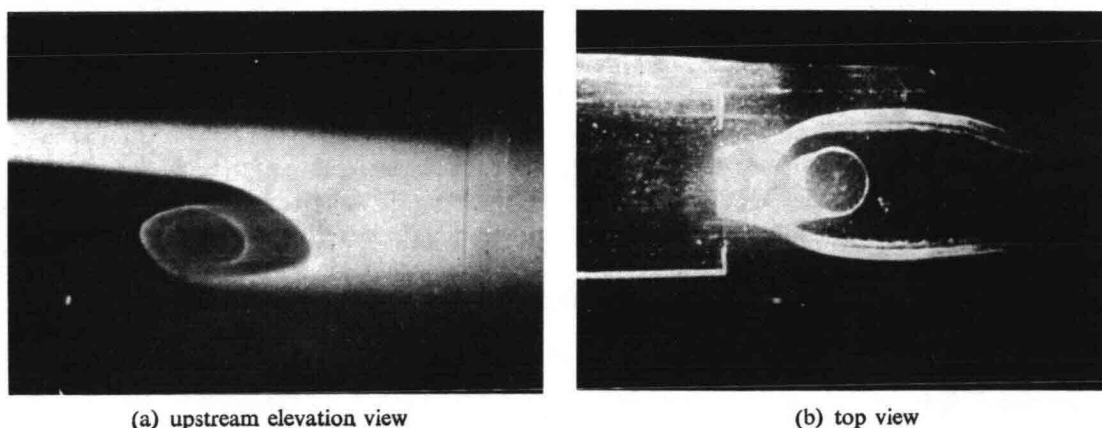


Fig. 2. Horse shoe-vortex after Taylor (1965).

The vorticity concentrated in the wake-vortex system is generated by the pier itself, contrary to the case of the horseshoe-vortex. The wake-vortex system is formed by the rolling up of the unstable shear layers generated at the surface of the pier, and which are detached from either side of the pier at the separation line. At low Reynolds numbers ($3 < \bar{R} < 50$), these vortices are stable and form a standing system downstream close to the pier. For Reynolds numbers of practical interest, however, the system is unstable, and the vortices are shed alternately from the

pier and are convected downstream. The strength of the vortices in the wake system varies greatly according to the pier shape and fluid velocity. A streamlined pier will create a relatively weak wake, but a blunt body produces a very strong one. The regularity of shedding ranges from the very stable VON KÁRMÁN vortex state ($80 < 90 < \bar{R} < 150$ to 300) to a practically chaotic state in the transcritical range [$3.5 \times 10^6 < \bar{R}$], ROSHKO (1961)].

The wake-vortex system is related to the so-called upflow which has been observed by POSEY (1949), MOORE and MASCH (1963), and others. Large scour holes may develop downstream from piers when the horseshoe-vortex system does not form or is adequately controlled, as demonstrated by the experiments of SHEN and others (1966). The wake-vortex system acts somewhat like a vacuum cleaner in removing the bed material which is then carried downstream by the eddies shedding from the pier.

MELVILLE (1975) found that:

“Under equilibrium conditions for the scour hole, vortex shedding occurs at a value of the Strouhal Number, based upon cylinder diameter and mean approach flow velocity varying from 0.229 to 0.238, that is, an increase of about 15% from that for the two-dimensional case. The vortex pattern generated is consistent with the occurrence of span-wise cells of constant shedding frequency separated at the discontinuities by longitudinal vortices. The shedding frequency between successive cells decreases with depth. The lower limit for consistent shedding appears to be at about the level of the undisturbed bed. Vortex convection speeds and separation distances downstream from the cylinder decrease with depth. Individual vortices are convected downstream at a speed initially less than that of the approach flow but becoming nearly constant and equal to the approach flow velocity at 8 cylinder diameters downstream. The vortices which are initially shed with their axes vertical are progressively bent by the mean flow as they are convected away from the cylinder. The cast-off vortices aid the erosion process at the cylinder. Each of the concentrated vortices acts with its low pressure centre as a vacuum cleaner. During the initial period of scour activity bursts of sediment transport away from the bed are evident with the generation of each vortex. A ripple is formed on the downstream mound coinciding with the path followed by the cast-off vortices. Based on observations of dye traces introduced into the flow, it is postulated that the arms of the horseshoe-vortex, extending around the circumference of the cylinder, oscillate laterally and vertically at the same frequency as the shedding of wake vortices. Consider the sequence involved in the shedding of two vortices, one from each side of the cylinder, that is, one period of wake-vortex generation: the decreased pressure within an individual cast-off vortex draws up fluid from the horseshoe vortex region, pulling the vortex arm with it. As this first wake-vortex passes downstream, the arm of the horseshoe-vortex recedes back into the scour hole, while the other arm of the vortex is similarly affected by the second wake vortex shed from the other side of the cylinder”.

The trailing-vortex system usually occurs only on completely submerged piers and is similar to that which occurs at the tips of finite lifting surfaces in finite wing theory. It is composed of one or more discrete vortices attached to the top of the pier and extending downstream. These vortices form when finite pressure differences exist between two surfaces meeting at a corner, such as at the top of the pier.

ROPER (1965 and 1967) gave a more detailed description of these vortex systems and many of the remarks made in the few preceding paragraphs were his.

HUNG (1968) made detail velocity and pressure distribution measurements near a circular cylinder in an open channel. The width of the channel was 1.2 m, the depth of flow was 0.195 m, the cylinder was 4.3 cm in diameter, and the average flow velocity was 0.39 m/s in the upstream approach section.

The pressure coefficient C_p is defined as follows:

$$C_p = \frac{p - p_y}{\frac{1}{2}\rho U_y^2} \quad (1)$$

where p is the local measured pressure, p_y is the upstream undisturbed flow static pressure at y , ρ is the fluid density, U_y is the upstream undisturbed flow velocity at level y , and y is the reference elevation above channel bottom.

The C_p measurements as a function of the elevation and relative cylinder location are shown in Fig. 3.

PETRYK (1969) observed under the same flow conditions as HUNG (1968) that the secondary flow along the front and back of the cylinder is downward, and at the back of the cylinder the pressure is higher near the surface than near the bottom.

The downward secondary flow along the front of the cylinder is attributed to the non-uniform approach velocity. The downward circulation pattern at the back of the cylinder disagrees with previous investigations where a two-dimensional object was placed in a non-uniform flow field.

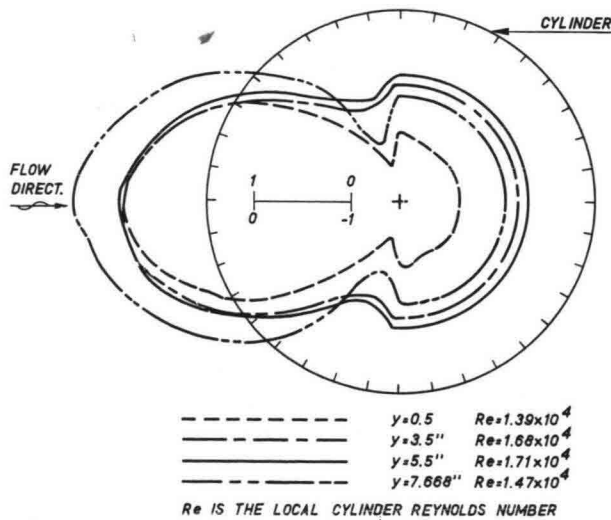


Fig. 3. Pressure coefficient C_p .

In shear flows it has generally been reported that the secondary flow in the near wake region of a cylinder is in the direction of increasing velocity head. This phenomenon has been deduced from the fact that generally as the approach velocity to the cylinder increases, the pressure at the back of the cylinder decreases. It follows that the secondary flow should be in the direction of decreasing pressure, or in the direction of increasing velocity head. All wind tunnel investigations report this circulation pattern [see BAINES (1965) and ROPER (1967)]. DALTON and MASCH (1968) also found that the secondary flow was in the direction of increasing velocity head. They placed a cylinder in

a water tunnel with a linear velocity profile, and demonstrated that this secondary flow pattern was applicable to flow without free surface effects.

MOORE and MASCH (1963) and ROPER (1965) reported the same secondary flow pattern downstream of a cylinder in an open channel flow with a non-uniform velocity profile. The downward circulation observed at the back of the cylinder under the flow conditions given in the beginning of this Section have been explained by PETRYK (1969): (i) the free surface effect, and (ii) the vortex shedding pattern at the back of the cylinder. The vortices are shed irregularly and their strength is relatively low. The flow in the separated region circulates quiescently.

The pressure throughout the separated region is expected to be approximately hydrostatic because of the relatively low flow velocities in that region. The re-entrainment velocity is expected to be higher near the surface than near the bottom because of the higher approach velocity near the surface. This higher re-entrainment velocity, impinging on the rear portion of the cylinder, appears to be enough to cause a pressure gradient downward. It follows that, with a downward pressure gradient, the secondary flow is also downward.

At lower velocities the vortex shedding pattern changes and the secondary flow is directed upward. The separated region swings from side to side as the strong vortices are shed alternately from the cylinder, causing separation points on the cylinder and the rear stagnation point to vibrate with the vortex shedding frequency. A very good description of this separation phenomenon is given by MATTINGLY (1962). A sketch showing a strong vortex in the upper half of the separated region is shown in Fig. 4. The upper vortex is shedded and then a strong vortex in the lower half is formed, it is shed, and so on.

Under these latter flow conditions, the higher velocity near the surface forms stronger vortices which are produced immediately behind the cylinder. Therefore it follows that the pressure behind the cylinder will decrease with increasing distance from the floor in a fully-developed channel flow. In this case, the free surface appears to have little effect and the secondary flow is upward.

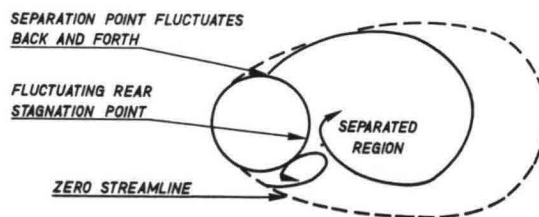


Fig. 4. Separation and oscillation behind cylinder (top view) (after Petryk, 1969).

VAUTIER (1972) measured flow characteristics around two-inch diameter vertical cylindrical piers in two separate flumes (0.45 meter and 2.4 meters wide) with the same approached flow conditions – flow depth 0.15 m, mean flow velocity range from 0.15 to 0.3 meter per second, and a fairly uniform sand of 0.4 mm in size. After a scour hole had reached its maximum size, the entire bed was stabilized, using PVA glue and shellac varnish. His measurements showed that (1) pier wake-vortex shedding frequencies were between 0.75 to 1.09 cycles per second; (2) pier nose-vortex shedding frequencies were in the range of 0.25 to 0.50 cycles per second; and (3) there was no significant difference in both the autocorrelation function and the spectral density for flow velocity measurements at correspondingly the same locations in the two flumes.

HJORTH (1975) studied the flow field around cylinders with circular and square cross sections. The theoretical part consisted of an analytical approach, using potential flow disturbed by a simple shear field, and the experimental part comprised measurements of wall shear stress and pressure field around the cylinders. For a circular cylinder it was found that the maximum average wall shear stress was 12 times that in the undisturbed approach flow. However, this is not in accordance with observations that scour near the pier starts at about 50% of the critical velocity for material transport in the undisturbed part of the bed.

2.2 Scour process

The dominant feature of scour process around a blunt-nosed pier is the horseshoe-vortex system. Since the horseshoe-vortex is being stretched the most at point A (about 70 degrees from the main flow direction, see Fig. 1) of a circular pier and near the corners of a square pier, the rotational velocity in the vortex core is the greatest in that neighbourhood. If the scouring potential created by this velocity is strong enough to overcome the particles' resistance to motion, scour will be initiated there. Sediment particles will be dislodged free along the front portion of the pier and carried out of the scour hole either by the horseshoe-vortex system and/or by the wake-vortex system like a vacuum cleaner.

Melville (1975) noted that:

"The horseshoe-vortex is initially small in cross-section and comparatively weak. With the formation of the scour hole, however, the vortex rapidly grows in size and strength as additional fluid attains a downwards component and the strength of the down flow increases. The down flow acts somewhat like a vertical jet in eroding the bed . . . Contours of [measured] bed shear stress, mean flow magnitudes and directions, and turbulent intensities on the bed of the scour hole remain remarkably similar throughout the development of the scour hole after its initial formation. This is a direct consequence of the similarity of shape of the scour hole which is apparent during its growth. As the scour hole enlarges, the circulation associated with the horseshoe-vortex increases, due to its expanding cross-sectional area, but at a decreasing rate, with the rate of increase being controlled by the quantity of fluid supplied to the vortex via the down flow ahead of the cylinder. This in turn is determined by the discharge of the approach flow; or, for a particular flow depth and width, by the magnitude of the velocity of the approach flow. The magnitude of the down flow near the bottom of the scour hole decreases as the depth of the hole increases. Hence the rate of erosion decreases. The armour coat, if present, helps to limit erosion. At a certain stage equilibrium is reached. The combination of the temporal mean bed shear and the turbulent agitation near the bed becomes incapable of removing further bed material from the scour area ahead of the cylinder and in the lower portion of the scour hole. Hence equilibrium is a condition at which the depth of scour ahead of the cylinder is just sufficient so that the magnitude of the vertically downwards flow ahead of the cylinder can no longer dislodge surface grains at the bed. This suggests that the equilibrium depth of scour for a particular bed material and under clear-water scour conditions should be a function of the magnitude of the downwards flow ahead of the cylinder, which in turn is primarily a function of the diameter of the cylinder and the magnitude of the approach flow velocity. Following this reasoning, the flow depth has only an indirect effect on the magnitude of the down flow and hence on the depth of scour. Although equilibrium is obtained for the depth of scour ahead of the cylinder, erosion continues in the downstream dune region. The mound immediately behind the cylinder is progressively flattened

and extended downstream by the flow out of the scour hole. This flow is directed up and out of the scour hole parallel to the downstream bed, and curves slightly inwards behind the cylinder. At equilibrium the flow near the bed of the scour hole has a greater concentration of energy in the low frequency range than the approach flow".

For a sharp nosed pier, in the absence of a strong horseshoe-vortex system large scour holes may develop downstream from piers by the wake-vortex system, as was demonstrated by the experiments of SHEN, SCHNEIDER and KARAKI (1966).

3 Analyses of scouring parameters

The magnitude which interests the designer for determining the pier foundation depth is the maximum depth to be reached by the scouring process. For this reason, the quantitative study will be limited to the maximum depth d_s reached by the scour hole around the pier after sufficient time has elapsed to reach the equilibrium. d_s is measured below ambient bed level.

Limiting the study to the case of the isolated bridge pier in a river whose flow is assumed to be steady and uniform, there are many parameters which may influence the scouring phenomenon:

Variables characterizing the fluid:

- g acceleration due to gravity,
- ρ density of fluid, and
- ν kinematic viscosity of fluid.

Variables characterizing the bed material:

- ρ_s density of the sediment,
- size distribution,
- grain form, and
- cohesion of material.

Variables characterizing the flow:

- d_0 depth of approach flow,
- \bar{U} mean velocity of undisturbed flow, and
- k the roughness of the approach flow.

Variables characterizing the bridge pier:

- its shape,
- its dimensions,
- its surface condition, and
- any protection systems.

The list of parameters is very long and some of them are, moreover, difficult to quantify, such as the particle size distribution, the grain form, or the cohesion of the bed materials.

For this reason, the analysis has been made mainly for the following restrictive conditions:

Bed material: the sediment is non-cohesive and has a uniform size D .

Flow: - channel sufficiently wide so that the bridge pier does not cause a significant contraction;
- flat bed, without dunes or ripples, so that the roughness k depends only on the diameter

- of the sediment D and the flow follows some resistance law relating mean velocity to hydraulic gradient I ; and
- only ultimate steady-state scour is considered.

Bridge pier: cylindrical, circular, perfectly smooth.

The parameters which remain are:

- for the fluid: ρ density, ν kinematic viscosity, and g acceleration due to gravity;
- for the bed material: D diameter of sediment and ρ_s its density;
- for the flow: d_0 the depth and \bar{U} the mean velocity of the undisturbed flow; and
- for the pier: its diameter b .

Therefore the scouring depth d_s depends on eight parameters:

$$d_s = f_1(\rho, \nu, g, D, \rho_s, d_0, \bar{U}, b) \quad (2)$$

These parameters may be replaced by the following ones:

$$d_s = f_2(\rho, \nu, g, D, \Delta, d_0, U_*, b) \quad (3)$$

with $\Delta = (\rho_s - \rho)/\rho$, the relative submerged density and $U_* = (gd_0I)^\frac{1}{2}$

It has been assumed therefore that only the relative density is of importance.

The theorem of Vaschy-Buckingham allows us to write:

$$\frac{d_s}{b} = f_3 \left(\frac{U_* D}{\nu}, \frac{U_*^2}{\Delta g D}, \Delta, \frac{d_0}{b}, \frac{D}{b} \right) \quad (4)$$

1 2 3 4 5 6

The justification for the choice of the dimensionless groups is the following:

- 1 Experiments have clearly demonstrated that it was possible to relate the scour depth to the diameter of the pier. This may be explained physically by the fact that scouring is due to the horseshoe-vortex system whose dimension is a function of the diameter of the pier.
- 2 and 3 These are classical parameters in the study of bed load.
- 5 and 6 These ratios relate the size of the pier to that of the flow and of the sediment.

The Equation (4) can be considerably simplified by the following considerations:

- The experimental studies conducted by CHABERT and ENGELDINGER (1956) and by RAMETTE and NICOLLET (1971) have shown that, for a pier with a given diameter b and a sediment of a given diameter D , the limiting scour depth d_s goes through a maximum d_{sm} for flow conditions corresponding to incipient movement in the absence of obstacles ($\tau = \tau_c$). Above τ_c , the scouring depth varies as a function of the inflow of particles and fluctuates owing to progression of bed forms. It is, therefore, very difficult to define the limit depth d_s . It is, however, possible to state that d_s is equal to or slightly lower than d_{sm} (about 10% according to SHEN). This important result has been confirmed by the study of HANCO (1971).
- The influence of the deformation of the free surface on the flow field is negligible if the Froude number of the flow is sufficiently low.

- There is an empirical relation for initiation of motion, relating

$$\frac{U_{*c}D}{\nu} \quad \text{and} \quad \frac{U_{*c}^2}{\Delta g D}$$

- The term Δ is constant by considering only natural sediments (pebbles, gravel or sand, $\Delta \approx 1.65$).

Under these assumptions Equation (4) may be simplified to:

$$\frac{d_s}{b} = f\left(\frac{U_*}{U_{*c}}, \frac{d_0}{b}, \frac{D}{b}\right) \quad \text{or} \quad \frac{d_{sm}}{b} = f\left(\frac{d_0}{b}, \frac{D}{b}\right) \quad (5)$$

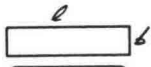
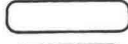
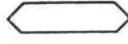



This means that the scour depth d_s will depend mainly on the ratio of mean velocity to mean critical velocity and the relative values of grain size, flow depth and pier diameter.

4 Description of model data

Numerous references on local scour experiments on piers can be found in literature. Few of them, however, are of a general nature with independent and sufficient variation of parameters. In most cases velocities were below or at the critical velocity for initiation of motion. Increasing the pier diameter was often done at constant water depth, thereby decreasing their ratio. Also scouring time will not have been sufficient in many cases to obtain the equilibrium scour depth. Some of the most interesting references are summarised below.

4.1 One of the first references on local scour is the article by DURAND-CLAYE (1873) (see also FLAMANT (1900) p. 281/282). He compared the scour for a square-nosed, a round-nosed and a triangular-nosed rectangular pier. The first one gave a maximum scour depth, whereas the triangular one gave the smallest scour depth.

4.2 TISON (1940 and summary in 1961). He has given much attention to the influence of shape, velocity profile and other parameters. The curvature of the flow at the upstream side of the pier is mentioned as the main cause of secondary vertical currents and local scour. Most tests were done in a flume with a width of 0.7 m, a discharge of 0.03 m³/s, a water depth of 0.105 m, a mean velocity of 0.41 m/s, and a medium-size sand, $D = 0.48$ mm.

shape	b (cm)	l (cm)	d_s (cm)
	6	24	11.4
	6	24	8.17
	6	24	7.0
	5.2	21.5	6.2
	6.0	24	5.45
	3.4	24	3.3

In a special test the bed upstream of the pier was roughened with gravel with $D = 1$ to 2 cm, thereby increasing the velocity gradient near the bed. The lenticular shape gave a maximum scour depth of 7.1 cm instead of 5.45 cm, showing the influence of the velocity profile. A gradual increase of the thickness of a lenticular pier from 5.3 cm at the water surface to 8.1 cm near the bed gave a decrease in scour depth from 7.1 to 4.6 cm, whereas a flared pier with a wide base gave very little scour under the same conditions. With a round-nosed circular pier a positive rake decreased the scour, whereas a negative rake increased the scour. The influence of the angle of attack was studied with the lenticular pier (6×24 cm).

$\alpha = 0^\circ$	6°	14.5°
$d_s = 5.45$ cm	6.95 cm	> 10.0 cm

Maximum scour depth occurred at the upstream nose for the rectangular pier and at the sides for the streamlined shapes. The length of a rectangular pier was not important at zero angle of attack. Tests with rectangular piers of 2.7×12 cm in a water depth of 6.0 cm at $\bar{v} = 0.32$ m/s showed no mutual influence on maximum scour depth for spacings equal to or larger than 11.6 cm (spacing/width ratio ≥ 4.3).

4.3 INGLIS (1948). Tests were performed on a rectangular round-nosed pier with $l = 19.2$ m and $b = 11.3$ m ($l/b = 1.7$) on lengths scales of $1:40$, $1:65$, $1:105$ and $1:210$ under zero angle of attack. The results are difficult to interpret because both \bar{U} and d_0 were varied simultaneously.

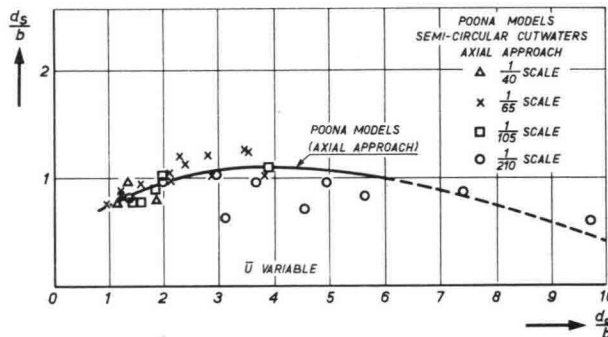


Fig. 5. Scour at bridge piers (Thomas 1962).

Maximum values of d_s/b were in the order of 1.3 (see Fig. 5, THOMAS 1962). Tests were carried out with sand with median grain sizes of 0.3 and 1.3 mm and were run until a zero net transport was obtained (no sand-feeding). From the experimental data the following relation was derived:

$$\frac{d_0 + d_s}{b} = 1.7 \left(\frac{q^3}{b} \right)^{0.78} \quad (\text{ft-units, coefficient} = 2.32 \text{ for m-units}) \quad (6)$$

The relation has limited applicability for $b \rightarrow 0$ and for increasing \bar{U} at constant d_0 , as has been shown by NEILL (1960, 1965). THOMAS (1967) stated that the formula should not be used outside the experimental range: $q^3/b = 2$ to 10 . A major disadvantage of the relation is the combination of undisturbed water depth and scour depth.

Several authors have converted the original relation thus:
 BLENCH (1962):

$$\frac{d_r + d_s}{d_r} = 1.8 \left(\frac{b}{d_r} \right)^{\frac{1}{2}} \quad d_r = \text{regime depth} \quad (7)$$

ARUNACHALAM (1965, 1967) with the aid of the Kennedy-relation:

$$\bar{U} = 0.84 d_r^{0.34} \quad (\text{ft-units}) \quad (8)$$

gave:

$$\frac{d_s}{b} = \frac{d_r}{b} \left[1.95 \left(\frac{d_r}{b} \right)^{-\frac{1}{2}} - 1 \right] \quad \text{in which } d_r = 0.9 q^{\frac{1}{3}} \text{ (ft-units) or } d_r = 1.334 q^{\frac{1}{3}} \text{ (m-units)} \quad (9)$$

or:

$$\frac{d_r + d_s}{d_r} = 1.95 \left(\frac{b}{d_r} \right)^{\frac{1}{2}} \quad (10)$$

4.4 CHABERT and ENGELDINGER (1956) performed an extensive programme of measurements on the various aspects of local scour around piers. The main variables were velocity, pier diameter (2.5 to 30 cm), water depth (0.1 to 0.35 m), grain size (0.26, 0.52, 1.5 and 3.0 m) and pier shape. Also many devices to reduce the scour were tested. The study on the influence of flow velocity showed that two regimes should be distinguished: for velocities at or below the threshold velocity of movement of the bed material scour depth approaches a limit asymptotically (see Fig. 6) whereas for a larger velocity scour depth fluctuates due to the periodic dumping of material in the scour hole by moving dunes (Fig. 7). Maximum scour depth was obtained at velocities near the threshold velocity, whereas scour started at about half the threshold velocity (see Fig. 8).

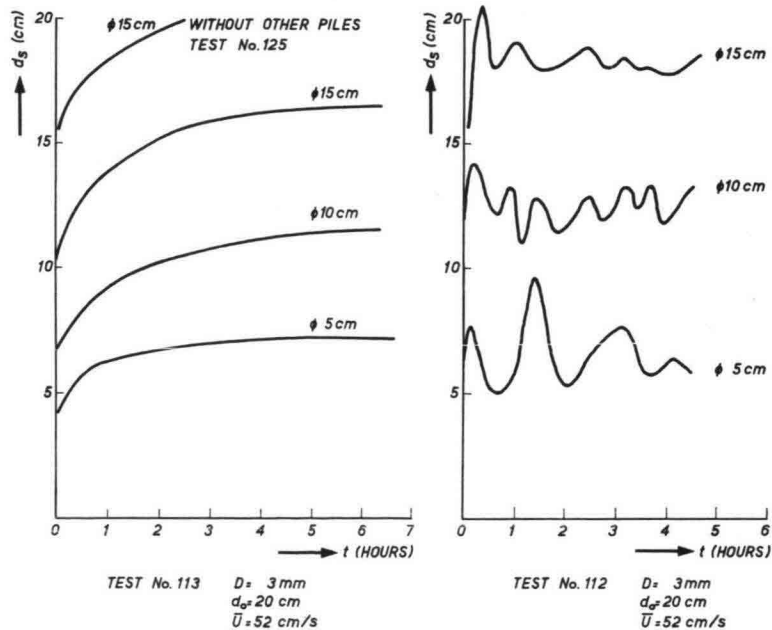


Fig. 6. Scour as a function of time $\bar{U} < \bar{U}_c$.

Fig. 7. Scour as a function of time $\bar{U} > \bar{U}_c$.

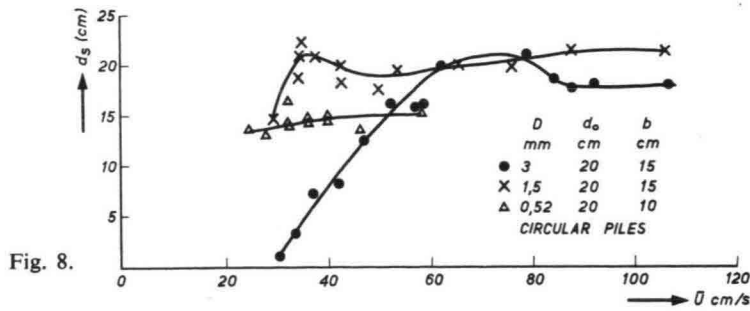


Fig. 8.

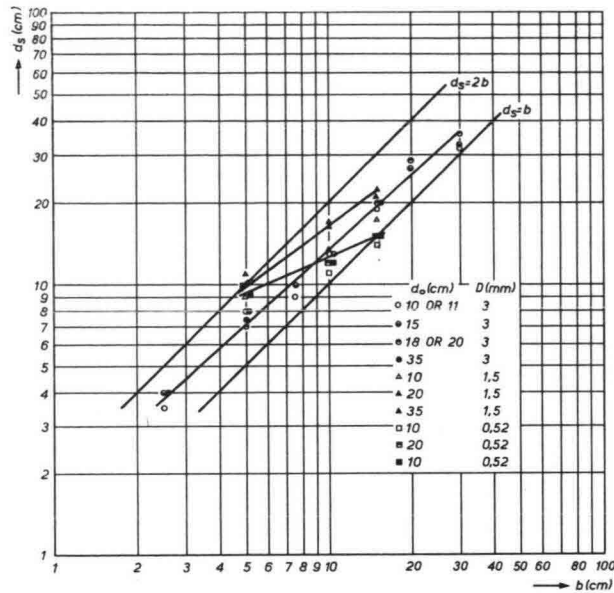


Fig. 9.

The influence of grain size, pier diameter and water depth can be seen from Fig. 9, which shows a small influence of grain size, a negligible influence of water depth for water depth/pier diameter ratios larger than one, and an increase of scour with b^α in which $\alpha \leq 1$. The latter influence may have been slightly obscured by the fact that the d_0/b ratio decreased with increasing pier diameter b for these tests.

The influence of pier shape and angle of attack can be seen from Fig. 10 which shows that at a zero angle of attack the scour depth may be minimised by streamlining the pier, but that this ad-

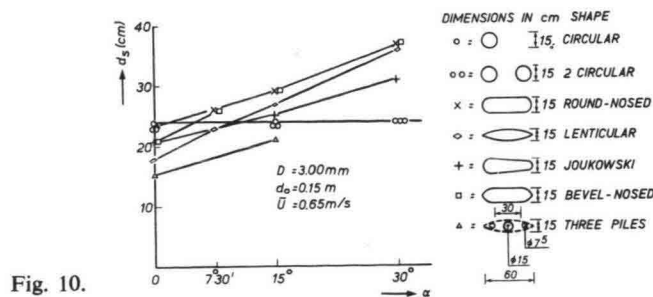


Fig. 10.

vantage disappears for angles of attack above 10°. An exception is formed by the system of 2 circular piers at a spacing of 3 pier diameters, which shows only a minor influence of the angle of attack.

Some care should be given to the interpretation of the results, because three piers were simultaneously tested in the flume at a separation of 6 m. Fig. 6 shows that some influence of the upstream piers was present.

4.5 LAURSEN and TOCH (1956, 1953) investigated the influence of pier shape, angle of attack, water depth, velocity and sediment size. The effects of pier shape and angle of attack were studied at the standard test condition: $b = 0.06$ m, $d_0 = 0.092$ m, $\bar{U} = 0.38$ m/s and $D = 0.58$ mm (see following Table):

angle of attack	l/b	relative scour depth *		
		round-nosed	elliptic	lenticular
0°	1:1	1.00		
	3:2	1.00		
	2:1	1.00	0.91	0.91
	3:1	1.00	0.83	0.76
10°	3:1	1.02	0.98	0.98
20°	3:1	1.13	1.06	1.02
30°	2:1	1.17	1.13	1.13
30°	3:1	1.24	1.24	1.24

* relative to scour for a circular pier with $b = 0.06$ m.

The influence of water depth, mean flow velocity and sediment size was studied with a dumb-bell pier under an angle of attack of 30°. The results are given in Fig. 11, from which it was concluded that there was no systematic influence of grain size and velocity in the range studied. There is an influence of water depth as might be expected in view of the large projected width of the pier (dimensions 0.06×0.4 m, $b = 0.06$ m, $b_{\text{eff}} = 0.25$ m). Scour depth varied with time due to the passage of dunes; the values given are averages.

The authors presented also a graphic design relation for rectangular piers under zero angle of attack, which was expressed by NEILL (1964b) as:

$$\frac{d_s}{b} = 1.5 \left(\frac{d_0}{b} \right)^{0.3} \quad (11)$$

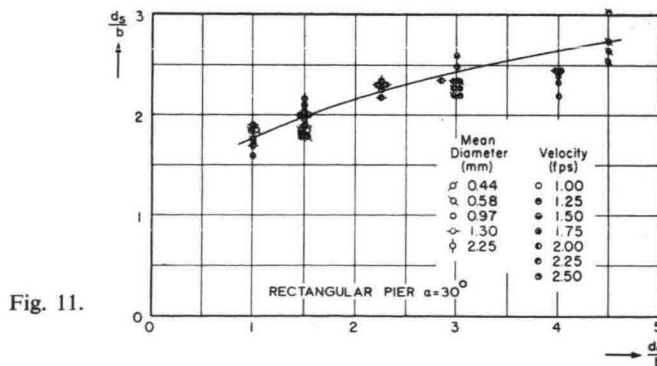


Fig. 11.

4.6 VARZELIOTIS 1960 (quoted from Neill 1964a). Varzeliotis did experiments with 1.7 mm sand with pier shape, angle of attack, velocity and water depth as variables. Standard test conditions were flow depth 0.107 m, mean velocity 0.48 m/s and $b = 0.025$ m. Here are some of his results:

Influence of shape:

square-nosed	0.067 m
round-nosed	0.038 m
bevel-nosed	0.041 m
lenticular	0.030 m

The length of a round-nosed pier had no influence for zero angle of attack and length/width ratios of 1 to 20. The influence of pier width was studied with constant depth with the results:

$b =$	0.025	0.05	0.075	0.1	m
$d_s =$	0.038	0.079	0.114	0.127	m

Variation of the angle of attack for a round-nosed pier with $l/b = 6$ gave the following result:

$\alpha =$	0°	7.5°	15°	30°	45°	
$d_s =$	0.035	0.041	0.048	0.083	0.132	m

Water depth and velocity were increased simultaneously during tests with increasing discharge intensity and a round-nosed pier of dimensions 0.05×0.15 m under zero angle of attack. Assuming that mean velocity has no great effect in the range used (0.4 to 0.58 m/s, see also Fig. 8), it may be concluded that d_s increases slowly with d_0 upto d_0/b equal 2 to 3:

$\bar{U} =$	0.40	0.45	0.48	0.51	0.53	0.56	0.58	m/s
$d_0 =$	0.073	0.091	0.107	0.122	0.134	0.146	0.159	m
$d_s =$	0.076	0.084	0.088	0.093	0.096	0.094	0.101	m

4.7 TARAPORE (1962) reported some experiments with circular piers ($b = 0.05$ m, $D = 0.15$ and 0.5 mm), from from which it may be concluded that d_s increases with d_0/b upto d_0/b equal to about one and remains constant thereafter ($d_s/b \approx 1.4$). The development of scour depth with time may be represented with a logarithmic relation. TARAPORE showed that this corresponds to an exponential decrease of velocity near the bed in the scour hole, assuming a standard type of bed-load transport relation to be valid in the scour hole.

4.8 LARRAS (1963, 1960) analysed the data given by CHABERT and ENGELDINGER (1956). He concentrated on the maximum scour depth near the threshold velocity of the undisturbed bed material and gave a relation expressing scour depth as a function of pier diameter, with water depth and grain size neglected:

$$d_{sm} = 1.05b^{0.75} \quad (\text{m-units}) \quad (12)$$

Tables were given for the influence of pier shape and angle of attack, with the circular pier as a

basis. Lenticular shapes gave a relative scour depth of 0.75, elliptical shapes 0.85, rounded piers 1.0 and rectangular ones 1.1 to 1.4. The advantage of the first two shapes disappears for angles of attack of 10° or more.

4.9 NEILL (1964a) gave an excellent review of the work of TISON, INGLIS, LAURSEN and TOCH, CHABERT and ENGELDINGER and VARZELIOTIS. He concluded in favour of relations expressing scour depth as measured from the original bed surface. Suggestions for design were given. For extrapolation to prototype conditions, NEILL suggested a linear increase of scour depth with pier diameter with a relative value of 1.5 to 2.5 for a round-nosed pier. The effects of grain size distribution, local conditions (contraction, embankments) should be investigated in more detail, preferably on the basis of field data.

4.10 NEILL (1964b). In this report detailed attention was given to the influence of the actual river on the scour phenomena, of which the local scour near the pier is only one aspect. A review of literature on model and field data as well as recommendations for design were presented.

4.11 ARUNACHALAM (1965). For the modification of the Inglis-relation see 4.3 The influence of an angle of attack can be taken into account by substituting the projected width of the pier in the relation given.

4.12 NEILL (1965) described some field data on local scour and gave a critical comparison of existing relations for local scour. This gave rise to an extensive discussion by people involved in the development of regime formulas (see Chapter 5).

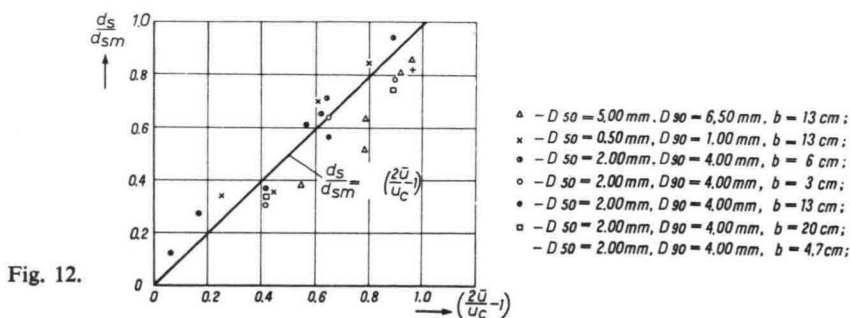


Fig. 12.

4.13 HÎNCU (1965, for a French translation see HANCO (1971)) gave experimental results for circular piers ($b = 3, 4.7, 6, 13$ and 20 cm) in coarse material ($D_{50} = 0.5, 2$ and 5 mm). The scour depth was constant ($d_s = d_{sm}$) above a certain velocity (\bar{U}_c). At lower velocities a linear relation with velocity was obtained:

$$\frac{d_s(\bar{U})}{d_{sm}} = \left(\frac{2\bar{U}}{\bar{U}_c} - 1 \right) \quad (\text{see Fig. 12}) \quad (13)$$

The influence of water depth was negligible for $d_0/b > 1$, and d_{sm} increased with grain size. The results were correlated with the expression:

$$\frac{d_{sm}}{b} = 2.42 \left(\frac{\bar{U}_c^2}{gb} \right)^{\frac{1}{3}} \quad \left(\frac{\bar{U}_c^2}{gb} = 0.05 \text{ to } 0.6 \right) \quad (14)$$

With a relation given for \bar{U}_c :

$$\bar{U}_c = 1.2 \sqrt{gD \frac{\rho_s - \rho}{\rho}} \left(\frac{d_0}{D} \right)^{0.2} \approx 1.54 D^{0.3} d_0^{0.2} g^{0.5} \quad (15)$$

for natural sands, the relation may be converted into:

$$\frac{d_{sm}}{b} = 3.3 \left(\frac{D}{b} \right)^{0.2} \left(\frac{d_0}{b} \right)^{0.13} \quad (16)$$

4.14 SHEN, SCHNEIDER, KARAKI (1966a, b, 1969), ROPER, SCHNEIDER, SHEN (1967), SHEN (1971). In the first reference (1966a) a review of existing literature is given. An analysis of the flow field and the horseshoe-vortex system near a circular pier gave the conclusion that the circulation of the vortex is proportional to $\bar{U} \cdot a$ ($a = b/2$). The next conclusion that the local scour depth will be a function of this factor divided by the kinematic viscosity, being a Reynolds number, is not so obvious.

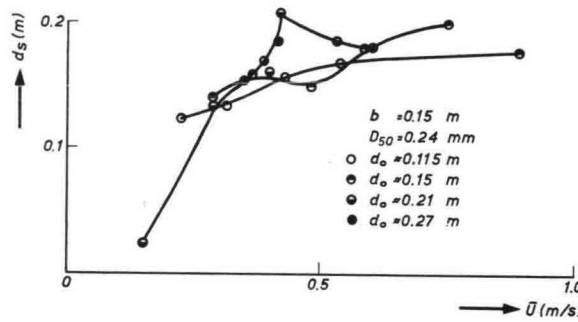


Fig. 13.

Experimental results (21 tests) were given for a circular pier with $b = 0.15$ m in 0.24 mm sand. One test was done with $b = 0.15$ m and 0.46 mm sand and two tests with $D = 0.9$ m in 0.46 mm sand. Results for the 0.24 mm sand are shown in Fig. 13. The scour depths for the 0.9 m pier were 0.67 m and 0.55 m respectively for $d_0 = 0.67$ m, $\bar{U} = 0.66$ m/s and $d_0 = 0.61$ m, $\bar{U} = 0.50$ m/s.

From these data and other results from literature a relation was derived of the form:

$$d_s = 0.000059 \text{ Re}^{0.512} \text{ (m-units) (SHEN 1966a)} \quad (17)$$

$$d_s = 0.00022 \text{ Re}^{0.619} \text{ (m-units) (SHEN 1969) see Fig. 14} \quad (18)$$

This relation must be considered as an upper envelope because scour depth does *not* increase with \bar{U} for $\bar{U} > \bar{U}_c$ (CHABERT and ENGELDINGER).

For d_{sm} another relation is given:

$$\frac{d_{sm}}{d_0} = 2 \{ F^2 (b/d_0)^3 \}^{0.215} \quad F = \bar{U} / \sqrt{g d_0} \quad (19)$$

or

$$\frac{d_{sm}}{b} = 2 F^{0.43} \left(\frac{d_0}{b} \right)^{0.355} \quad (20)$$

which is similar to the design relation given by LAURSEN and TOCH. The latter may be approximated by:

$$\frac{d_{sm}}{b} = 1.35 \left(\frac{d_0}{b} \right)^{0.3} \quad \text{for a circular pier} \quad (21)$$

d_{sm} fluctuates with time for $\bar{U} > \bar{U}_c$. The authors advised to take $d_{sm} + 0.5$ dune height for design purposes.

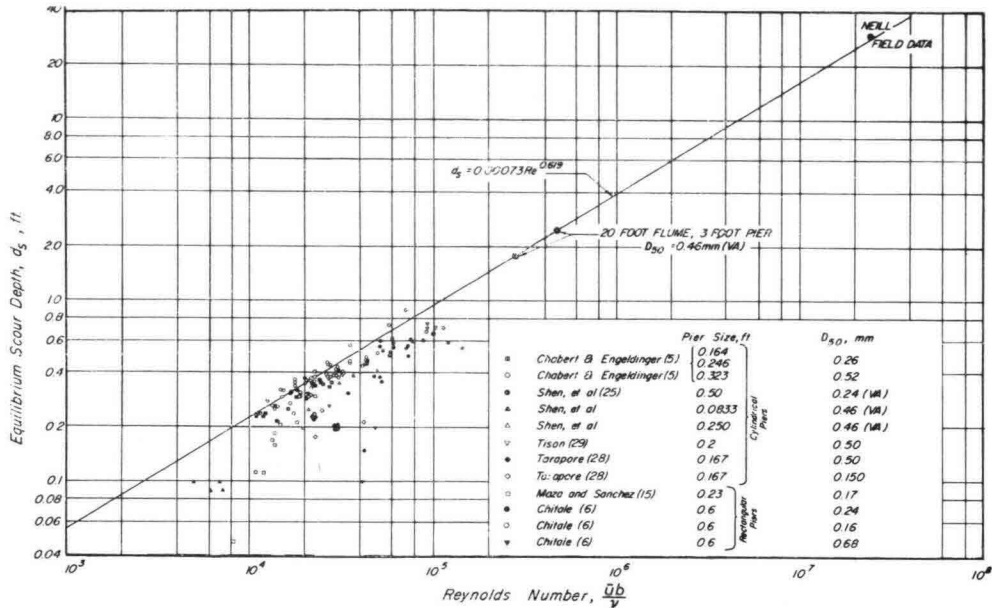


Fig. 14.

The influence of grain size was considered to be negligible for $D < 0.5$ mm (SHEN et al 1966a). The influence of pier shape was studied by SHEN et al (1966b). Adding a sharp nose (top angle 15° or 30°) to a blunt-nosed pier gave a reduction in maximum scour depth. Roughening the upstream face of the pier to decrease the vertical velocities or the strength of the vortex had no effect. SHEN et al (1969) gave a summary of SHEN (1966a, b) and new experiments. The data were also compared with other design relations such as given by LARRAS (1963): $d_s = 1.05 kb^{0.75}$ (m-units) in which $k = 1.0$ for a circular pier and 1.4 for a rectangular pier, and by BREUSERS (1965): $d_s = 1.4b$ for circular piers. These relations were considered as an upper limit for scour with continuous transport.

In the discussion on SHEN et al (1969), BREUSERS (1970) stressed the empirical knowledge that in general a linear scaling-up of scour depth with pier dimensions may be expected. Comparisons of model and prototype data were given which pointed to this linear relationship (Fig. 15). VEIGA DA CUNHA (1970) stated that the relation given by SHEN et al (1966a) can be valid for clear-water scour only because scour is independent of velocity for velocities above the threshold velocity (Fig. 16), as was shown by CHABERT and ENGELDINGER (1956). The Reynolds number is apparently an unsuitable parameter to characterise the scour depth. According to VEIGA DA CUNHA, also the ratio of water depth to pier diameter should be considered (Fig. 17).

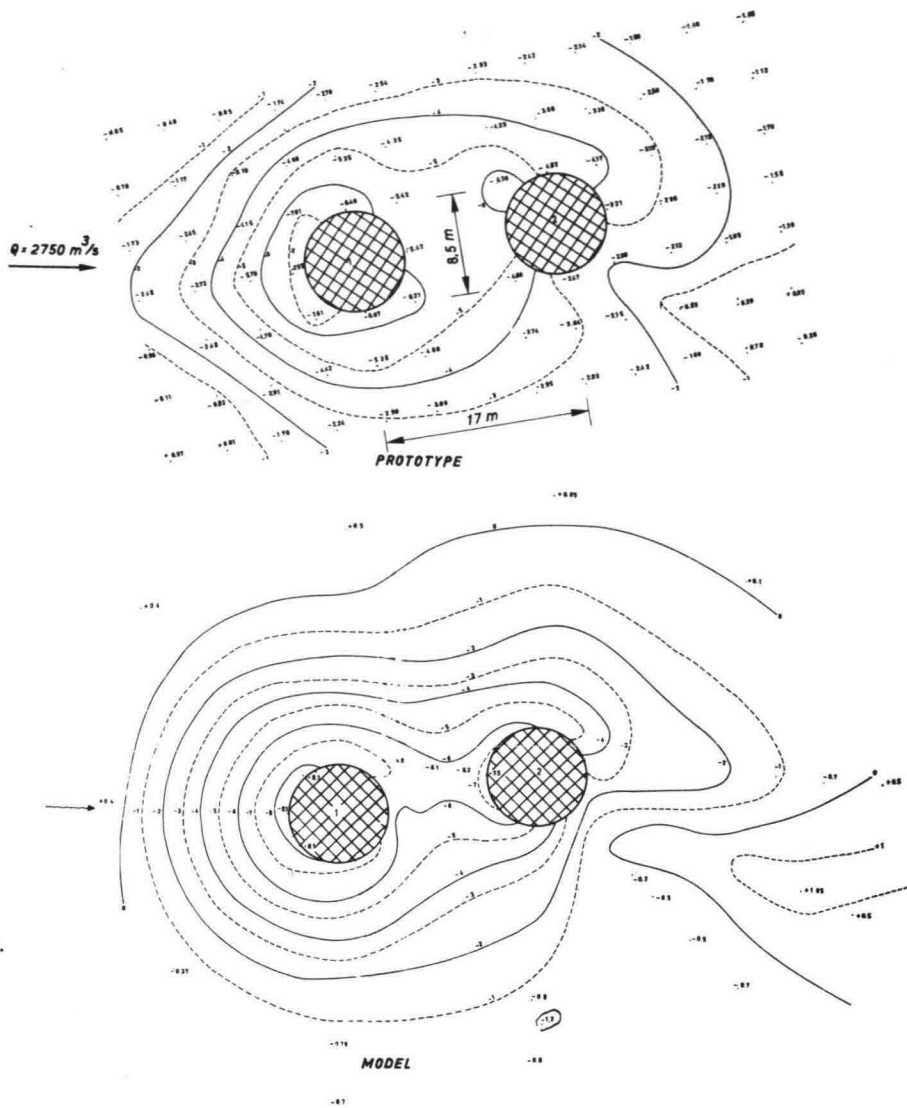


Fig. 15.

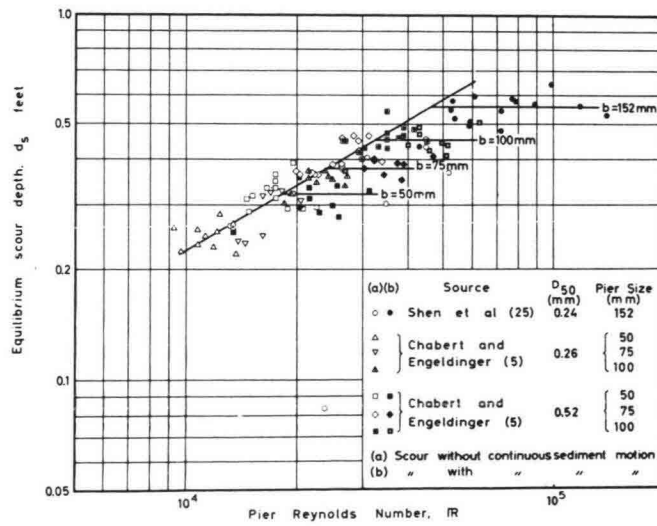


Fig. 16. Scour with and without continuous sediment motion.

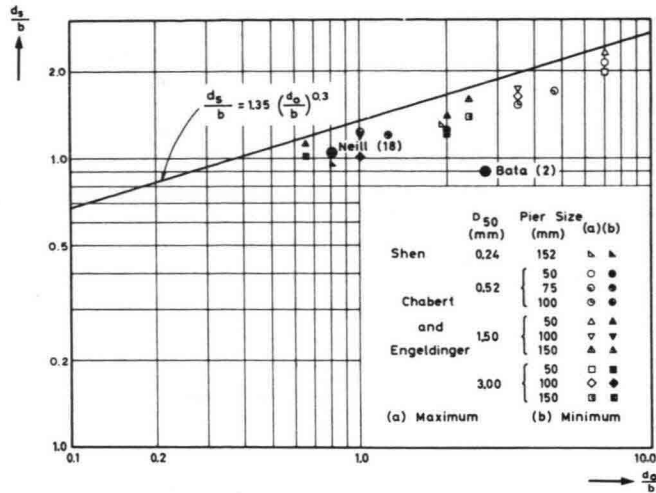


Fig. 17. Influence of d_0/b .

4.15 MAZA ALVAREZ and SANCHEZ BRIBIESCA (1966, 1967, 1968) presented a general discussion on the various types of scour in a river and gave results of flume tests on circular, rounded and rectangular piers in sand with diameters of 0.17, 0.56 and 1.3 mm. Some results for a circular pier \varnothing 13.3 cm are shown in Fig. 18. Maximum scour depth is in the order of 1.5 times the diameter for a circular cylinder and 2.0 for a rectangular pier under zero angle of attack. The influence of water depth seems insignificant, whereas a linear increase of scour depth with velocity is observed for velocities below the threshold value.

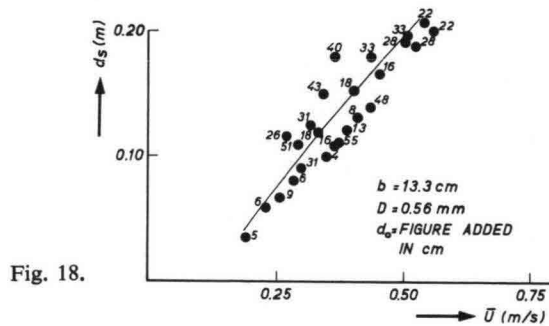


Fig. 18.

4.16 COLEMAN (1971) analysed data from SHEN et al (1969) and results from experiments on circular piers with $b = 0.045$ and 0.076 m in sand with $D = 0.1$ mm under conditions of continuous sediment transport. The correlation obtained was:

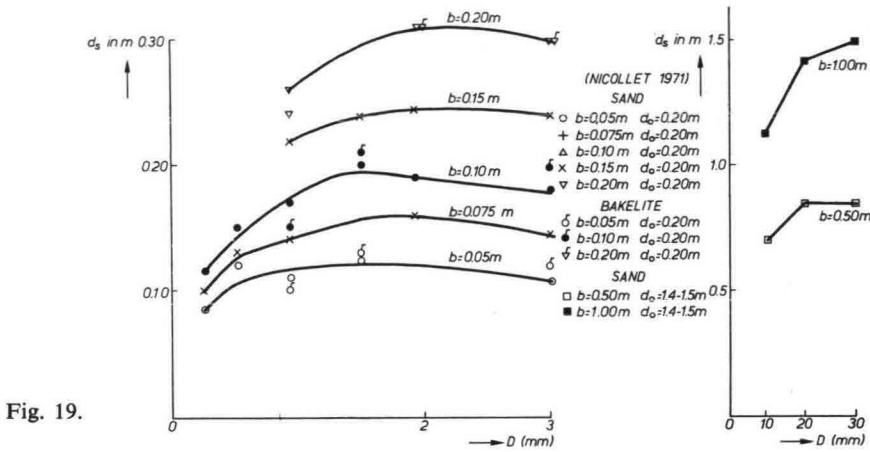
$$\frac{d_s}{b} = 1.49 \left(\frac{U^2}{gd_0} \right)^{1/10} \quad (22)$$

which can be transformed into $d_s = 1.4b$ (BREUSERS 1965) with a minor change of coefficients.

4.17 NICOLLET (1971a, b) extended the experiments by CHABERT and ENGELDINGER (1956) with respect to the following variables:

- Grain size and gradation,
- the velocity at which the scouring process starts,
- the influence of bed material density, and
- the influence of aspect ratio for a round-nosed pier.

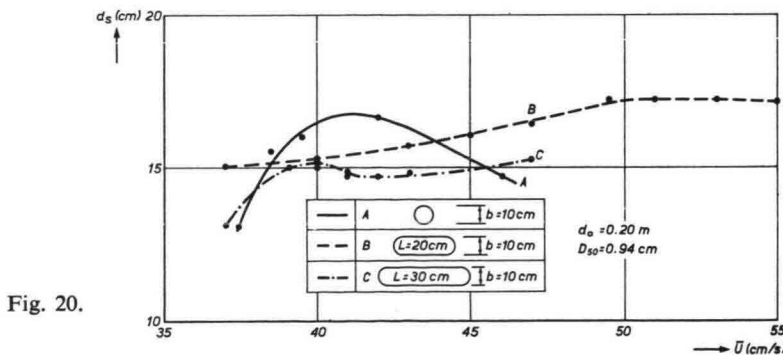
The first aspect was studied by performing tests with grain sizes of 0.94, 1.93 and 3 mm in the flume used by CHABERT and ENGELDINGER and with gravel (7, 15 and 25 mm) in a large channel (4 m wide) with a water depth of 1.5 m and pier sizes of 0.5 and 1.0 m. The results for d_{sm} , the maximum value of d_s are presented in Fig. 19. Scour depth increases with grain size upto $D = 2$ mm for constant water depth.



Tests with a widely graded material ($D_5 = 0.24$ mm, $D_{50} = 0.7$ mm, $D_{90} = 4$ mm) gave a much lower value of d_s/D (in the order of 0.5 instead of 1.5) than with uniform sand under similar conditions (see also Para. 6.6).

Results for bakelite ($\rho_s = 1320$ kg/m³) are also plotted in Fig. 19 from which it may be concluded that ρ_s is not a significant parameter as far as d_{sm} is concerned. The influence of aspect ratio was studied with $b = 0.1$ m and $l/b = 1, 2$ and 3 (see Fig. 20), which shows that the aspect ratio only has a slight influence on d_{sm} .

Special attention was given to the velocity for initiation of scour. The ratio of this velocity to \bar{U}_c , the velocity for initiation of movement of the undisturbed bed material, was 0.42 to 0.53 for a



circular pier and 0.5 to 0.65 for round-nosed piers. For design of scour protection by rip-rap, the ratio given by HANCO (0.5) is suggested.

4.18 From the tests by DIETZ (1972) on circular piers with various bed materials it may be concluded that scour depth increases with d_0/b upto $d_0/b = 3$ (see Fig. 21). Scour increased linearly with b for $b = 0.043$ to 0.135 m. Several shapes were investigated. When the cylindrical pier was taken as a reference, the following ratios were measured:

shape	round-nosed	elliptical			rectangular		
aspect ratio	—	1:2	1:3	1:5	1:1	1:3	1:5
ratio	0.95	0.9	0.85	0.72	1.4	1.2	1.1

4.19 Systematic tests were performed under geometrically similar conditions by BONASOUNDAS (1973) on circular piers ($b = 0.05, 0.10, 0.125$ and 0.15 m, grain size $0.63, 1.15$ and 3.3 mm). The results are summarised in Fig. 22 for $\bar{U}/\bar{U}_c \geq 1.0$. The scour depth given is that measured after 2 hours and is not the equilibrium value. The figure shows that d_s increases with d_0/b upto $d_0/b = 2$. The influence of grain size is relatively unimportant for constant D and d_0 . Scour depth increases roughly with b , keeping d_0/b and grain size constant.

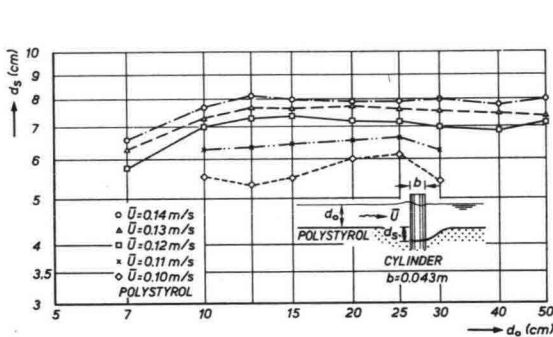


Fig. 21.

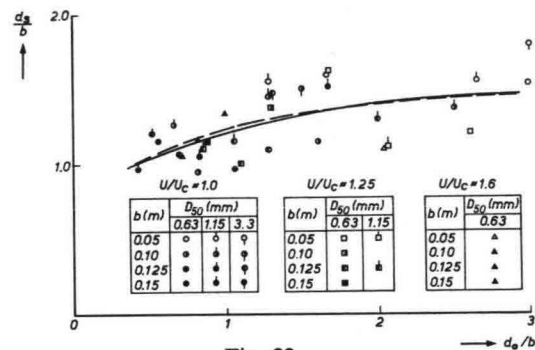


Fig. 22.

4.20 WHITE (1975a, b) presented experimental data for various pier shapes in a coarse sand ($D_{50} = 0.9$ mm, $D_{90} = 3.4$ mm) for high Froude numbers (0.8 to 1.2). The influence of the Froude number was only small in this range. The influence of the pier width decreased with decreasing water depth. The results are difficult to interpret because of interdependence of the variables. The tests were done for scour prediction in steep mountain streams.

4.21 CARSTENS and SHARMA (1975) argued that for large values of b (offshore oil storage tanks) the scour depth will not increase linearly with b for several reasons: the special velocity distribution (Ekman spiral), the large ratio of b/d_0 , and the absence of thick layers of sand. They also stated that protections against scour should not increase linearly with b as far as dimensions are concerned.

4.22 NICOLLET (1975) gave results for a test in cohesive material ($D_{50} = 2.2$ μm). Initiation of scour occurred at 60% of the critical velocity without the presence of the pier. The scour depth

was in the order of 0.045 to 0.065 m for a circular pier, with $D = 0.05$ m at velocities of 0.7 to 0.8 m/s. The scour hole was more elongated in the downstream direction and more irregular than with sand as bed material.

4.23 Tests with a large diameter pier (up to 0.75 m) were described by TORSETHAUGEN (1975). Polystyrene was used as bed material and special attention was given to the time-history of the scour:

$$d_s/d_{se} = \exp[-(t_0/t)^{0.5}] \quad (23)$$

The correlation obtained for d_{se} was:

$$d_{se}/b = 1.8(\bar{U}/\bar{U}_c - 0.54)d_0/b \quad d_0/b < 1.0 \quad (24)$$

where most experiments were for $\bar{U}/\bar{U}_c = 0.8$ and $d_0/b = 0.2$ to 0.65. The scouring depths given are below those found by other investigators for similar conditions, but no explanation is given.

4.24 BASAK et al (1975) performed tests with square piers in coarse sand ($D_{50} = 0.65$ mm, $D_{90} = 1$ mm). Pier width ranged from 0.04 to 0.5 m but the water depths were small (up to 0.14 m). For most of the tests $\bar{U} > \bar{U}_c$, but as both depth and velocity were varied simultaneously, no independent variation of parameters was obtained. The results for square piers were correlated with the equation:

$$d_s = 0.558b^{0.586} \quad (\text{m-units}) \quad (25)$$

for varying d_0 , which can be interpreted only as a decrease of d_s/b with increasing b/d_0 . The results are interpreted in a better way by plotting d_s/b versus d_0/b , which shows that for constant d_0/b , d_s increases linearly with b (see Fig. 23). Increasing the length width ratio of rectangular piers gave no increase in scour depth for $l/b = 1$ to 6. For rectangular piers under an angle of attack $0 \leq \alpha \leq 90$,

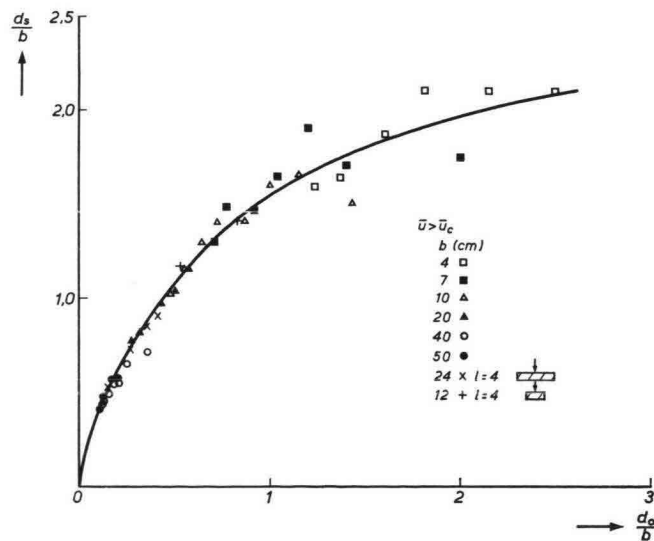


Fig. 23.

the relation given above was also valid if the projected width was taken for b . Interesting results were obtained with rows of square piers. For a row aligned with the flow, maximum scour always occurred at the upstream face of the first pier, so that no influence of spacing and number of piers on d_s was found. For the other piers minimum scour was observed for a centre spacing /width ratio of 4.

For rows perpendicular to the flow, scour depth decreased with increasing spacing upto a spacing/width ratio of 5.

4.25 MELVILLE (1975) made very detailed measurements of the turbulent velocity field around a circular pier and in the scouring hole. For a brief summary see Chapter 2. Also field data are given, (see Section 5.9).

4.26 ETTEMA (1976) studied the influence of median grain size ($D_{50} = 0.55$ to 6.0 mm) and gradation (σ/D_{50} upto 1.6) on local scour near a circular pier with $b = 0.1$ m and $d_0 = 0.6$ m. The experiments were carried out at or below the critical flow velocity. For a discussion of the results, see Sections 6.2 and 6.6. The development of the scour depth with time was described satisfactorily with a $\log(t)$ -relation.

5 Description of field data

Field data should give a final proof of the relations established on the basis of small-scale experiments. It is unfortunate, therefore, that the availability of well-documented field data is limited. Use of the data is also hampered by complicated geometrical shapes, variability of bed material, and inaccuracy of measured quantities. It is, however, possible to present a few cases, mainly taken from NEILL (1964a, b) and MELVILLE (1975).

5.1 INGLIS (1949), Indian Rivers. Observations in the period 1924–1942 on 17 bridges in rivers with discharges from 850 tot 63,000 m^3/s were recorded. Data were presented as a table of total scoured depth, measured from the water surface to the bottom of the scour. This total depth is the sum of general scoured depth, scour due to contraction and local scour due to the piers. The depths were compared with the Lacey regime depth:

$$d_{\text{Lacey}} = 0.473(Q/f)^{\frac{1}{3}} \quad (\text{m or ft-units}) \quad (26)$$

in which f = silt factor = $1.76 (D)^{\frac{1}{2}}$, D = median grain size in mm. The average value was 2.09 with a r.m.s. value of 12.9% (see ARUNACHALAM, 1965). Individual values of the ratio varied between 1.73 and 2.62. For design purposes generally a value of 2.0 is used, therefore:

$$d_0 + d_s = 0.95(Q/f)^{\frac{1}{3}} \quad (27)$$

ARUNACHALAM (1965) re-analysed the data and found that the correlation could be improved by leaving f out of the correlation. The result was:

$$d_0 + d_s = (2.09)0.473Q^{\frac{1}{3}} \approx 0.95Q^{\frac{1}{3}} \quad (28)$$

The r.m.s. value reduced to 8.45% with individual ratios varying from 1.72 to 2.59. ARUNACHALAM stated that it may not be concluded that the grain size is not important as the grain size only varied from 0.17 to 0.39 mm (f from 0.71 to 1.10).

5.2 LAURSEN and TOCH (1956), Skunk River. Field observations at the nose of a single rounded pier in the middle of a straight reach of a sand-bed river were obtained with an electric resistivity device. The width of the pier is not exactly defined but was approximately 1.2 m. The maximum value of d_s was 2.0 m at a flow depth of 3.7 m. Neither velocities nor bed material were given. Scale models (1:12 and 1:24) with 0.58 mm sand and a velocity of 0.53 m/s gave a good correspondence with the field observations (see Fig. 24).

5.3 LARRAS (1960) gave two tables with scoured depths around bridge piers. The first table contained depths observed *after* a flood had passed and must, therefore, as is clearly stated in the paper, have been smaller than the maximum depths during the flood. Pier widths ranged from 0.5 to 6.5 m and scoured depths from 0.6 to 4.3 with d_s/b ratios from 0.4 tot 1.2.

The second table presented *estimated* scoured depths, *including* general scour, based on accidents or incidents with bridge piers. Values of pier widths ranged from 0.7 to 4.2 m, estimated d_s/b values from 1.3 to 2.0.

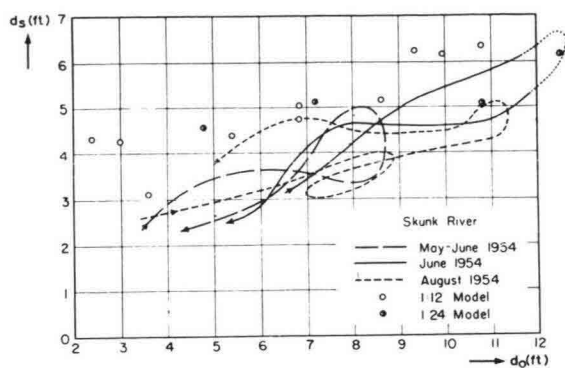


Fig. 24.

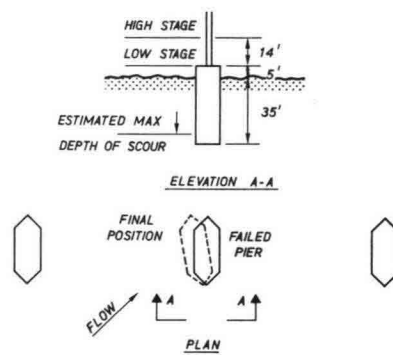


Fig. 25.

5.4 NEILL (1964a, b) reported several cases of scour near bridges which in some cases led to bridge failure. The following cases are of interest for the aspect of local scour:

Bridge C. Figure 25 shows the principal features of this case. Slender piers were supported by a concrete caisson from 10.6 m below the bed to 1.5 m above it. The bed was composed of sand and the pier was skewed at least 40° to the current. During a flood one caisson settled and tipped sideways towards the flow, as shown. The maximum scoured depth was estimated at 9.4 m below low-water bed on the exposed face of the caisson. General scour was not known, but using Laursen's design data a scour depth almost equal to the observed depths was predicted.

Bridge F. Scour in a stable gravel-bed river. In this case a total scoured depth ($d_o + d_s$) of about 15.9 m at the nose of a 6 m wide pier at zero angle of attack was observed. Using Blench's method to determine a "zero flood depth" and a multiplication factor of 2.0 (INGLIS) resulted in a depth of 15.3 m.

5.5 NEILL 1965, Beaver River. Scour data on two bridges (la Corey and Beaver Crossing) were given. Scouring was mainly due to constriction of the flow; only limited local scour near the piers was observed. The scoured depth was compared with the two-dimensional LACEY depth:

$$d_{2,Lacey} = 0.9(q^2/f)^{1/3} \quad (\text{ft-units, 1.34 for metric units}) \quad (29)$$

f was taken equal to 1.0 ($D = 0.5$ mm).

To compute q , the clear water-surface width beneath the bridge at a low-water stage was taken. The ratios of total scoured depth and $d_{2, \text{Lacey}}$ were 1.22 and 1.3 respectively. The article about this gave rise to interesting discussions by several authors involved in the development of regime relations (LACEY, INGLIS, THOMAS, BLENCH).

5.6 ARUNACHALAM (1965). ARUNACHALAM also re-analysed the data given by INGLIS with a relation developed from the Inglis/Poona relation (developed from model tests on the Hardinge bridge). The resulting equation was:

$$d_s/b = d_r/b[1.95(d_r/b)^{-\frac{1}{2}} - 1] \quad (30)$$

in which some influence of pier width is present. For $d_r/b \approx 1$, this relation reduces to $d_s + d_r \approx 1.95d_r$.

Correlation with 11 out of the 17 bridges where b was known, resulted in a r.m.s. value of 10% instead of 12.7% with Equation (27). The relation also gave good results for some other cases, but overestimated the scour for the data given by NEILL (1965).

5.7 Ministry of Railways, India (1967, 1968, 1972).

5.7.1 1967 Report. At the request of the Indian Railway Board a measuring campaign on railway bridges in all parts of India was started. After a careful selection, only 8 bridges out of 48 were used, because many bridges were protected with stone pitchings or because observations were incomplete. The bridges had spans from 9 to 23 m, the bed material was coarse sand to gravel with silt factors from 1.83 to 2.9 ($D = 1$ to 3 mm). Discharges varied from 35 to 600 m³/s. The computed LACEY depths varied from 1.35 to 3 m and the observed total scour depths ($d_0 + d_s$) from 2.3 to 5.5 m. The dimensions of the piers were not given (in one case $b = 2.44$ m). For flow parallel to the pier, maximum scour occurs at the nose and an average ratio of $(d_0 + d_s)$ to LACEY depth of 1.71 was found (r.m.s. value 19%). For currents inclined to the pier upto 35°, maximum scour occurred on the side of the pier under attack and averaged $1.99d_{\text{Lacey}}$ (r.m.s. value 15%). Combination of all data gave $(d_0 + d_s)/d_{\text{Lacey}} = 1.93$.

The correlation with Q was better than with the discharge intensity computed from an estimated stream width near the piers. In this case the depth was computed from the "two-dimensional" Lacey relation.

$$\begin{aligned} d_{2, \text{Lacey}} &= 1.34(q^2/f)^{\frac{1}{3}} && \text{(m-units)} \\ &= 0.9 (q^2/f)^{\frac{1}{3}} && \text{(ft-units)} \end{aligned} \quad (31)$$

5.7.2 1968 Report. Scour around the piers of Ganga Pul at Makameh. This bridge has 14 spans of 123 m, and the width of the wells was 9.75 m. 18 observations are given for various monsoon floods (5,000 to 34,000 m³/s) in the period 1958–1967. Corresponding LACEY depths were 7.5 to 14.5 m using a silt factor of 1.15 (sediment size not given). Average scoured depth at the nose of the piers gave a ratio $(d_0 + d_s)/d_{\text{Lacey}} = 1.75$, whereas for an inclined attack scour along the sides averaged $2.15d_{\text{Lacey}}$.

It was observed that during non-monsoon floods the value of $(d_0 + d_s)/d_{\text{Lacey}}$ was larger, possibly due to a lower silt content, according to the author. Corresponding values from 13 observations were $2.94d_{\text{Lacey}}$ at the nose and $2.7d_{\text{Lacey}}$ for scour along the sides of the piers. Measured scour

depths during non-monsoon floods were slightly smaller, however, than during the largest monsoon flood.

5.7.3 1972 Report. Further observations (50) on 4 out of the 8 bridges mentioned in the 1967 Report are given with discharges from 60 to 500 m³/s, d_{Lacey} 1.5 to 3 m and $(d_0 + d_s)$ values from 2.1 to 6.8 m. Maximum scoured depth was generally found along the sides of the piers.

The final correlation for all (93) observations was (see Fig. 26) $(d_0 + d_s) = 1.92 d_{Lacey}$ (r.m.s. value 15%, correlation coefficient 0.79). Correlation with the two-dimensional LACEY depth gave the result (see Fig. 27): $(d_0 + d_s) = 1.46 d_{2Lacey} = 1.46 [1.34(q^2(f)^{\frac{1}{3}})]$ (r.m.s. value 15%, correlation coefficient 0.80; q is the local discharge intensity near the piers). In 36 out of the 50 observations also the depth between the piers was measured and correlated with Q and q . The best correlation was obtained with the Lacey expression (correlation coefficients of 0.74 and 0.76 respectively for the three and two-dimensional cases).

In this series of observations pier width was also measured and a Laursen type of plot (d_s/b vs d_0/b) was given after reduction for effects of shape and angle of attack. In 14 cases d_0 was estimated from Lacey's formula. The result was discouraging. No correlation with Reynolds or Froude number was obtained. The authors also tried correlations of the form

$$d_s + d_0 = kQ^{af^b} \quad \text{or} \quad kq^{af^b}$$

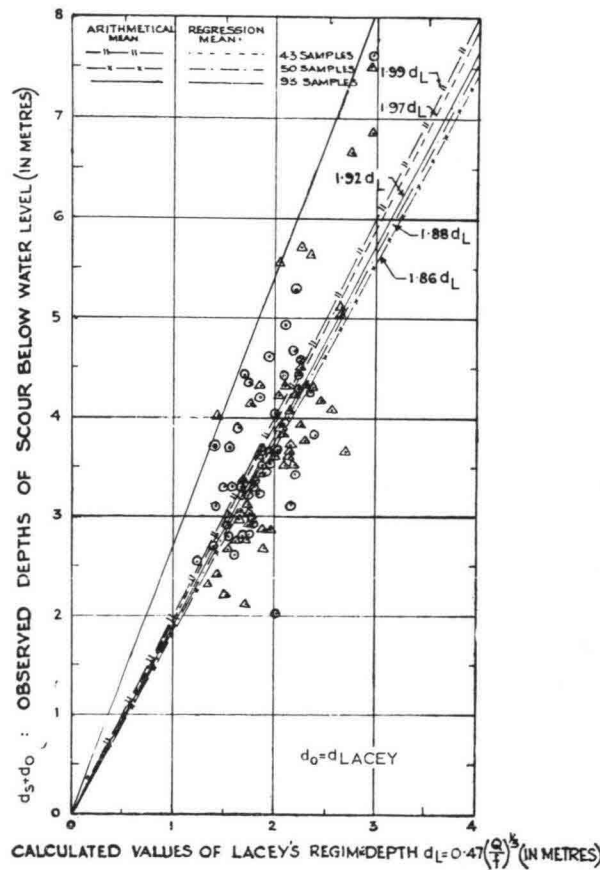


Fig. 26. Scour depth as a function of total discharge.

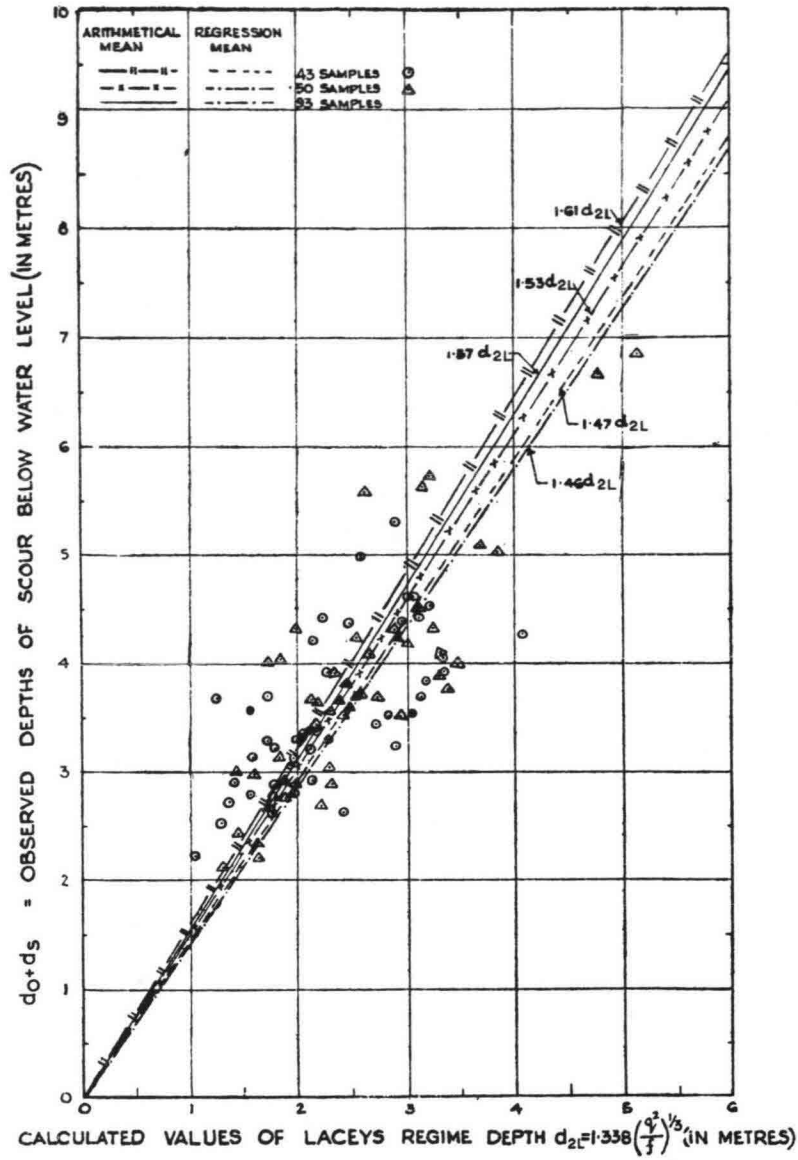


Fig. 27. Scour depth as a function of local discharge intensity.

It appeared that the effect of the silt factor was insignificant, so that the following relations were given:

$$(d_s + d_0) = 0.72Q^{0.33} \quad (32)$$

and

$$(d_s + d_0) = 2.31q^{0.37} \quad (33)$$

(*m*-units, r.m.s. value 16%, correlation coefficient 0.74 in both cases).

5.8 BREUSERS (1971) gave a comparison between the local scour measured in nature and in a model for the Onitsha Bridge on the Niger River. The piers consisted of two circular piles with a diameter of 8.5 m and a centre-line separation of 17 m. At a low stage of the river ($\bar{U} = 0.7$ m/s

$d_0 = 9$ m) scour was measured and reproduced in model tests (scale 1 : 53) under the condition that the scale of mean velocity and critical velocity for all fractions was equal. For the result see Fig. 15.

5.9 MELVILLE (1975) gave a literature review and compared the predictions with field data from New Zealand. The cases in which local scour depth was clearly defined are:

5.9.1 Tuakau Bridge, lower Waikato River. Data: mean depth 3.0 m, mean velocity 0.87 m/s, bed material $D_{15} = 0.38$ mm, $D_{50} = 0.78$ mm, $D_{85} = 2.09$ mm. The pier shape was rectangular with dimensions 8.85 by 2.44 m with chamfered corners and an angle of attack of 10% (estimated LAURSEN and TOCH correction factor 1.3). Maximum scour depth was estimated at 2.75 m but can have been greater in view of the limited number of depth observations.

5.9.2 Big Wanganui River Bridge. Mean water depth 3.8 m, mean velocity 4.27 m/s, bed material $D_{50} = 0.23$ m with $\bar{U}_c = 5.9$ m/s. The scour for a pier measuring 8.5 by 1.63 m at a supposed angle of attack of 10° (LAURSEN-TOCH factor 1.5) was estimated at 4.88 m.

5.9.3 Matawhera Railway Bridge. Water depth 3.0 m, mean velocity 2.25 m/s, bed material $D_{50} = 7$ mm, $\bar{U}_c = 1.12$ m/s. Estimated scour depth 4 m for a pier measuring 6.8 by 1.5 m (see Fig. 28). Maximum angle of attack was 45°, LAURSEN-TOCH correction factor 1.75.

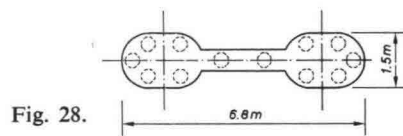


Fig. 28.

5.9.4 Bull's Bridge, Rangitikei River. The river bed was composed of a shingle surface stratum ($D_{50} = 11$ mm) overlying a thin layer of silty clay and a thick layer of fine river sand ($D_{50} = 0.15$ mm). This combination proved extremely dangerous with respect to scour. Once the upper layers were eroded, scour proceeded in the fine sand without an upstream supply. A scoured depth in the order of 12 m developed which caused the complete failure of the bridge. Water depth before scour was 2.7 m and mean velocity 2.8 m/s. Fine sediments underlying coarse sediments or less erodible layers are, therefore, a potential danger.

MELVILLE (1975) concluded from his study at the above four bridge sites that for *Clear Water Scour* Shen's Equation (18) for the equilibrium depth of scour forms an envelope to all the available experimental data and should be used for clear water scour at bridge piers. For *Sediment-transporting Scour* Laursen's relationship appears to be reliable. For flows in which the Froude number is greater than 0.5, the larger of the scour depths given by Laursen and Shen's Equation (19) should be used. MELVILLE apparently misquoted Shen's Equation (19). However, using the corrected equation, it was found that the results were in even better agreement with Melville's field data.

5.10 NORMAN (1975) collected and analyzed depths of scour around piers at seven bridge sites in Alaska, U.S.A., plus four other bridge sites, and found that all scour depths were below the curve $d_s = 3b^{0.8}$. The two largest scour depths were about 7 meters.

6 Comparison of data with dimensional analysis and theoretical work, and influence of parameters

A theory in the sense of a complete model for computing the velocity field and the related local sediment-transport rate in the scouring hole has not yet been developed, mainly because the flow field is too complicated. Some attempts have, indeed, been made (TARAPORE (1962), GRADOWCZYK (1968), ZAGHLOUL (1975) and others), but they can only be considered as explanatory in view of the underlying assumptions.

An analysis of experimental data, with dimensional analysis as some kind of framework, seems, therefore, the only possibility to derive general relationships. The dimensional analysis resulted in a relation of the form:

$$\frac{d_s}{b} = f\left(\frac{\bar{U}}{\bar{U}_c}, \frac{D}{b}, \frac{d_0}{b}\right) \quad (5)$$

neglecting the influence of shape, Froude number, bed-material density and gradation. In this chapter the influence of various parameters and other factors is discussed.

6.1 Influence of \bar{U}/\bar{U}_c

From the results of various investigations a reasonable picture of the influence of this parameter can be obtained. The following regimes may be distinguished:

- a. $\bar{U}/\bar{U}_c \leq 0.5$ – no scour (see HANCO 1967, NICOLLET 1971a, b)
- b. $0.5 \leq \bar{U}/\bar{U}_c \leq 1.0$ – clear water scour. In this interval some investigators found that the scour depth increases almost linearly with \bar{U} . (See Fig. 8 for $D = 3$ mm (CHABERT and ENGELDINGER 1956), Fig. 17 (HANCO 1967), and Fig. 18 (MAZA 1968)). The function:

$$d_s/d_{sm} = (2\bar{U}/\bar{U}_c - 1) \quad (13)$$

given by HANCO is a good approximation in this interval. The limiting scour depth is approached slowly (Fig. 6).

- c. $\bar{U}/\bar{U}_c \geq 1.0$ – scour with sediment motion. Here scour depth does not increase further with velocity, apparently because the dynamic equilibrium between transport out of the scouring hole and the supply is not influenced by the magnitude of the transport rate. Sometimes a slight decrease of d_s with \bar{U} is observed. Scour depth fluctuates with time due to the influence of moving bed forms (Fig. 7). The limiting scour depth is defined here as the time-averaged value (NEILL 1964a). The maximum d_{sm} is defined as the maximum with respect to velocity. For most practical problems an estimate of d_{sm} is sufficient because in a natural river the condition $\bar{U}/\bar{U}_c \geq 1.0$ will almost certainly be met during floods. Therefore further discussions will be concentrated on d_{sm} .

6.2 Influence of D/b

NICOLLET (1971a, b) reported systematic tests with a large variation in grain size, and the results were interpreted as giving an influence of D/b . If the results are replotted as d_s against D for constant b and d_0 , it follows that scour depth is a function of D (Fig. 19). The influence of b is mainly due to a simultaneous variation of d_0/b (d_0 was constant and equal to 0.2 m in most tests). Maximum scour depth as a function of grain size occurred at $D = 2$ mm.

LAURSEN and TOCH (1956) did not observe an influence of D for $D = 0.5$ to 5 mm.

The results by BONASOUNDAS also show some increase of scour depth with increasing grain size in the range 0.6 to 3.3 mm.

The results of ETTEMA (1976) for $\bar{U}/\bar{U}_c \approx 1.0$ show some increase of d with D (uniformly graded) upto $D \approx 4$ mm, as can be seen from the following table:

D_{50} (mm)	0.55	0.70	0.85	1.9	4.1	6.0
d_s/b	1.45	1.75	2.0	2.05	2.2	2.1

In conclusion, it may be stated that the influence of grain size is limited for single particle size sediment. The main effect of D/d_0 is the influence on the velocity profile which is a function of this parameter. An increase in velocity gradient (with increasing D/d_0) will increase the strength of the vortex system, as has been shown by TISON (1940).

6.3 Influence of d_0/b

This factor gives the most conflicting statements. The following schools may be distinguished:

- a. The regime theory which gives the scour depth as a function of the regime water depth. As an example the Inglis relation is taken:

$$d_s \approx d_{Lacey} = 0.473(Q/f)^{\frac{1}{3}} \quad (27)$$

- b. Modification of this type of relation to introduce some effect of d_0/b , for example, ARUNUCHALAM (1965):

$$d_s/d_r = 1.95(b/d_r)^{\frac{1}{3}} - 1 \quad (d_0 = d_r = \text{regime depth}) \quad (30)$$

or BLENCH:

$$d_s/d_r = 1.8(b/d_r)^{\frac{1}{3}} - 1 \quad (7)$$

- c. Relationships expressing d_s/b as a function of b/d_0 :

LAURSEN and TOCH (1956), NEILL (1965):

$$d_s/b = 1.5(d_0/b)^{0.3} \quad \text{for rectangular piers} \quad (11)$$

This relation was also given by VEIGA DA CUNHA (1970):

$$d_s/b = 1.35(d_0/b)^{0.3} \quad \text{for circular piers} \quad (34)$$

HANCO (1971):

$$d_s/b = 3.3(D/b)^{0.2}(d_0/b)^{0.13} \quad (16)$$

- d. Relations giving scour depth as a function of pier diameter:

$$\text{LARRAS (1963)} \quad d_s = 1.05b^{0.75} \quad (\text{m-units}) \quad (12)$$

$$\text{SHEN (1969a)} \quad d_s \sim b^{0.619} \quad (\text{for constant } \bar{U}) \quad (18)$$

$$\text{BREUSERS (1965)} \quad d_s = 1.4b \quad (\text{circular piers}) \quad (35)$$

$$\text{BARAK (1975)} \quad d_s = 0.558b^{0.586} \quad (\text{rectangular piers}) \quad (25)$$



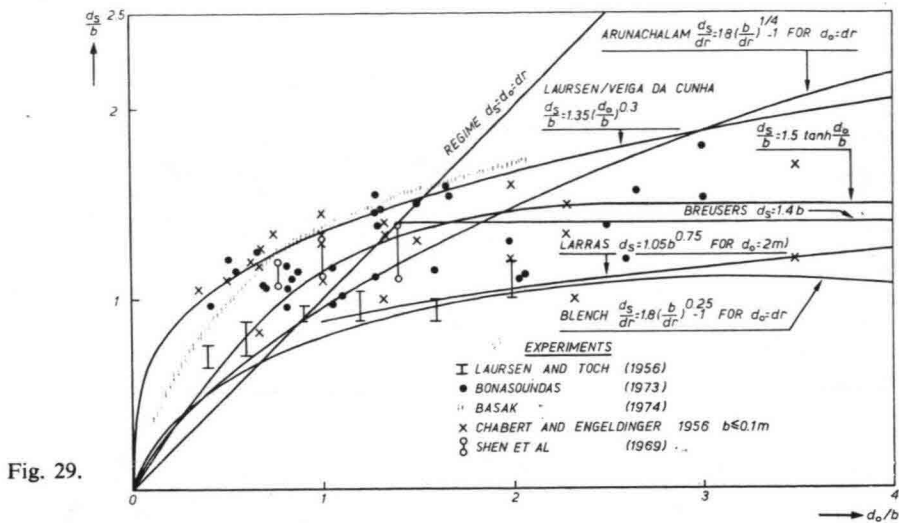


Fig. 29.

The experimental evidence is compared with some of these expressions in Fig. 29. The results of LAURSEN were scaled with the effective width (0.6 ft) instead of the real width (0.2 ft) because a pier under an angle of 30° was used ($k_a = 2.5$), and they were also corrected for pier shape (1.1). The results of BASAK were also reduced with a factor 1.2 because rectangular piers were used in the experiments.

Many authors state that the influence of water depth can be neglected for $d_0/b > 1$ or 2. It is not clear whether this is due to the experimental set-up (not fully developed velocity profiles or inlet conditions). Also the influence of simultaneously testing more piers (CHABERT and ENGELDINGER) is not clear. From the experimental results it may be concluded, however, that for $d_0/b > 3$ the influence of this parameter can be neglected. For smaller values some empirical relation is necessary. The following relation gives a good description for the full range of d_0/b :

$$d_s/b = 1.5 \tanh \frac{d_0}{b} \tag{36}$$

For $d_0/b \rightarrow 0$ the relation over-estimates the scour depth if compared to the regime theory, but experiments also point to higher d_s/b values for $d_0/b = 0.4$ to 1.

Relations of the type *b* and *c* and BREUSERS (1965) satisfy the basic linear relationship between scour depth and pier dimension for geometric similarity. This linear relation is considered essential for model studies and is stressed by LAURSEN and TOCH (1956) in these words:

“On the basis of all the accumulated evidence, both laboratory and field, it appears that the depth of scour can be regarded as a function of the geometry alone, and that the scour depth can be treated like any other length in the comparison of model and prototype” (under the condition d_0/b is constant).

NEILL (1964a) puts it this way:

“The available evidence suggests that if the pier dimension and depth of flow are scaled up uniformly, then the scour depth may be scaled up by approximately the same factor” (also for constant d_0/b).

These statements are only valid, of course, under the condition that $\bar{U}/U_c \geq 1.0$.

6.4 Shape of the pier

TISON (1964) showed qualitatively that scour around piers can be affected by the curvature of streamlines. SHEN, SCHNEIDER and KARAKI (1969) classified pier shapes in two categories:

- (i) Blunt-nosed pier where a strong horseshoe-vortex system and thus the maximum scour depth occur at the pier nose. The upstream pier shape should have a strong influence on the scour depth, and the length of the pier and downstream pier shape should have a minimum effect if the blunt-nosed pier is aligned with flow.
- (ii) Sharp-nosed pier, where the horseshoe-vortex system is very weak and the maximum scour depth occurs near the downstream end. For long piers under an angle of attack the point of maximum scour depths shifts towards the downstream end of the pier (LAURSEN and TOCH, 1956, MAZA ALVAREZ, 1968).

The effect of pier shape on scour depth is significant, and some important studies have been conducted by FLAMANT (1900), REHBOCK (1921), YARNELL and NAGLER (1931), KEUTNER (1932), TISON (1940), ISHIHARA (1942), SCHNEIBLE (1951), LAURSEN and TOCH (1956), CHABERT and ENGELDINGER (1956), ROMITA (1960), KNEZIVIC (1960), VARZELIOTIS (1960), LARRAS (1962), MAZA and SANCHEZ (1964), PAINTAL and GARDE (1965) and SHEN and SCHNEIDER (1970). CHABERT and ENGELDINGER (1956) tested scour around six pier shapes (shown in Fig. 30). See also Fig. 10.

Their results indicate that (i) Group 1 for shapes 1, 2, 4 and 6 have approximately the same maximum scour depths for correspondingly the same flow conditions; (ii) the maximum scour depths for shape 3 were between 33% to 86% of that for the same corresponding flow velocities of Group 1 (with greater scour depths ratios for greater corresponding flow velocities); and (iii) the maximum scour depths for shape 5 varied between 50% to 100% of that for the same corresponding flow velocities for Group 1 (with greater scour depths ratios for greater flow velocities).

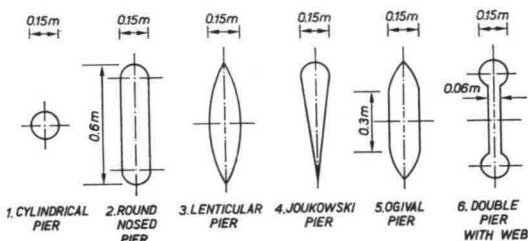


Fig. 30.

NOSE FORM	LENGTH-WIDTH	SHAPE	SHAPE COEFFICIENT
RECTANGULAR			1.00
SEMICIRCULAR			0.90
ELLIPTIC	2:1		0.80
	3:1		0.75
LENTICULAR	2:1		0.80
	3:1		0.70

Fig. 31.

PAINTAL and GARDE (1956) observed that the upstream nose of the pier plays an important part in the phenomenon of scour and that the rear of the pier had no effect. Some of their tests were conducted on piers with upstream triangular noses having different apex angles (15° to 180°), and their results indicated that maximum scour depth increased with increasing apex angles. They also found that the length of pier has a negligible effect on maximum scour depths for their pier shapes with a sediment size of 2.5 mm (the pier was aligned with flow direction).

LAURSEN (1960) found that the shape coefficient (defined as the ratio between scour depth of a particular shape to that of the rectangular shape) varies with the shape of pier as shown in Fig. 31.

SHEN and SCHNEIDER (1970) tested nine pier shapes and found that (i) maximum scour depth occurred at the downstream end of a sharp-nosed pier with a wedge nose angle of 30° , (ii) a rectangular pier with roughened upstream face and roughened horizontal apron seemed to have no

effect on scour, and (iii) a rectangular pier on a flat footing supported on piers with a vertical lip around the edge of the footing is an effective device for reducing scour (40–50%) if the top of the flat footing with vertical lip is placed at the proper elevation (see also Para. 7).

A pier consisting of two or more circular piers seems to be an attractive one where there is an appreciable angle of attack (CHABERT and ENGLEDINGER 1956). According to DIETZ, who made systematic tests with a system of 2 circular piers, d_{sm} is not influenced by the angle of attack for centre-line spacings larger than $3b$.

Taking together all evidence, it is concluded that if the circular or the round-nosed pier is taken as a reference, a reduction in the order of 25% in scour depth can be obtained by streamlining the pier, although his positive effect disappears for angles of attack larger than 10 to 15°. On the other hand, a rectangular pier gives 20 to 40% more scour than the reference pier.

6.5 Influence of angle of attack

The influence of an angle of attack has been studied by LAURSEN and TOCH (1956). See Fig. 32 for an empirical relation for k_α , which is the ratio of scour depth at an angle of attack α to that at a zero angle of attack. The results of CHABERT and ENGLEDINGER (1956) for $l/b = 4$ (see Fig. 10) and VARZELIOTIS (1960) for $l/b = 6$ (both rounded piers) are also given in this figure. It may be concluded that the LAURSEN and TOCH relation gives a good estimate for k_α . Some authors have proposed the use of the projected width in their formulas (ARUNACHALAM (1965) and BARAK (1974), but this gives an overestimate in most cases.

For piers consisting of circular piers with a spacing of more than $3b$ (DIETZ 1973) and, of course, for a single circular pier, no influence of an angle of attack has to be considered.

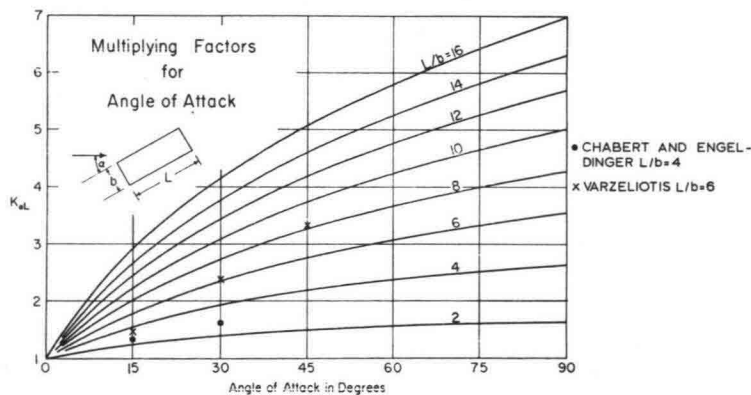


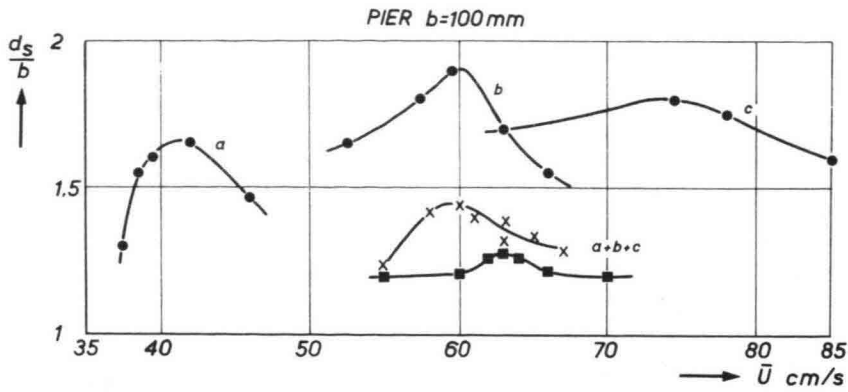
Fig. 32.

6.6 Influence of sediment particle distribution

To determine the influence of sediment particle size distribution, a series of tests were conducted by RAMETTE and NICOLLET (1971) with the same hydraulic conditions and the same circular piers as those used for tests with uniform bed materials. The sand for these tests was a 33% mixture of the sands a, b and c previously used, giving a rather straight grading curve between 0.8 and 3.2 mm.

Experimental data on scouring depth limits are presented as a function of flow velocity in Fig. 33, for a pier with a 10 cm diameter. Tests with materials of uniform size carried out for velocities

Fig. 33.



SAND OF UNI-FORM TEXTURE	●—●	TEST WITHOUT NOURISHMENT	SAND	SIEVE SIZES mm	
			a	b	c
			a	0,77-1,12	0,94
			b	1,62-2,24	1,93
			c	2,77-3,17	2,97
SAND MIXED TEXTURE	X—X	WITHOUT NOURISHMENT	SAND MIXTURE 33% a + 33% b + 33% c		
	■—■	WITH NOURISHMENT			

near incipient movement did not show any significant change in the bed upstream of the pier, and it was therefore not necessary to feed bed load in the channel. For the mixture, the flow velocities corresponded to an intense movement of the fine elements with the formation of dunes in certain cases. Two series of tests were conducted: the first one with additional sediment ensuring the stability of the bed upstream, and the other without any feeding. The scouring depth was measured in all cases with respect to the mean level of the bed upstream.

In Fig. 33, it can be seen that:

- For the mixture, the maximum scouring is obtained for a flow velocity in the vicinity of the velocity giving the maximum scouring for the component *b* alone;
- the maximum scouring depth limit for the mixture is about 25% smaller than those obtained with each of the components taken separately;
- in the case of the mixture, the variation in scouring depth for the flow velocities giving a significant bed load transport is always far below the limit values of d_s obtained with the components of the mixture; and
- the scouring depths are greater in the absence of solid addition upstream, i.e., when the bed load is provided only by the materials in place.

These results tend to demonstrate that the values of d_s around the beginning of bed load transport for a material of uniform gradation cannot be exceeded if a certain particle size gradation is considered and that this conclusion is independent of the flow conditions.

ETTEMA (1976) also studied the influence of bed material gradation on local scour, and found that for σ/D_{50} ratios above 0.3 scour depth decreases dramatically with σ/D_{50} (σ = standard deviation of grain size distribution). These experiments were done at or slightly below the critical velocity, so that no general conclusions can be drawn. The reduction in scour depth is due to armouring effects in the scouring hole.

6.7 Influence of bed material density

Several authors have carried out experiments with various bed material densities (NICOLLET (1971a) and DIETZ (1972)) under identical conditions. The conclusion of these experiments is that the density only has an influence on the maximum scour depth. There is some tendency for scour depth to increase with decreasing bed material density for identical \bar{U}/\bar{U}_c , but the use of low material densities in model tests seems to be possible in cases where reproduction of a Froude number is necessary.

6.8 Influence of flow duration

The limiting scour depth, on which this Report concentrates, will be reached only during floods of a sufficiently long duration. For very short floods time may be important, because maximum scour will occur on the receding flood. At this stage the river bed has been lowered to its lowest level and with decreasing flow the general sediment transport is already greatly reduced so that clear-water scour conditions prevail. Here the rate of scour development can have an important influence on the maximum scour depth (RAUDKIVI, 1976, personal communication).

7 Scour protection

After making the best choice of the pier shape for minimizing scour, additional arrangements can be considered to prevent the formation of the scour hole, thereby permitting smaller foundation depths. In the final analysis, it is the cost criterion which will allow a decision as to the suitability of these arrangements.

The main scour protection systems which have yielded valid results are a caisson placed around the pier and whose top is under the average level of the river bed, additional structures such as small piles placed above the main pier, and mats of riprap (see Fig. 34).

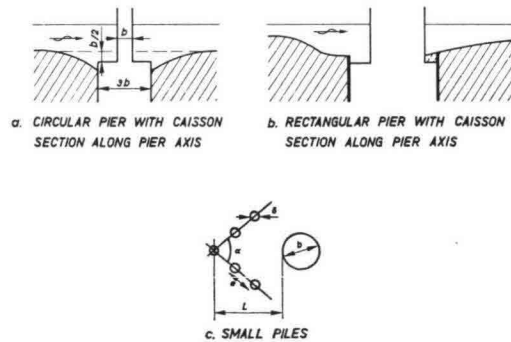


Fig. 34.

7.1 Foundation caisson

Engineering requirements may call for the founding of the pier on a caisson of larger dimensions. In this field, CHABERT and ENGELDINGER (1956) investigated a circular pier founded on a circular caisson. Tests in an experimental channel enabled them to conclude that the best system appeared to be a caisson having a diameter three times the diameter of the pier, and a top elevation about half the diameter of the pier below the natural bed. This would reduce scour to only one-third of that reached with the pier alone.

SHEN and SCHNEIDER (1970) investigated a variant of the caisson system in which the caisson is surrounded by a vertical lip (cut-off sheet-pile). The main idea was to contain the horseshoe-vortex inside an enclosure allowing it to escape downstream. These tests were conducted on rectangular piers, and under the optimum conditions of overall dimensions, it was possible to obtain a bed level corresponding to the lip, above and on the sides of the pier, and even to get an accretion downstream.

This system made it possible to reduce scour by half. However, the dimensions of the platform and of the lip in relation to the pier and to the other parameters (flow and sediment) were not examined in a sufficiently systematic manner to enable general laws to be formulated on the valid dimensions in the general case. The lip certainly allows a reduction in the dimensions of the caisson. Reduction of scour depth up to 50% can be obtained by placing a horizontal flat plate with a diameter of at least 3 times the pier diameter some distance (0.3 to 0.4D) below the undisturbed bed level (see CIABERT and ENGELDINGER 1956, TANAKA 1969, THOMAS 1967).

7.2 Additional structures placed upstream: piles

Additional structures are sometimes provided to protect the bridge piers from collision with floating bodies: example of dolphins on navigable waterways.

CIABERT and ENGELDINGER (1956) investigated the installation of small piles above the pier itself, the main purpose being to break the incident current and in this way weaken the vortex generating the erosion.

A large number of parameters are necessary for the definition of such a structure: n piles of diameter δ , spaced e from each other, open according to the angle α and a distance L from the pier (five parameters). No general law could be formulated concerning such a system, but laboratory tests have made it possible to observe scour reductions as high as 50%. Similar reductions were mentioned by LEVI and LUNA (1961) for a vertical strip placed at $2b$ upstream of an rectangular pier. The optimum width of the strip was equal to the pier width b .

It must be mentioned, however, that all these constructions were not tested under general conditions, so for practical applications special tests are advised.

7.3 Riprap mats

The most usual method for remedying erosion is the dumping of stones into the scour hole. Many authors have examined this problem (see list in H. W. SHEN "River Mechanics", 1972) and have made recommendations regarding the choice of materials. Experience has shown that this type of protection is the only one allowing scour to be totally prevented.

CARSTENS (1966) used the fact that the maximum velocity around the cylinder in two-dimensional flow is approximately twice the velocity in undisturbed flow in order to state that the flow velocity giving the initial scour at the base of the pier must be half that corresponding to general bed load movement. The tests of S. HANCU (1971), confirmed by RAMETTE and NICOLLET (1971), have in fact shown that for a given sediment scour begins to appear at the foot of a circular pier at a flow velocity equal to half the critical velocity, irrespective of the diameter of the pier. These results make it possible to determine the weight of riprap capable of preventing any scour. In fact, in a river where the extreme flood velocity is \bar{U}_{\max} , it is enough to place boulders whose critical velocity is $\bar{U}_c = 2\bar{U}_{\max}$. Velocities are defined here as mean-on-vertical values.

The diameter of the boulders D as a function of \bar{U}_c can be determined, for example, by means of the ISBASH (1935) formula:

$$\bar{U}_c = 0.85 \sqrt{2g \frac{\rho_s - \rho}{\rho} \cdot D} \quad (37)$$

where ρ_s and ρ denote the specific weight of the boulders and of the water. For $\rho_s = 2650 \text{ kg/m}^3$ this reduces to $\bar{U}_c \approx 5\sqrt{D}$ (m-units), which covers also the data given by MAZA and SANCHEZ (1964) and NEILL (1973).

The horizontal dimensions of the protection to prevent any scour should be at least 2 times the width of the pier measured from the face of the pier. For the thickness it is suggested to take at least three times the diameter of the stone. A good inverted filter is necessary to prevent leaching of the bed material (POSEY, 1974). The top of the protection should be at some distance below the normal bed level to prevent excessive exposure.

7.4 Conclusion

Although valid results can be obtained by means of foundation caissons below the bed level or by means of piles placed upstream of the main pier, no general law as yet enables the dimensions of these protective structures to be determined.

On the other hand, an effective method of preventing any scour consists of providing a riprap protection in which the stone dimensions, stone gradation and the location for protection can be evaluated by estimating the river flow velocity.

8 Practical aspects for design

From the material presented it is concluded that the scour depth may be described by a function of the form:

$$\frac{d_s}{b} = f \left\{ \frac{\bar{U}}{\bar{U}_c}, \frac{d_0}{b}, \text{shape, angle of attack} \right\} \quad (38)$$

For practical applications the following relation is suggested:

$$\frac{d_s}{b} = f_1 \left(\frac{\bar{U}}{\bar{U}_c} \right) \cdot \left[2.0 \tanh \left(\frac{d_0}{b} \right) \right] \cdot f_2(\text{shape}) \cdot f_3 \left(\alpha, \frac{l}{b} \right) \quad (39)$$

(the constant has been taken as 2.0 instead of 1.5 to be on the safe side).
in which

$$\begin{aligned} f_1 \left(\frac{\bar{U}}{\bar{U}_c} \right) &= 0 \quad \text{for} \quad \frac{\bar{U}}{\bar{U}_c} \leq 0.5 \\ &= \left(2 \frac{\bar{U}}{\bar{U}_c} - 1 \right) \quad \text{for} \quad 0.5 \leq \frac{\bar{U}}{\bar{U}_c} \leq 1.0 \\ &= 1 \quad \text{for} \quad \frac{\bar{U}}{\bar{U}_c} \geq 1.0 \end{aligned} \quad (40)$$

f_2 (shape) = 1.0 for circular and rounded piers
 = 0.75 for stream-lined shapes
 = 1.3 for rectangular piers

f_3 ($\alpha, l/b$) – see Fig. 32

Suggestions for bottom protections to decrease the scour depth have been given in Chapter 7. Generally speaking a flexible protection at some depth below the normal river bed will give the best results. The necessary stone size for a given maximum mean velocity \bar{U}_{\max} can be obtained from:

$$\bar{U}_{\max} = 0.5\bar{U}_c = 0.42 \sqrt{2g \frac{\rho_s - \rho}{\rho} \cdot D} \quad (41)$$

A good filter construction is necessary.

Rigid footings should be designed carefully and be placed at some depth below the level of general scour.

If the footing is exposed to the flow, scour depth will increase due to the greater effective width.

Attention had to be given to the following special effects:

- *Debris and ice* can increase the effective size of the piers and therefore the local scour.
- *Flash floods* can give a greater scour depth because of unsteady transport conditions. Also non-monsoon floods can give relatively large scour depths (Min. of Railways India, 1968). LAURSEN and TOCH (1956) suggest a 50% increase in design scour depth.
- *Dunes and sand waves* can change the angle of attack and increase the local depth near the pier. SHEN, SCHNEIDER and KARAKI (1969) suggest adding 50% of the dune height to scour depth.
- *A cohesive upper layer* can be disturbed near the pile and cause an increase in scour depth because upstream supply is not present (MELVILLE 1975). The same effect is caused by vegetation in a dry period.
- *General scour* due to degradation, contraction, shifting channels, or bed level variations during floods has to be added to the local scour near the piers (see for example, NEILL 1973).
- Intensive *suspension* of sediment in large fine-bed rivers may invalidate the empirical relations.
- *Bad placement of riprap* can provoke scour.

9 Discussion, research needs

Although it has been possible here to present a wealth of experimental data and useful design relations have been developed, it cannot be said that all aspects of local scour near bridge piers have been cleared up. Theoretical developments are limited, and there is not much hope for a rapid success in this complicated interaction of flow field and sediment transport. More experimental data for large diameters piers ($b > 0.5$ m) in the full range of water depths ($d_0/b = 0.5$ to 4) and sufficiently large flow velocity would be helpful to test the relations given.

Also prototype data are needed to improve the relations developed on the basis of model experiments. The data would have to give all relevant information on geometry, bed material and flow field, and are therefore difficult to obtain because maximum scour depth will occur during floods.

It is hoped that the present Report will encourage comprehensive studies on large-scale models. Perhaps certain sites could be selected for more precise data collection, while other secondary field sites could be chosen from which to obtain order-of-magnitude estimates on scour depth.

Acknowledgement

The assistance of Prof. A. J. RAUDKIVI and Mr. C. R. NEILL in reviewing the manuscript and giving suggestions for improvement is gratefully acknowledged.

References

Bibliographie

- ARUNACHALAM, K., 1965, Scour around bridge piers; J. of the Indian Roads Congress (No. 2), August, pp. 189/210.
- ARUNACHALAM, K., 1967, Discussion to Neill (1965); Proc. Inst. Civ. Eng., London, **36**, pp. 402/404.
- BAINES, W. D., 1965, Effect of velocity distribution on wind loads and flow patterns on buildings; Wind effects on buildings and structures; Vol. 1, H.M.S.O. London, England, pp. 197/224.
- BASAK, V., Y. BASAMISLI and O. ERGUN, 1975, Maximum equilibrium scour depth around linear-axis square cross-section pier groups (in Turkish). Devlet su isteri genel müdürlüğü, Rep. No. 583, Ankara.
- BATA, C., 1950, Erezija eke novesadskeg mastorskog stube (scour around bridge piers), Inst. za Vodoprivedu, Jaroslav Cerni Beograd, Yugoslavia.
- BONASOUNDAS, M., 1973, Strömungsvorgang und Kolkproblem; Diss. T.U. München (Bericht no. 28, Versuchsanstalt für Wasserbau, T.U. München).
- BREUSERS, H. N. C., 1965, Scouring around drilling platforms; Hydr. Res. 1964/65, IAHR Bulletin, **19**, p. 276.
- BREUSERS, H. N. C., 1970, Discussion on Shen et al (1969); Proc. ASCE, **96**, HY 7, pp. 1638/1639.
- BREUSERS, H. N. C., 1971, Local scour near offshore structures; Proc. Symp. on Offshore Hydrodynamics, Wageningen, 1971, (also Delft Hydraulics Laboratory Publication No. 105).
- CARSTENS, M. R., 1966, Similarity laws for localized scour; Proc. ASCE **92**, (HY 3), pp. 13/36.
- CARSTENS, T. and H. R. SHARMA, 1975, Local scour around large obstructions; Proc. 16th IAHR Congress, Sao Paulo, **2**, pp. 251/262.
- CHABERT, J. and P. ENGELDINGER, 1956, Etude des affouillements autour des piles de ponts; Lab. Nat. d'Hydr. Chatou, Octobre.
- CHITALE, S. V., 1960, Discussion on Laursen (1960); Trans. ASCE, **127**, pp. 191/196.
- COLEMAN, N. L., 1971, Analyzing laboratory measurements of scour at cylindrical piers in sand beds; Proc. 14th IAHR Congress, Paris, **3**, pp. 307/313.
- VEIGA DA CUNHA, L., Discussion to Shen et al (1969); Proc. ASCE, **96**, (HY 8), pp. 1742/1747.
- DALTON, C. and F. D. MASCH, 1968, Influence of secondary flow on drag forces; Proc. ASCE, **94**, (EM 5).
- DIETZ, J. W., 1972, Ausbildung von langen Pfeilern bei Schräganströmung am Beispiel der BAB-Mainbrücke Eddersheim; Mitt. blatt der Bundesanstalt für Wasserbau, Karlsruhe, (No. 31), pp. 79/94.
- DIETZ, J. W., 1973, Kolkbildung an einem kreiszylindrischen Pfeilerpaar; Die Bautechnik, **50**, 1973 (6), pp. 203/208.
- DURAND CLAYE, A., A., 1873, Expériences sur les affouillements; Ann. des Ponts et Chaussées, 1er semestre, p. 467.
- ETTEMA, R., 1976, Influence of bed material gradation on local scour. M. Eng. Thesis. Univ. of Auckland, School of Engineering, Rep. no. 124, Auckland, New Zealand.
- FLAMANT, A., 1900, Hydraulique, Paris, Béranger, pp. 281/282.
- GRADOWCZYK, M. H., O. J. MAGGILOLO and H. C. FOLGUERA, 1968, Localized scour in erodible bed channels; J. Hydr. Res., **6** (4), pp. 289/334.
- HANCO, S., 1971, Sur le calcul des affouillements locaux dans la zone des piles de ponts, Proc. 14th IAHR Congress, Paris, **3**, pp. 299/313.
- HINCU, S., 1965, Cu privire la calculul a fuierilor locale in zona pilelor podului; Hidrotehnica, Gospodăria Apelor, Meteorologia, **10** (1), pp. 9/13.
- Highway Research Board, 1970, Scour at bridge waterways; Nat. Acad. of Sciences, Washington.
- HJORTH, P., 1975, Studies on the nature of local scour. Dept. of Water Resources Eng. Univ. of Lund, Bull series A, No. 46.
- HUNG, C. S., 1968, A preliminary study on the resistance of cylinders in open channel flow: unpublished report, Colorado State University.
- INGLIS, C. C., 1949, The behaviour and control of rivers and canals; Chapter 8, C.W.I. & N., Research Station Poona, Res. Publ. 13.
- ISHIHARA, T., 1942, Experimental study of scour at bridge piers (in Japanese); Trans. Jap. Soc. of Civ. Eng., **28** (11), pp. 974/1007.
- ISBASH, S. V., 1935, Construction of dams and other structures by dumping stones into flowing water; Trans. Res. Res. Inst. Hydrot. Leningrad, **17**, pp. 12/66.

- KEUTNER, C., 1932, Strömungsvorgänge an Strompfeilern von verschiedenen Grundrissformen und ihre Einwirkung auf die Flüss-sohle; *Die Bautechnik*, **10**, (12), März.
- KNEZERIA, B., 1960, Prilog proucaranju erozije oko mostovskih stubova; *Inst. za vodoprivedu. Jaroslav Cerni Beograd, Yugoslavia.*
- LARRAS, J., 1960, Recherches expérimentales sur l'érosion au pied d'une pile de pont; *C. R. Acad. Sciences*, **251** (3) pp. 330/331.
- LARRAS, J., 1963, Profondeurs maximales d'érosion des fonds mobiles autour des piles en rivière; *Ann. Ponts et Chaussées*, **133** (4), pp. 411/424.
- LAURSEN, E. M. and A. TOCH, 1953, A generalized model study of scour around bridge piers and abutments; *Proc. IAHR Int. Hydr. Conf., Minnesota*, pp. 123/131.
- LAURSEN, E. M. and A. TOCH, 1956, Scour around bridge piers and abutments; *Bull. No. 4, Iowa Highway Res. Board.*
- LAURSEN, E. M., 1960, Scour at bridge crossings; *Proc. ASCE*, **86**, (HY 2), pp. 39/54 (also 1962, *Trans. ASCE*, **127** (1), p. 166/209).
- LAURSEN, E. M., 1970, Bridge design considering scour and risk; *Proc. ASCE* **96**, (TE 2), pp. 149/164.
- LECLERC, J. P., 1971, Recherches des lois régissant les phénomènes d'affouillement au pied des piles de pont. Premiers résultats; *Proc. 14th Int. IAHR Congress*, **3**, pp. 323/330.
- LEVI, E. and H. LUNA, 1961, Dispositifs pour réduire l'affouillement au pied des piles de pont; *Proc. 9th IAHR Congress, Dubrovnik*, pp. 1061/1069.
- MATTINGLY, G. E., 1962, An experimental study of the three-dimensionality of the flow around a circular cylinder; *Inst. of Fluid Dyn. and Appl. Math. Univ. of Maryland TN BN-295.*
- MAZA ALVAREZ, J. A. and J. L. SANCHEZ BRIBIESCA, 1964, Contribucion al estudio de la socavación local en piles de puente; *Universidade Federal do Rio Grande do Sul.*
- MAZA ALVAREZ, J. A. and J. L. SANCHEZ BRIBIESCA, 1966, Socavación y protección al pie de pilas de puente; *Segundo Congr. Latin-americano de Hidraulica, Caracas.*
- MAZA ALVAREZ, J. A., 1967, Erosión del cause de un rio por el cruce de un puente. *Ing. Hidr. en México*, **20** (1/2), pp. 93/106.
- MAZA ALVAREZ, J. A., 1968, Socavación en cauces naturales; *Inst. de Eng., Univ. Nac. de México, Publ. No. 177.*
- MELVILLE, B. W., 1975, Local scour at bridge sites, *Univ. of Auckland, School of Engineering, Auckland, New Zealand, Rep. No. 117.*
- Ministry of Railways, India, 1967, 1968, 1972, Scour around bridge piers; *Bridges and floods reports No. RBF 1, 2, 3.*
- MOORE, W. L. and F. D. MASCH, 1963, The influence of secondary flow on local scour at obstructions in a channel; *Proc. Federal Interagency Sed. Conf. Misc. Publ. No. 970*, pp. 314/320.
- NEILL, C. R., 1964a, Local scour around bridge piers; *Res. Council of Alberta, Highway and River Eng. Div.*
- NEILL, C. R., 1964b, River bed scour, a review for bridge engineers; *Res. Council of Alberta, Contr. No. 281* (also *Techn. publ. No. 23, Canadian Good Roads Assoc., reprinted 1970*).
- NEILL, C. R., 1965, Measurements of bridge scour and bed changes in a flooding sand-bed river; *Proc. Inst. Civ. Eng., London*, **30**, pp. 415/436, Discussion in **36** (1967), pp. 397/421.
- NEILL, C. R., 1967, Mean velocity criterion for scour of coarse uniform bed material; *Proc. 12th IAHR Congress Ft. Collins*, **3**, pp. 17/25.
- NEILL, C. R., 1970, Discussion on Shen et al (1969), *Proc. ASCE*, **96**, HY5.
- NEILL, C. R. (ed.), 1973, *Guide to bridge hydraulics*, Univ. of Toronto Press.
- NICOLLET, G. and M. RAMETTE, 1971a, Affouillements au voisinage de piles de pont cylindriques circulaires; *Proc. 14th IAHR Congress, Paris*, **3**, pp. 315/322.
- NICOLLET, G., 1971b, Déformation des lits alluvionnaires; affouillements autour des piles de ponts cylindriques, E.D.F., *Dep. Lab. Nat. d'Hydr., Chatou, HC/043/689.*
- NICOLLET, G., 1975, Affouillements au pied des piles de pont en milieu cohesif; *Proc. 16th IAHR Congress, Sao Paulo*, **2**, pp. 478/484.
- NORMAN, V. W., 1975, Scour at selected bridge sites in Alaska, *U.S. Geol. Survey Water Resources Div., Anchorage, Alaska.*
- PAINTAL, A. S. and R. J. GARDE, 1965, Effect of inclination and shape of obstruction on local scour; *Res. Journal, Vol. 8, Univ. of Roorkee, Uttar Pradesh, India.*
- PETRYK, S., 1969, Drag on cylinders in open channel flows; *Diss. Colorado State Univ. Ft. Collins, Colorado.*
- POSEY, C. J., 1949, Why bridges fail in floods; *Civ. Eng.*, **19**, pp. 42/90.
- POSEY, C. J., 1974, Tests of scour protection for bridge piers; *Proc. ASCE* **100**, HY12, Dec., pp. 1773/1783.
- REHBOCK, TH., 1921, Transformations wrought in stream beds by bridge piers of various shapes of cross sections and experiments on the scouring action of the circular piers of a skew railroad bridge across the Wiesent River for the Nürnberg Railroad; see *Hydraulic Laboratory Practice*, John R. Freeman, ed. ASME, New York, 1929
- ROMITA, P. L., 1960, Discussion on Laursen (1960); *Proc. ASCE*, **86**, HY9, pp. 151/152.

- ROPER, A. T., 1965, Wake region of a circular cylinder in a turbulent boundary layer; M.Sc. Thesis, Colorado State Univ. Ft. Collins, Colorado.
- ROPER, A. T., 1967, A cylinder in a turbulent shear layer; Diss. Colorado State University, Ft. Collins, Colorado.
- ROPER, A. T., V. R. SCHNEIDER and H. W., SHEN, 1967, Analytical approach to local scour; Proc. 12th IAHR Congress, Ft. Collins, 3, pp. 151/161.
- ROSHKO, A., 1961, Experiments on the flow past a circular cylinder at a very high Reynolds number; J. Fluid Mech., 10, pp. 345/356.
- SCHNEIBLE, D. E., 1951, An investigation of the effect of bridge-pier shape on the relative depth of scour; M.Sc. Thesis, Dept. of Mechanics and Hydraulics, Graduate Coll. of the State Univ. of Iowa.
- SCHWIND, R. G., 1962, The three-dimensional boundary layer near a strut; Gas turbine Lab. Rep. No. 67, Mass. Inst. of Techn.
- SHEN, H. W., V. R. SCHNEIDER and S. KARAKI, 1966a, Mechanics of local scour; Colorado State Univ., CER 66 HWS-VRS-SK22.
- SHEN, H. W., V. R. SCHNEIDER and S. KARAKI, 1966b, Mechanics of local scour; Supplement: Methods of reducing scour. Colorado State Univ., CER 66 HWS 36.
- SHEN, H. W., V. R. SCHNEIDER and S. KARAKI, 1969, Local scour around bridge piers; Proc. ASCE, 95, (HY6), pp. 1919/1940.
- SHEN, H. W. and V. R. SCHNEIDER, 1970, Effect of bridge pier shape on local scour; Prepr. No. 1238, ASCE Nat. Meeting on Transport Eng., Boston, Mass., July.
- SHEN, H. W., V. R. SCHNEIDER and S. KARAKI, 1971, Closure on Shen et al (1969); Proc. ASCE, 97, HY 9.
- SHEN, H. W., 1971, River Mechanics, Vol. 2, Chapter 23, Scour near piles; Ft. Collins.
- TANAKA, S. and YANO, M., 1967, Local scour around a circular cylinder; Proc. 12th IAHR Congress, Ft. Collins, 3, pp. 193/201.
- TARAPORE, Z. S., 1962, A theoretical and experimental determination of the erosion patterns caused by obstructions in an alluvial channel with particular reference to a vertical circular cylindrical pier; Ph. D. Thesis, Univ. of Minnesota.
- TAYLOR, E. S., 1965, The horseshoe-vortex; silent movie film, B/W-Nos-FM 020, Encyclopedia Britannica.
- THOMAS, A. R., 1962, Discussion on Laursen 1960; Trans. ASCE, 127 (1), p. 196/198.
- THOMAS, Z., 1967, An interesting hydraulic effect occurring at local scour; Proc. 12th IAHR Congress, Ft. Collins, 3, pp. 125/134.
- TISON, L. J., 1940, Erosion autour de piles de pont en rivière; Ann. des Travaux Publics de Belgique, 41 (6), pp. 813/871.
- TISON, L. J., 1961, Local scour in rivers; J. Geoph. Res., 66 (12), p. 4227/4232.
- TORSETHAUGEN, K., 1975, Lokalerosjon ved store konstruksjoner Modellforsøk (Norwegian); Vassdrags-og Havnelaboratoriet, Trondheim.
- VARZELIOTIS, A. N., 1960, Model studies of scour around bridge piers; M.Sc. Thesis Dept. of Civil Eng., Univ. of Alberta.
- VAUTIER, E. W., 1972, Flow around a cylindrical pier with scour hole formation; M.E. Thesis, Civil Eng. Dept. Univ. of Auckland, New Zealand.
- WHITE, W. R., 1975b, Scour around bridge piers in steep streams; Proc. 16th IAHR Congress, Sao Paulo, 2, pp. 279/284.
- WHITE, W. R., 1975b, The design of bridge piers for steep streams in Jamaica; H.R.S. Wallingford, EX 690.
- YARNELL, D. L. and F. A., NAGLER, 1931, A report upon a hydraulic investigation of North Carolina standard reinforced concrete bridge pier, No. P-401-R and modifications thereof; Iowa Inst. of Hydr., Res., Univ. of Iowa Iowa City.
- ZAGHLOUL, N. A. and J. A. MCCORDQUODALE, 1975, A stable numerical model for local scour; J. Hydr. Res. 13 (4), pp. 425/444.

RIJKSWATERSTAAT - DELTA DIRECTORATE
AND
DELFT HYDRAULICS LABORATORY

PUBLICATION NO. 64

CLOSURE OF ESTUARINE CHANNELS IN TIDAL REGIONS
BY

J.J. DRONKERS, H.N.C. BREUSERS, J.J. VINJÉ, W.A. VENIS, F. SPAARGAREN

JUNI 1967

SERIES 1 : FLUID MECHANICS

Group 16 . Unsteady motion: waves, tides, oscillations, etc. of fluids
Section 16.32: Tidal motion in river mouths and estuaries

SERIES 2 : EXPERIMENTAL HYDRAULIC RESEARCH

Group 28 : Experiments on movement of sediments
Section 28.80: Local scour-general

Closure of estuarine channels in tidal regions

I. Considerations on fluid motion in and around closure gaps

by dr. J. J. Dronkers

II. Two-dimensional local scour in loose sediments

by ir. H. N. C. Breusers

III. Local scour caused by vortex streets

by ir. J. J. Vinjé

IV. Behaviour of dumping material when exposed to currents and wave action

by ir. W. A. Venis

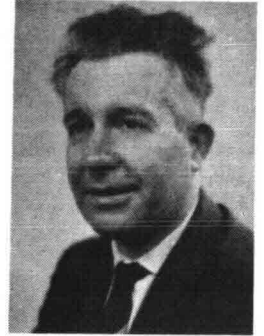
V. Results of model tests applied to an actual project

by ir. F. Spaargaren

Closure of estuarine channels in tidal regions¹⁾

I. Considerations on fluid motion in and around closure gaps

by dr. J.J. Dronkers



Summary: The closure of the final gaps is the most difficult part of the construction of the dams in the 'Delta plan' of the Netherlands. In this contribution various factors concerning the water motion in closure gaps are discussed in general terms. These factors are: the tidal motion in the region, the changes of velocities in and near the closure gap during the closure period, and the way in which they can be computed. Remarks are made about the interaction of water motion and soil mechanics.

1. Introduction

A primary consideration when closing an estuary is the interaction of water and soil. Fluid and soil mechanics figure prominently in studies on channel closures. For the fluid motion causes sediment transport which is followed by changes in the structure and pattern of the bedprofile, and this in turn affects the flow pattern. When a channel is closed the fluid motion in the area undergoes a drastic change, which affects the bed and sometimes also the sides of the channel. This influence does not only make itself felt at the surface but also in the deeper layers of the ground masses. Whenever changes in pore-water pressure occur in ground water as a result of changing levels of the bed and changes in water pressure, the ground-water may start moving. Consequently, changes will take place in effective stresses, which in turn may cause the ground masses to shift. This interplay of movements is of a complex nature. It would be a far less difficult subject if only we could get to know more about the soil properties that occur in a given situation. In this respect there is a great difference with the knowledge we can acquire of fluid motion. For water is a homogeneous substance, whereas soil as a rule is not. In soil properties, such as effective granular stresses, pore-water pressure and initial density, irregular changes may take place, and variations of this kind are very difficult to determine accurately by measurement. In the case of water it is the motion which interests us most and this can be measured sufficiently accurately to be of practical use. Micromotion, however, which occurs in turbulent fluid motion and which is of a statistical nature, is also difficult to determine with the required measure of precision.

As a result of our inadequate knowledge of soil properties, it is difficult to predict the interaction between fluid motion and

soil properties; consequently, we can never be certain about the effect of fluid motion on soil displacements during channel closures. This uncertain factor must be taken into account when planning channel closures and it is important that our studies be aimed at limiting this uncertainty as much as possible.

The main subject of this article, is determining the fluid motion during closure of a channel. Since lack of space does not permit of a more thorough analysis of studies on soil mechanics, we cannot do more than give some further general information regarding these studies at the end of the paper.

2. Remarks on tidal movement in general

When an estuary is to be closed off from the sea, or a dam is to be built splitting a tidal area into two parts – as is the case with the Volkerak and Grevelingen dams – it is necessary first of all to investigate how such a construction will affect the existing tidal movement (fig. 1). The boundaries of the area thus affected then determine the tidal area involved in the hydraulic calculations for closure. In the first place the initial and final fluid motion patterns must be studied, that is to say the pattern before and the pattern after construction of the barrier dam, followed in turn by the patterns that may be expected in the transition period.

The initial pattern must be determined as accurately as possible by measuring the vertical tide and the tidal velocities, after which tidal calculations can be made to determine the necessary hydraulic parameters or factors, such as Chézy's coefficient, and to verify and control the schematization. There are various methods of determining the final pattern, such as tidal computation, an electric model or a hydraulic model. To a greater or lesser degree, they are all based on a schematization of reality. In order to verify this schematization, tests also have to be made under the existing conditions. Tidal calculations and an electric model can then be regarded as a mathematical model in which all the determining factors are indicated in figures. In

¹⁾ Engelse weergave van de voordrachten gehouden tijdens het Symposium over 'Geulafsluitingen in Getijgebieden' onder auspiciën van de Afdeling voor Bouw- en Waterbouwkunde van het K.I.v.I. op 7 juni 1967 te 's-Gravenhage. Aangekondigd in *De Ingenieur* 1967, nr. 20, blz. A 317.

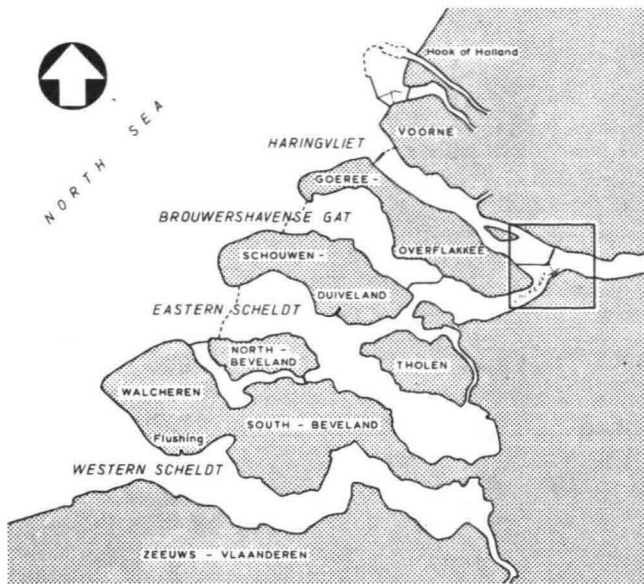


Fig. 1. Delta region, completed dams and dams under construction are denoted. The area within the square is given in greater detail in fig. 4.

the hydraulic model on the other hand, certain information, such as elements of resistance, can be inserted on a more experimental basis, and profiles of the channels can be reproduced in more detail, depending on the scale. In this way the model can reproduce the fluid motion at certain points more accurately than would be possible when using either of the former methods. For this reason several large-scale tidal models have been built at the Hydraulics Laboratory at Delft (horizontal ratio 1:300, vertical ratio 1:100). Such models are obviously very expensive and we must be sure that the details they produce are important enough for our research before deciding to build them.

For all practical purposes we are able to calculate the tidal motion accurately enough in rivers and channels. We refer to such calculations as one-dimensional, disregarding the dimension of time. Our knowledge and experience of how to compute the tides in a sea area, which is of a two-dimensional nature on the horizontal plane, is increasing rapidly. A new method has been developed by Leendertse.

It is obvious that such computations at the seaside with respect to conditions before and after completion of the Delta Project are also very important in connection with the closure of the various estuaries. We have already obtained some useful results. Naturally, computations of this kind will also affect future requirements for tidal models.

In order to determine the final flow pattern, we must introduce certain boundary conditions. This involves no extra difficulty. However, it is doubtful whether a tidal model showing the bed shape as it is at present can still be used after the enclosure has been completed.

In most cases it will be possible to do so until immediately after the complete closure, provided this is accomplished within a short period lasting not more than a few months and provided that the preparatory work done previously has not greatly affected the topography of the bed. However, important changes may occur during the closure period, usually in a limited area in the immediate vicinity of the dam.

When the final tidal pattern has been computed it will generally be found that the tidal patterns expected to occur during the closure period correspond to interpolations between the

initial and the final patterns. This gives rise to the question whether we could use a corresponding linear interpolation if we narrow down the cross-profile at the place in question. As a rule this is not so. Initially the fluid motion in the tidal region changes more slowly than it does at the final stage.

At first the total amount of water flowing through the closure gap at ebb and flood decreases only very slowly so that the velocity of the water in the gap increases in proportion as the gap becomes narrower. This means that changes in the fluid motion in the immediate vicinity of the place where the gap is closed make themselves felt at once. Changes in the tidal area further away from the closure appear only slowly. Usually it is not before the profile is reduced to about $\frac{1}{4}$ that any changes in the tide become really noticeable in the whole area.

3. The water motion in the closure-gap area

The flow of water through one or more closure gaps of course depends on the tide on both sides, which in turn is influenced by the size of the closure gap. The water from the side with the highest water-level then flows to the closure gap at an ever greater rate. This is known as the acceleration zone.

If there is a broad crest, i.e. if the breadth of the crest equals or exceeds the depth (d) above the sill of the closure gap, the acceleration will in any case continue as far as the downstream end of the sill (fig. 2). If the flow is subcritical, meaning that it has a velocity of less than \sqrt{gd} , it may even be fastest at the downstream side of the sill. This is due to the contraction which the flow undergoes as it passes through the closure gap. It may cause such strong trains of vortices at the downstream side of the actual closure gap that the gap itself is extended to the downstream side and even becomes narrower. This phenomenon also depends on the height of the sill in relation to the height of the bed beyond the downstream end of the closure gap. If there is a high sill the water can disperse into the depth. Moreover, the eddy with horizontal axis (counter-current) which may occur on the downstream slope of the sill and beyond it can also be of influence. The measure of roughness at the sill also plays an important part in this phenomenon.

When critical flow occurs with a velocity equal to \sqrt{gd} , the maximum velocity will occur at the downstream end of the crest of the sill.

If the sill has a sharp crest (fig. 3) the maximum velocity will occur a few metres beyond the top. If there is a smooth sill, there may be what is called a diving jet, in which the water shoots down the side slope of the sill.

As the water flows out of the closure gap it slows down. This takes place in the deceleration zone. There is a strong building-up of eddies and increased turbulence as a result. A distance away from the closure gap, however, the fluid motion of the tide reverts to normal. This distance depends on the measure in which the velocity of the water decreases until a normal distribution over the whole tide channel is restored.

The area in and around the closure gap, in which the velocity distribution over the profiles differs from the distribution before the closure gap was formed, will henceforth be referred to simply as the *closure-gap area*. We now propose to concentrate especially on this area. The water level in this area is lowest at the place where acceleration changes to deceleration. Since at ebb the water flows in the opposite direction to that at flood and since it is subjected to about the same force in each case, we may assume that the areas on either side of the closure gap are of equal extent (fig. 4).

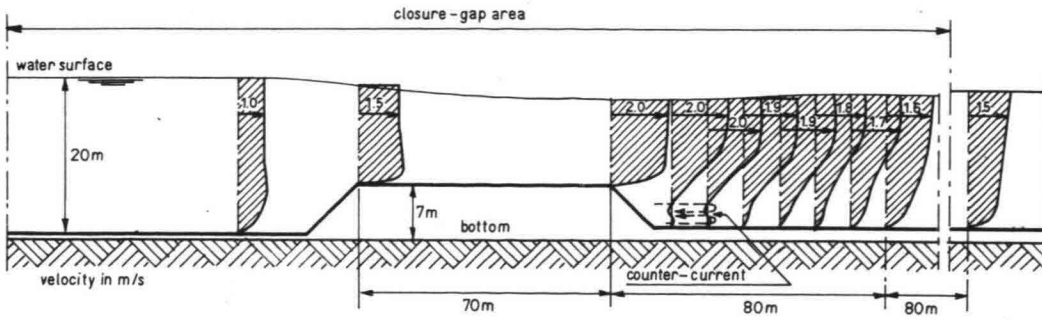


Fig. 2. Example of velocity distributions in the vertical plane in a closure-gap area in case of a sill with a horizontal crest.

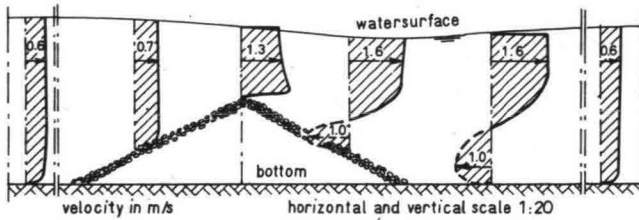


Fig. 3. Example of velocity distributions in the vertical plane in case of a sill with a sharp crest.

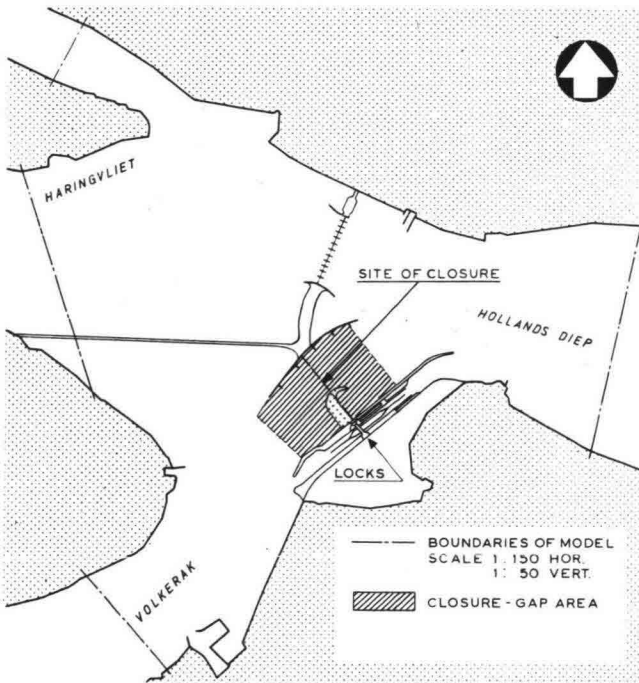


Fig. 4. Locations of boundaries of the hydraulic and the computational model of 'Volkerak': the closure-gap area (see also square in fig. 1).

It is difficult to indicate the exact boundary of this area, since it expands as the velocity in the closure gap increases in relation to the velocity outside the closure-gap area. It should be visualized as a wide strip facing the closure gap, for instance 300 metres wide, or in exceptional cases 1000 m, running parallel with the dam, with flow velocities of three to four metres per second in the gap and for instance one metre per second outside the closure-gap area. The extent of this area depends on the shape and dimensions of the gap. Outside of this area the turbulence of

the water may remain stronger than before over a distance of hundreds of metres. This depends on the shape of the closure gap. It is one of the aims of the model studies to determine the shape of the gap in such a way that the closure-gap area is as small as possible and the development of turbulence is weakest.

The flow pattern also depends on the position of the closure gap in relation to the original channel. Besides acceleration or deceleration there may also be cross-currents, and it is very important to site the closure gap in such a way as to reduce them to a minimum. Cross-currents tend to intensify the contraction in the closure gap and should be avoided as far as possible.

The forces of resistance acting on the motion of the water are subject to alteration, depending on the changed profile of the closure-gap area during the closure operation and the materials present for the protection of the bed.

Provided the river-bed is practically horizontal, the flow in the original channel can be regarded as one-dimensional with respect to both magnitude and direction. In that case the distribution of the velocity in the vertical plane, as well as the turbulent motion as a result of which the velocity continually undergoes slight changes, are disregarded in tidal computations.

The fluid motion in the closure-gap area is said to be two-dimensional if, although there is no change in the direction of the current, there are important changes of velocity in the vertical plane as a result of the area being narrowed. This usually happens when raising the sill, the closure gap narrows more or less evenly along its whole length. If, however, the narrowing varies from one place to another or if it is effected from the extremities of the closure gap, causing a contraction of the flow pattern, the direction of the current also changes over the closure gap and we then speak of a three-dimensional flow pattern.

There may be important side-effects in such two- and three-dimensional flow patterns. If the sill in the closure gap is high enough this may produce an eddy (counter-current) against and behind the downstream slope of the sill; the rotating fluid motion in it has a horizontal axis at right angles to the direction of the current then. This means that rotation takes place in the vertical plane.

If contraction is caused by narrowing the closure gap at the ends it may produce trains of vortices in the closure gap, particularly at discontinuous transitions where the vortices actually originate. These trains of vortices continue into the deceleration area; they may be very stable and screen off the main flow from the area downstream of the completed part of the dam (fig. 5). The vortices are continually being created at the source. The trains of vortices also may set the water downstream of the completed part of the dam in motion, which is apt to cause counter-currents in that region, rotating in the horizontal plane, with the highest velocity on the periphery.

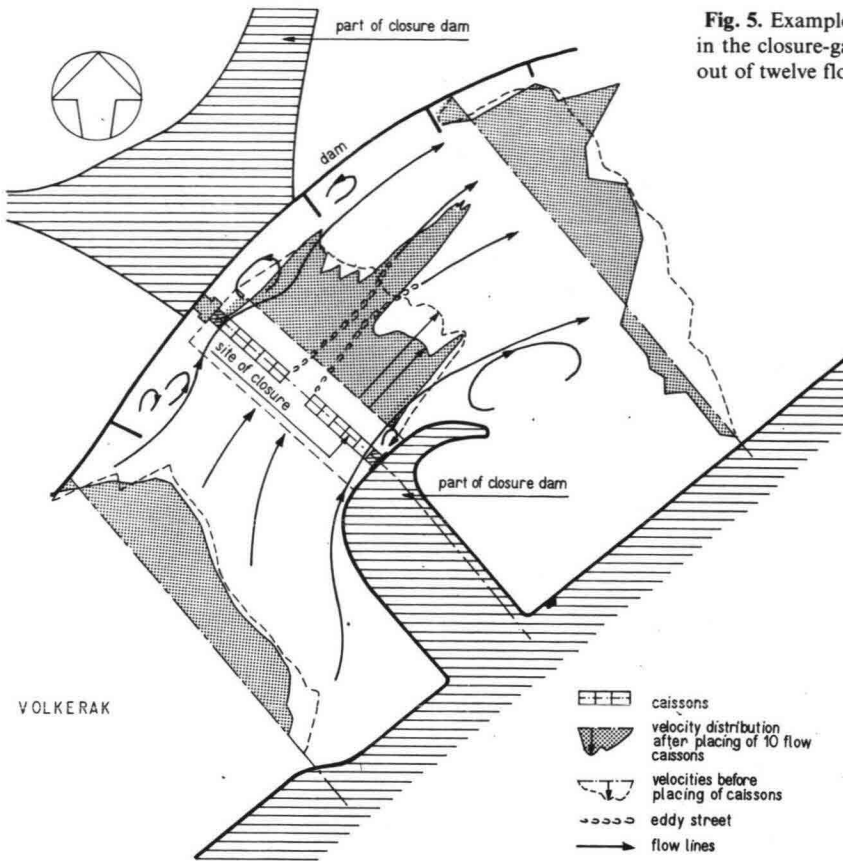


Fig. 5. Examples of velocity-distributions in the horizontal plane in the closure-gap area of 'Volkerak' before and after placing of ten out of twelve flow caissons on the sill.

Often, however, part of the flow pattern in the middle of the closure gap can safely be regarded as two-dimensional. This is the case, for instance, in gaps that are to be closed with caissons. There will of course be a three-dimensional flow pattern at the extremities.

Changes in the bed topography and in the tide while the dam is being built must of course be followed closely and compared with forecasts based on calculations and on conditions observed during previous closures. Should the actual conditions be found to differ from the forecasts, the latter can then be revised in accordance with this more exact information for the further procedure in closing the gap.

It is particularly important to see that the gauges for these tide measurements are put in the right places; they should be capable of continuous automatic registration so that we can also obtain information about abnormal conditions, for instance in gales. Preferably, the gauges should be placed at the boundaries of the closure-gap area, in line with the channel. If important changes in the two-dimensional flow pattern are expected in wide closure gaps (with a width of say 1000 metres), it is advisable to place at least two gauges, on each side of the closure gap, both on the ebb side and on the flood side. Our calculations will then have to be made in such a way that it will be possible to correlate the results with the information thus obtained about the vertical tide. Velocity measurements should be made, if possible, in the cross-profiles where the velocities are highest, since these velocities, combined with the flow volume, are the factors which determine the degree of scouring.

If possible, velocity measurements should be made in a cross-section above the sill, where there is only limited contraction. Measurements in areas with eddies are difficult to make and the

results are often inaccurate. Further velocity measurements in the closure-gap area will be used mainly for purposes of study, for instance to determine the distribution of velocities and the degree of turbulence in the closure-gap area. It is also important to know the distribution of velocities in counter-currents and eddies.

4. Remarks concerning the forces which determine the equations for the currents flowing through a closure gap

In a one-dimensional flow pattern where the bed is practically horizontal the usual equations for long waves apply, whereby the average velocity at any time in a cross-section of the river is taken as the basis for all computations. In the equation of forces the inertia forces then balance the gravity (slope) and frictional forces.

Two terms can be distinguished in the inertia forces; viz.: the force which at a given spot depends on the change of velocity with respect to time, and the Bernoulli term, indicating the force at any given moment as a result of the variation in velocity along the flow lines. In the case referred to above, where the bed is horizontal, the velocity going in the direction of the flow line changes due to the filling or emptying of the tidal prism situated alongside the channel during the tide.

In the closure-gap area, the Bernoulli force is also influenced by the height and shape of the sill which deflects the direction of the flow lanes. The flow and consequently the forces exerted on the fluid motion near the downstream slope of the base may be affected by a counter-current. However, if there are broad crests we may safely assume that the Bernoulli forces at the sill

predominate over those at the beginning of the acceleration area. If the channel is narrowed, for instance by raising the sill, this becomes even more marked. In view of the comparatively limited space covered by the closure-gap area the influence of the storage in that area on the magnitude of the Bernoulli term can usually be disregarded in view of the far greater effect of the accelerated fluid motion caused by narrowing the closure gap. This even applies to the local inertia term.

If the depth in the closure gap changes, or if the gap is narrowed, either or both factors have a steadily increasing influence on the value of the Bernoulli terms. In addition, the frictional forces increase, due to the varied velocity distribution as the water flows over the sill and due to the roughness of any bed protection there may be. If the sill is high, the friction is generally strongest at the sill, in which case estimates can be made of its magnitude. However, if the closure gap is deep, the influence of friction is usually negligible. The situation in the deceleration area defined above is even more complicated. In that area the effect of the Bernoulli force is the opposite of what it is in the acceleration area. However, its value is greatly affected by the fact that the increased turbulence causes a dissipation of energy. The influence of this strongly increased turbulence can be regarded as an extra friction to which the fluid motion is subjected. Moreover, it depends on the kind of bed protection and changes in profile due to scouring, etc. The magnitude of this resistance must be determined empirically from slope measurements of the water surface. This is one of the objects of laboratory research on the subject of closure gaps.

The above was a brief survey of the factors which influence the flow of water through closure gaps. We shall now give the equations for a subcritical flow, the various terms of which we have discussed above. Critical flow will not be discussed here; in that case the equations are quite different.

5. Discussion of the formulae

The equation of motion for the one-dimensional fluid motion is as follows:

$$\frac{\partial u}{\partial t} + u \frac{\partial u}{\partial x} = -g \frac{\partial h}{\partial x} - \frac{g|u|u}{C^2 a} \quad (1)$$

and the equation of continuity is:

$$\frac{\partial Q}{\partial x} + b \frac{\partial h}{\partial t} = 0 \quad (2)$$

The analogous equations for the two-dimensional fluid motion in the length and the vertical directions are:

$$\frac{\partial u}{\partial t} + u \frac{\partial u}{\partial x} + w \frac{\partial u}{\partial z} = -\frac{1}{\rho} \frac{\partial p}{\partial x} + \frac{\xi_1}{\rho} \left(\frac{\partial^2 u}{\partial x^2} + \frac{\partial^2 u}{\partial z^2} \right) \quad (3)$$

$$\frac{\partial w}{\partial t} + \frac{\partial w}{\partial x} + w \frac{\partial w}{\partial z} = -\frac{1}{\rho} \frac{\partial p}{\partial z} + g + \frac{\xi_2}{\rho} \left(\frac{\partial^2 w}{\partial x^2} + \frac{\partial^2 w}{\partial z^2} \right) \quad (4)$$

and the equation of continuity:

$$\frac{\partial u}{\partial x} + \frac{\partial w}{\partial z} = 0 \quad (5)$$

In these and further expressions u and w denote velocity components in x and z direction (z is in the vertical direction);

h = height of water level

a = depth

C = coefficient of Chézy

A = area of cross-section

b = storage width

Q = the total flow through a transverse section

ρ = density

g = gravitational acceleration

t = time.

In equations (3) and (4) the shear stresses due to turbulence are taken account of by adding the terms comprising a coefficient ξ . The coefficient ξ depends generally on x and z ; it is here assumed that the variation of ξ is slow in comparison with the other factors in the equations. Even equations (3) and (4) are simplified equations for the study of the influence of turbulence and eddies on the water motion. No eddies are produced in a frictionless fluid if they are not already present.

In view of the difference in scale between x and z , the coefficient ξ will be found to have a different value in the two directions. Initial ($t = 0$) and boundary values, for instance the vertical tide on either side of the closure gap, must also be added to equations (1) and (2). So far the case of one-dimensional motion. However, boundary values for the velocity components at the bottom of the river and the water surface must also be added, besides the vertical tide on either side of the closure gap, to equations (3), (4) and (5) for the two-dimensional motions.

The equations must be solved in each particular case by a numerical method, using a computer. A more simple case occurs if we may assume $\frac{\partial u}{\partial t} = 0$ and $\frac{\partial w}{\partial t} = 0$, thus calcu-

lating a stationary current example, for instance supposing that there is a current with given water levels on either side of the closure gap. For the three-dimensional case we must consider the well-known three-dimensional Navier-Stokes equations. Equations (3) ... (5) are a particular case. It is very remarkable that we are able to deal with the problem in practice much more simply, when the closure gap has a sufficiently small area. A simple formula may be drawn up for determining the flow volume through the closure gap. The formula which is a simplification of equation (1), is based on the fact that in the closure gap the Bernoulli term predominates over all other terms in the equation of motion, although the friction value, which is also proportional to u^2 may be important (see section 4). This is the case when, for instance, the velocity in the gap exceeds 2 metres per second and in the region outside the closure area the velocity is about one metre per second or less.

The velocity also varies across the width of the closure gap, for instance if the water level above the closure gap has a transversal slope, as is often the case in broad channels. In practice we are mainly interested in two magnitudes, namely the maximum velocity in the gap (u_{\max}^2), and the maximum total mass of water (Q) flowing through the closure gap per second: or more precisely the discharge per unit of width (Q/b) where b is the width of the channel. These values are important in connection with scouring. If a gap is closed with caissons the change of the velocities at the turns of the tide (slackwater periods) is of great importance.

The total mass of water (Q) is one of the factors which also determine the tidal motion at both sides of the closure gap.

Let u be the average velocity of the current across the closure gap over the flow profile (A) at a point of time t .

According to the simplifications which are based on the discussions in section 4, the following very simple relation can then be deduced from equation (1): $u = \sqrt{2g\Delta h}$, if Δh is the drop in head across the closure gap, while further $Q = A\sqrt{2g\Delta h}$. There are, however, several difficulties involved in applying it. We know the total profile of the closure gap as it was designed. However, in order to determine Q we must know

the effective flow profile, since part of the closure gap may not be effective due to contraction and in the further part the velocities vary. Moreover, the resistance of the sill influences the water motion etc. (see section 4). The effect of this is absorbed by a coefficient μ . Moreover we should determine the drop in head not merely across the closure gap itself but also across the entire closure gap area, at the edges of which gauges will have been placed. It is extremely difficult to measure the level of water in the closure gap itself. In view of this, μ is replaced by a new coefficient φ , which includes the drop of head over the acceleration and deceleration areas. The formula finally applied is:

$$Q = \varphi A' \sqrt{2g(h_1 - h_2)}$$

The maximum velocity in the closure gap at an instant t then is:

$$u = \varphi' \sqrt{2g(h_1 - h_2)}$$

$h_1(t)$ and $h_2(t)$ are the water-levels measured at the gauges; their difference is positive, otherwise they are taken in the reversed way (flood or ebb).

The value of φ' differs from that of φ as a result of the distribution of the velocities across the closure gap.

The values of φ and φ' are unknown when planning the closing of a gap. The initial calculations are therefore made for the cross-section of the closure gap, in which φ and φ' are taken to equal one, unless these values are known from comparable data gained from experience in the past and can be introduced.

We then calculate the values of Q for various A' -values. The coefficients φ and φ' in this formula are determined by means of tests on a closure gap model at the hydraulics laboratory. The ratio of such models is 1 : 30 to 1 : 60. They are not distorted.

The values of φ , which were originally determined for A' , belong to profile area $\varphi A'$. As regards the computation of Q , such computations are nowadays generally done by computer. By this method a normal tide calculation is combined with a calculation of the flow through the closure gap.

The values of φ and φ' vary for each closure, whether it be a closure using caissons or a gradual closure by building up a barrier dam by dumping. During the closure, too, the values change.

A special case is the one in which part of the gap is closed with open sluice caissons. In that case the values of φ and φ' for the open sluice caissons are very different from those in the stretch of the closure gap which is still fully open (see fig. 5). In the open part φ is considerably high and differs little from 1. In the open caissons φ' has a value of about 0.8 or even lower, depending on the manner of inflow into the caisson. The values of φ and φ' must be determined by means of laboratory tests.

6. Considerations on soil-mechanical problems

We pointed out at the beginning of this article that the increasing power of fluid motion can produce disturbances in the ground mass. A direct result of the increased water velocities is the occurrence of scouring which will be described in more detail in the ensuing article.²⁾ Such scouring is liable to be a great danger to the ground body on which the closure dam is being built, even if the dam itself can stand up to the pressure

²⁾ Cf. this issue, p. B 133.

of the overflowing water. The properties of the subgrade which consists mainly of sand in the Netherlands Delta area, are highly important in this aspect.

The initial density of the sand is one of the determining factors in problems of this kind and is a measure of its looseness.

There seems to be a critical value, meaning the porosity belonging to the so-called critical density (fig. 6).

If the value of the percentage of voids in nature is greater than the critical value the sand is said to be loosely packed. If shear stresses are exerted on sand of this kind its volume decreases. As the pores are full of water, pressure of it will build up inside the mass of sand, diminishing the effective stresses and thus reducing the shear resistance. Not until sufficient water is drained out, the pore-water pressure decreases, enabling the effective stresses as well as the shear resistance to build up once more. The shear resistance in this period of high pore-water pressure is low and as a result sliding or even liquefaction may occur in the sand body. It is obvious that scourings reduce the resistance of the construction base to sideways sliding. Sudden variations of overburden pressure, caused for instance by the placing of caissons, may be particularly risky, since over-pressured pore-water has no opportunity of flowing away in the short time available, so that stresses in the water do not diminish quickly enough.

The same thing occurs if there is a sudden sliding in the slope of a scouring pit beyond the sill.

If however the percentage of voids equals or exceeds the critical value there is less to fear, since in that case the volume of voids increases as soon as a shear stress is exerted. The shear resistance also increases as a result.

Hence, when making a design it is very important to know the critical density; this is determined in the Delft Soil Mechanics Laboratory. The test in question consists in determining the change in volume of a dry sample of sand obtained by drilling, while subjecting it to a shear stress increasing from zero on. The initial density in the sand sample is varied in order to find out what porosity of the sand still just shows no decrease in volume when subjected to this test.

The Delft Soil Mechanics Laboratory has developed a method for measuring the porosity or compaction in nature based on comparing the specific electrical resistance of the soil (which actually consists of sand-particles and water), and the electrical resistance of the ground-water proper. The measuring device is fixed either on or in a sounding rod. A similar kind of measu-

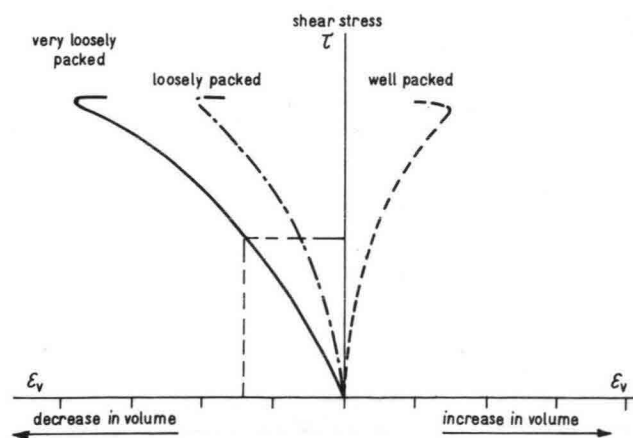


Fig. 6. The relation between shear stress and volume, under the effect of external forces on the sand sample, for different initial densities.

rement takes place in the laboratory by measuring separately the specific electrical resistance of the saturated sand proper for different degrees of compaction, and that of the water.

In this way a relation is determined between porosity on the one hand and electrical magnitudes on the other, after which the values measured in the field can be translated into a percentage of voids. After this initial density has thus been determined we can compare it with the critical density.

It is obvious that it is not only the greater or lesser compactness of a sand body that counts, but particularly the degree to which shear stress variations are liable to occur and the rapidity with which they may crop up. This poses a problem, since it means that one has to know both the initial stresses in the ground masses and the stress conditions after changes in surcharge have occurred as a result of the closure works, caused by the construction of a sill and by scouring effects. Efforts are being made at the moment to work these problems out by way of computation. Calculations of this kind are made at the Tech-

nological University, Delft, on highly schematized examples in which the soil is taken to be an elastic, isotropic medium, while the scouring pit is taken to be an arc of a circle in a semi-infinite region.

Finally the following remarks are made. It is obvious that the parameters used in the practical computations of the water motion and soil mechanics determine only roughly the complex circumstances in nature. For instance the principles of turbulence are not introduced into the equations of water motion and the variations in the components of stresses and tensions are not considered in soil mechanics. Otherwise the theory of tensors and probability must be applied. Still the limitations of the results of practical applications in soil mechanics are greater than those in case of water motion. Especially in soil mechanics tendencies are found instead of sufficient conditions. For the time being we have to accept these limitations for the practical solution of design problems.

627.223:532.582

II. Two-dimensional local scour in loose sediments

by ir. H. N. C. Breusers, research engineer Delft Hydraulics Laboratory

Summary: The conformity and time scale of local scour is studied from model experiments. A description of the flow pattern in the scouring hole and the development of the scouring process with time is given. A time-scale relationship is derived from experiments with a wide range of scales. The influence of the velocity profile and turbulence intensity on the scouring process is demonstrated with some examples.

1. Introduction

The study of scour and the consequential erosion behind structures is necessary in order to safeguard the stability.

In a number of cases structures have failed due to local scour, e.g. around bridge piers.

In the Delta area in the Netherlands this problem is further aggravated by the danger of landslides, because many sand layers are loosely packed.

The measures required for protection against scouring are costly and consequently a careful design is of the utmost importance.

In case of small structures like river-weir and bridge piers the knowledge of the maximal scour in the equilibrium situation is usually sufficient and good results are obtained in a geometrically similar model, provided that the ratio of bottom shear stresses in model and prototype is the same as the ratio of the critical shear stresses of the bottom materials in model and prototype.

Critical shear stress is the shear stress at which sediment movement starts.

With large structures like the Haringvliet discharge sluices however, the time necessary to reach the equilibrium scour depth is very extensive. For closure of an estuarine channel like the Brouwershavensche Gat the scouring process is even slow as compared to the construction speed in question. In such cases knowledge of the time history of the scouring process is of paramount importance.

To solve these problems investigations with models present possibilities, provided the time scale is established, viz. the appropriate correlative interpretation of actual and model time.

The description of the scouring process and the time scale (confined to the contemplation of a two-dimensional case) is the subject of this paper.

2. Problem

The large amount of empirical knowledge on sediment transport of non-cohesive material in uniform flow, justifies a study on the value of the parameters involved in this type of flow. Their relationships may be reduced to a relation between the rate of transport, the sediment characteristics and the bottom shear stress.

This simplification is due to the fact that the bottom shear stress determines the structure of the turbulent flow for a greater part.

Determination of shear stresses in a scour hole is difficult due to the fluctuating character of the flow; even if an average shear stress is obtained, this value does not govern the average rate of sediment transport. It is necessary therefore to use other quantities which determine the sediment transport. Once a



relationship between these quantities and the transport has been obtained a second step is necessary: the determination of these characteristic quantities from the given flow geometry. Generally the flow geometry is so complicated that a purely theoretical solution is impossible. Only a model experiment (with all the difficulties of scale effects and limitations in instrumentation) can provide the required information. To overcome these difficulties it is necessary to predict the scouring directly from the movable bed models.

For problems in which the time element for development of the scouring process is important (like the closure of a tidal channel), the determination of the time scale for scouring is essential to interpret the model results. It is clear that for a definition of a time scale, which is constant during the process, conformity of the scour hole in model and prototype is necessary; hence:

$$\frac{h_{(x,t)}}{h_0} = f\left(\frac{t}{t_1}, \frac{x}{h_0}\right) \quad (1)$$

in which $h_{(x,t)}$ = scouring depth,
 h_0 = water-depth at the end of the bottom-protection,
 x = distance from the end of the bottom-protection,
 t = time,
 t_1 = a characteristic time of the scouring process.

If the function f is the same in model and prototype then the time scale can be defined as the ratio of the t_1 -values.

As there are hardly any prototype test cases which can be used for comparative tests, it is necessary to study the validity of (1) by means of scale tests. Subsequently the influence on the time scale of the length scale, the velocity scale and the material characteristics in the model must be derived from series of those tests with adequate variations in the characteristic quantities.

3. Flow patterns

Although a study of the flow pattern gives no direct solution it may be helpful to get some insight and also for practical problems like determination of the required length of the bottom-protection. It is known that in decelerating turbulent flows high turbulence-intensities are possible, due to the formation of layers with great velocity gradients. This effect is very strong in an abrupt expansion (see fig. 1). In this figure are shown the distribution of the mean velocity and the turbulence intensity (r.m.s. deviation) as measured with a propeller current-meter (fig. 2) [1]. The rotor diameter of the meter is rather large (15 mm) but a greater part of the large-scale turbulence is measured. This large-scale turbulence is of paramount importance in the scouring process.

After reattachment of the flow an equalization of mean velocity and turbulence intensity takes place and the ultimate distribution is gradually approached. From this type of measurement an optimal length of a bottom-protection can be deduced.

Behind the bottom-protection a second region with decelerating flow is formed in the scour hole. The mean velocity near the bottom decreases rapidly as the erosion depth increases, whereas the turbulence intensity remains more constant (fig. 3).

An example of the velocity distribution is shown in fig. 4. From observations of the scouring process it is clear that especially eddies of large dimensions and low frequencies are important. Because viscosity has nearly no influence on these eddies a reasonable conformity between the important parts of the turbulence structure in model and prototype may be expected.

4. Description of the scouring process

To study the scouring process many laboratory experiments have been performed, with variations in velocity, water-depth, material and flow geometry. An example of a test is illustrated in fig. 5 where the scouring downstream of a rough bottom-protection at a water-depth h_0 is given. Generally the scouring

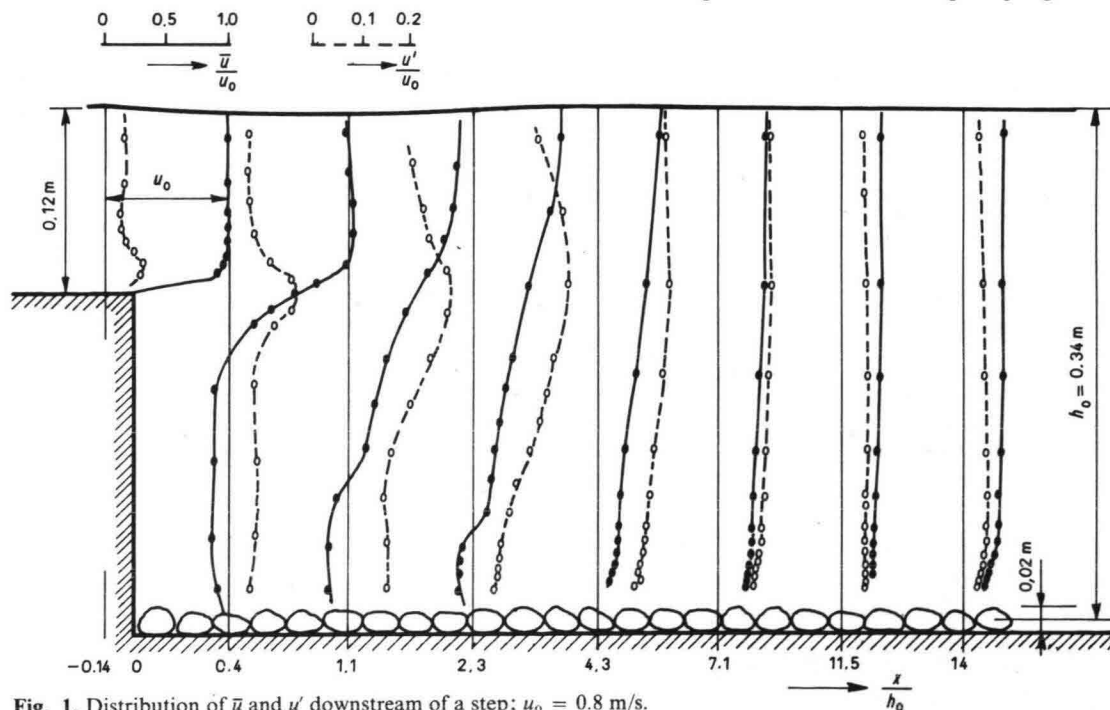


Fig. 1. Distribution of \bar{u} and u' downstream of a step; $u_0 = 0.8$ m/s.

depth h_x , at a point a distance x from the end of the bottom-protection, increases with time as:

$$h_x/h_0 = A(x) \ln(t/t_0(x)) \quad (2)$$

For small values of x/h_0 an equilibrium erosion depth is reached after a certain time. From observations it was deduced that both $A(x)$ and $t_0(x)$ increased exponentially with x [2]. From this fact and (2) it may be deduced that the maximum scour depth h_{max} also increases exponentially with time:

$$h_{max}/h_0 = (t/t_1)^\alpha \quad (3)$$

From the experiments it appeared that for a certain flow condition the value of α was nearly independent of the mean velocity, the bottom material or the water-depth h_0 (see fig. 6). Also for different types of inflow condition, e.g. a smooth bottom-

protection or a dam, the variation of α was small with an average value of 0.38.

If for a certain flow condition besides h_{max} as a function of time also the shape of the scouring hole is similar, then the value of t_1 determines the whole process. An example is given in fig. 7. From this figure it appears that even if the velocity scale is different from the scale of the critical velocities of the bottom sediments, good similarity is obtained.

The ratio of the t_1 -values of two tests may be taken now as the time scale of the tests. Because the variation in α is small for different flow conditions, the influence of these conditions on the rate of scouring may be compared directly by means of t_1 .

5. Time scale

The conformity in the scouring process with different flow

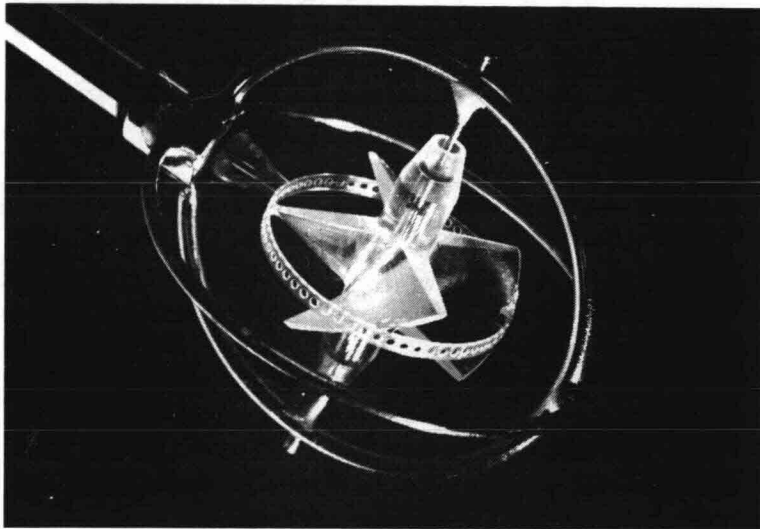


Fig. 2. Propeller current-meter. Rotor diameter = 15 mm.

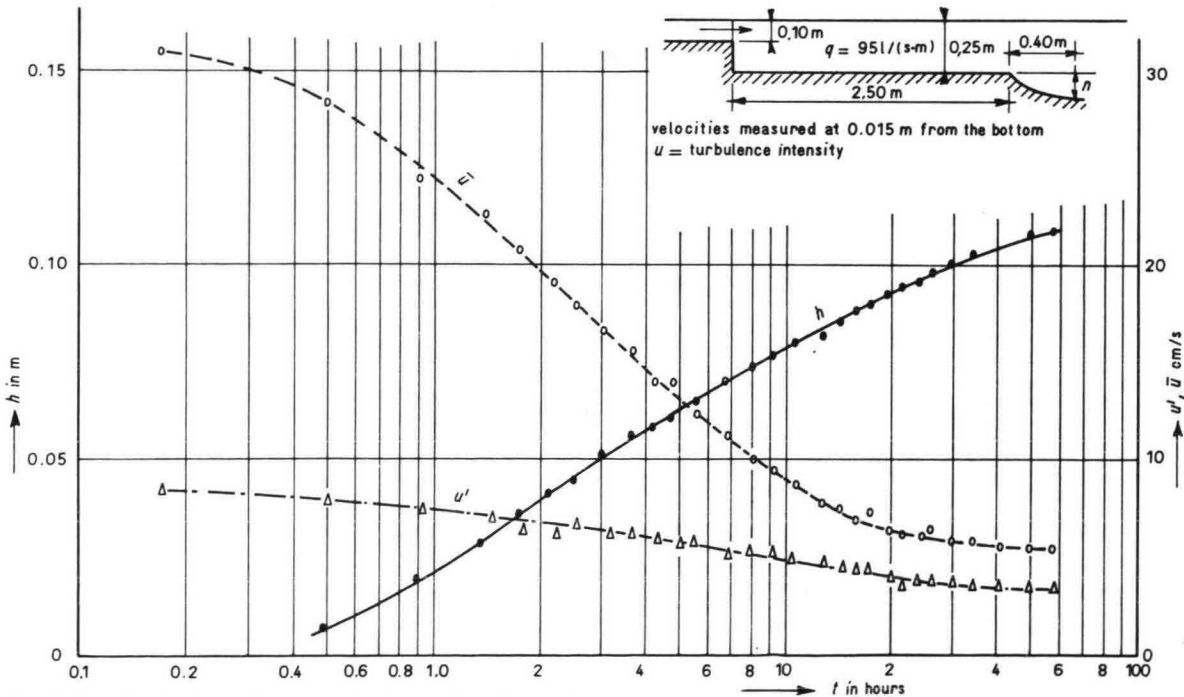


Fig. 3. Scouring-depth and bottom velocity as a function of time.

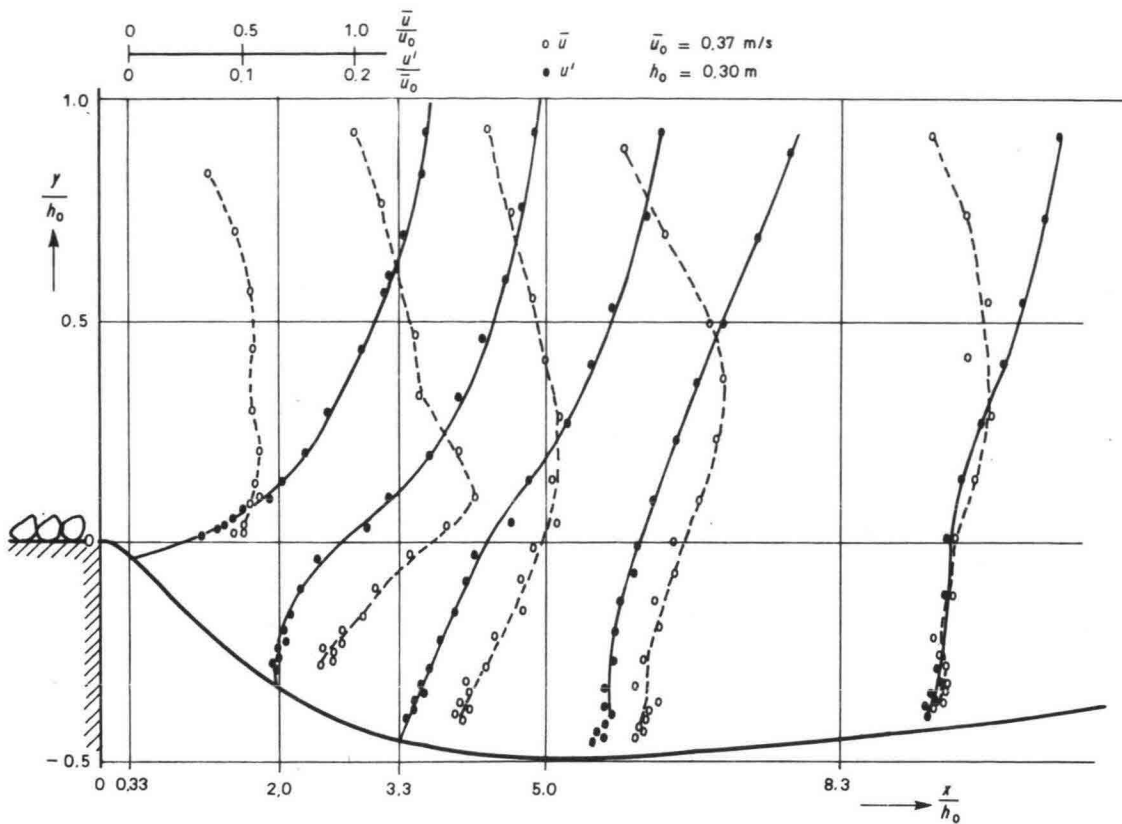


Fig. 4. Velocity and turbulence-intensity profiles in the scouring hole.

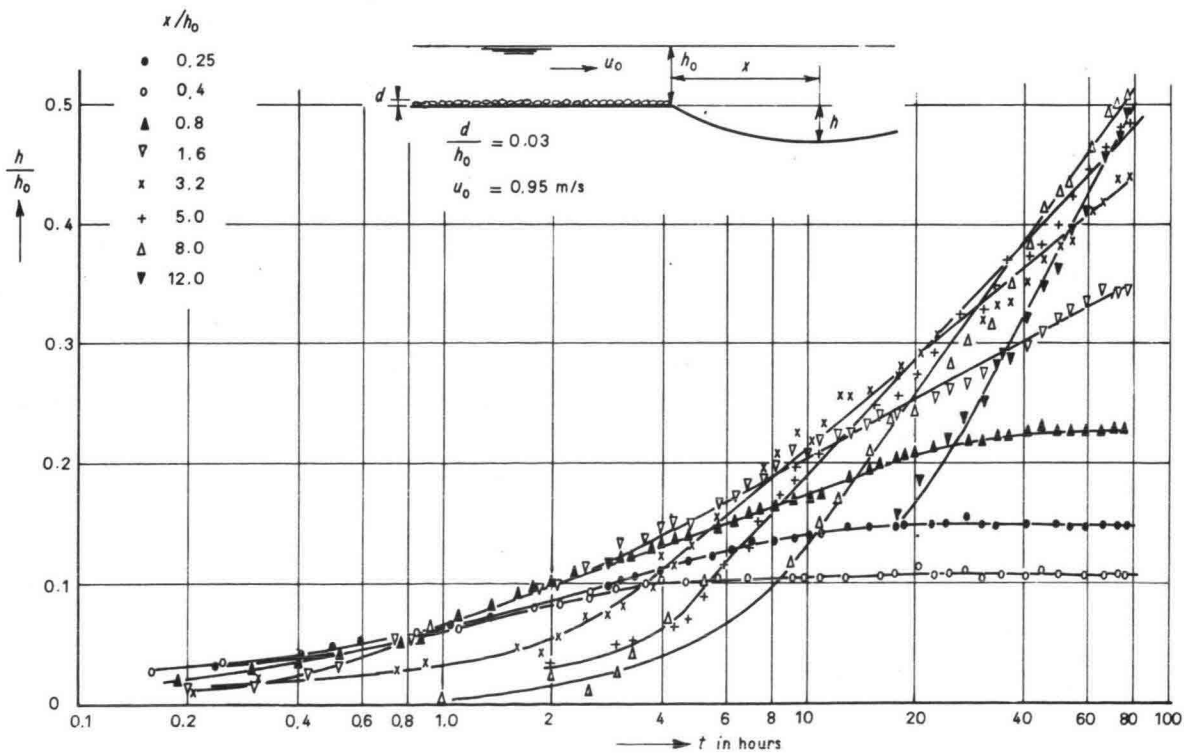


Fig. 5. Local scouring-depth as a function of time.

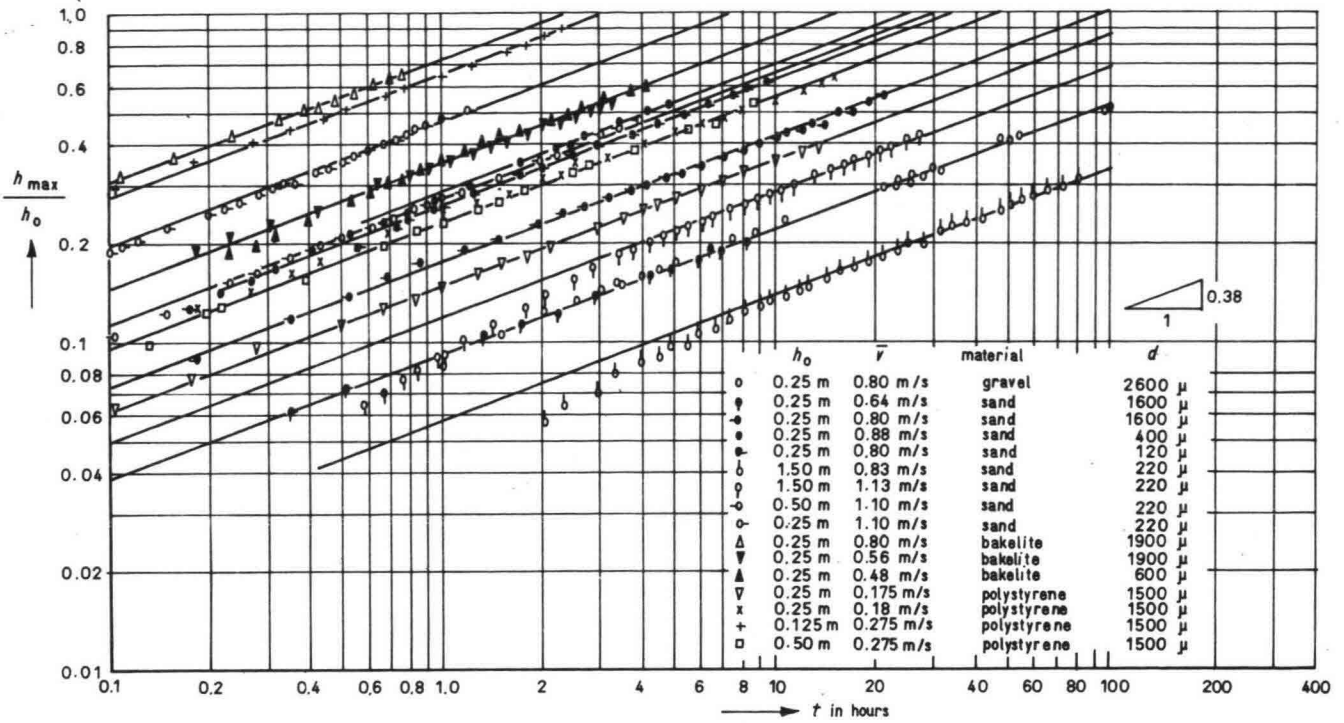


Fig. 6. h_{max} as a function of time. Scouring downstream of a rough bottom.

conditions, velocities and materials is of great value because it is possible now to express the time scale as a function of the initial conditions and sediment transport. For this correlation existing sediment-transport relations could be used.

If the amount of material which goes directly in suspension is small compared with the bed-load transport then the equation of continuity of the bottom material:

$$\frac{\partial h}{\partial t} = \frac{\partial T}{\partial x} \quad (T = \text{transport in } m^3/(s \cdot m)) \quad (4)$$

gives the scale relationship:

$$n_t = (n_{h_0})^2 \times (n_{T_0})^{-1} \quad (5)$$

It is assumed that for local scour only geometrically undistorted models are used, hence $n_x = n_h$.

A simple approximation of the existing relations between the parameters used in describing sediment transport,

$$\Phi = T \cdot d^{-1.5} (g \Delta)^{-0.5}$$

$$\text{and } \Psi = (u^*)^2 \cdot (\Delta g d)^{-1} \left(\text{with } \Delta = \frac{\rho_s - \rho_w}{\rho_w} \right)$$

$$\text{is given by: } \Phi = c \left(\Psi^2 - \Psi_{crit}^2 \right)^4 \quad (6)$$

From this follows that:

$$n_T = \left(n_{(u^*-u^*_{crit})} \right) 4 \times (n_\Delta)^{-1.5} \times (n_d)^{-0.5}$$

so that

$$n_t = (n_{h_0})^2 \times (n_\Delta)^{1.5} \times (n_d)^{0.5} \times \left(n_{(u^*-u^*_{crit})} \right)^{-4} \quad (7)$$

This relation will be compared with experimental results.

The experimental determination of the time scale for different conditions required many tests. A great part of these tests on the scouring influence was done in three flumes (width 0.5, 1.0

and 3.0 m, water-depth 0.25, 0.5 and 1.5 m) downstream of a long horizontal bottom-protection consisting of stones: $d_{stone} = (0.02 \dots 0.04) h_0$.

This was taken as a reference case.

Tests (see fig. 8) with different mean velocities and sediment diameter (sand: $d = 0.12 \dots 2.6$ mm) could be correlated by:

$$n_t = \left(n_{(U_{max} - U_{crit})} \right)^{-4} \quad (8)$$

in which $U_{max} = (1 + 3r) \bar{U}$, and U_{crit} is the critical mean velocity computed from the critical shear velocity as given by Shields. Values of U were used instead of u^* for practical reasons; r is the mean relative turbulence intensity, measured with the propeller current-meter at the end of the bottom-protection. The factor $(1 + 3r)$ was determined from the experiments. The influence of the grain diameter on the critical velocity was adequate to take into account the influence of the grain diameter on the time scale (see fig. 8).

By comparing tests with various h_0 (viz. 0.25 ... 1.5 m) it was found that on the average $n_t \sim (n_L)^{2.05}$ (fig. 8). The exponent was slightly greater than 2 due to the fact that with increasing h_0 the ratio \bar{U}/u^* increases and that the value of u^* is more appropriate for sediment transport.

The influence of the material density was studied with sand, bakelite and polystyrene ($\rho = 1.65, 0.35$ and 0.050). By comparing the materials it was found that relationship (8) was valid and that n_t varied with $(n_\Delta)^{1.6}$ (see fig. 9).

Other flow conditions, e.g. scouring downstream of low dams and long bottom-protections, could be correlated equally well with (7). The velocity profiles were reasonably similar to the profile found at the end of a rough bottom. In case of deviating velocity profiles, e.g. flow over a smooth bottom-protection or downstream of high dams, a correction factor α_u had to be introduced:

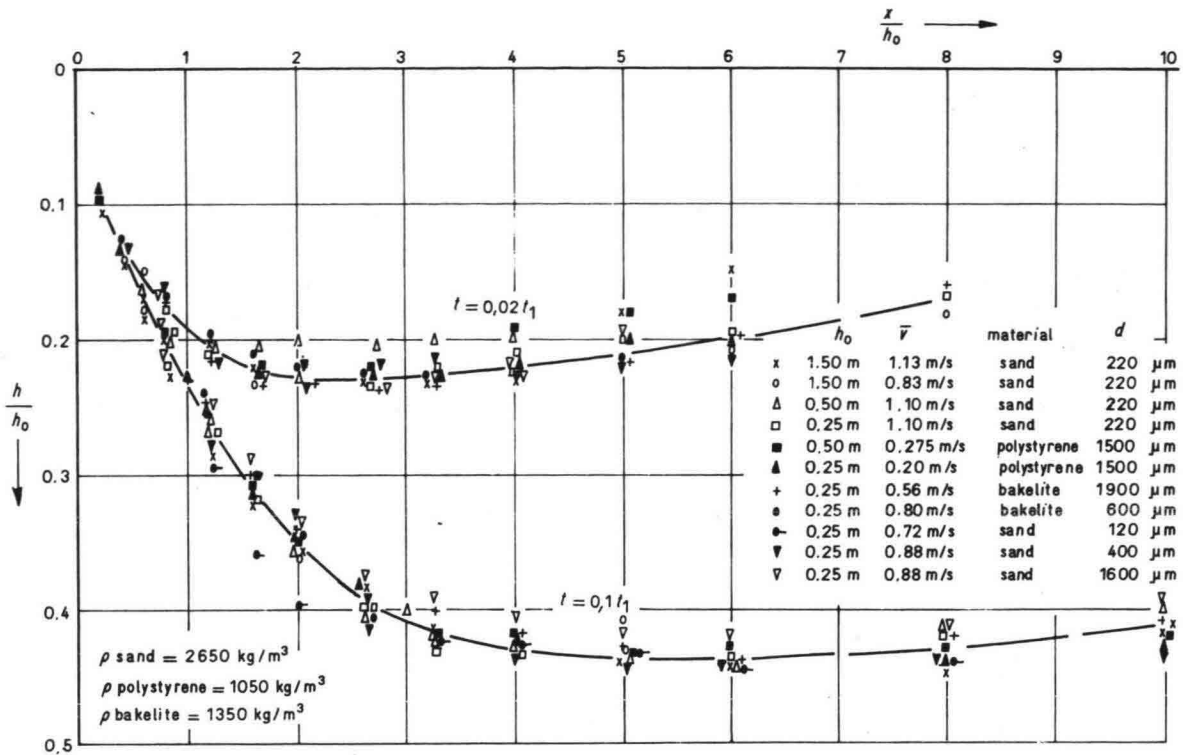


Fig. 7. Comparison of scour profiles.

scouring downstream of a rough bottom protection

sand	d in mm
∇	0.12
\bullet	0.225
Δ	0.28
\blacktriangle	0.39
x	0.84
o	1.6
∇	2.6

for any $u_{\max} - u_{\text{crit}} : t_1 :: h_0^{2.05}$

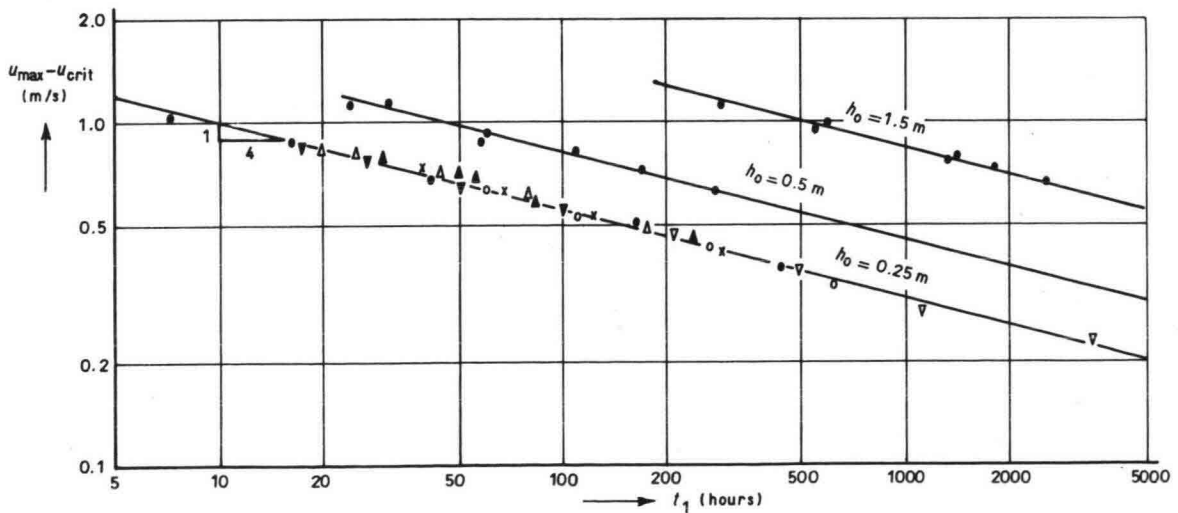


Fig. 8. Relation of t_1 vs. $(U_{\max} - U_{\text{crit}})$.

Scouring downstream of a rough bottom protection

—	sand	$d = 0.12 - 2.6 \text{ mm}$	$\Delta = 1.65$
•	bakelite	$d = 0.6 \text{ mm}$	$\Delta = 0.35$
o	bakelite	$d = 1.9 \text{ mm}$	$\Delta = 0.35$
Δ	polystyrene	$d = 1.5 \text{ mm}$	$\Delta = 0.050$

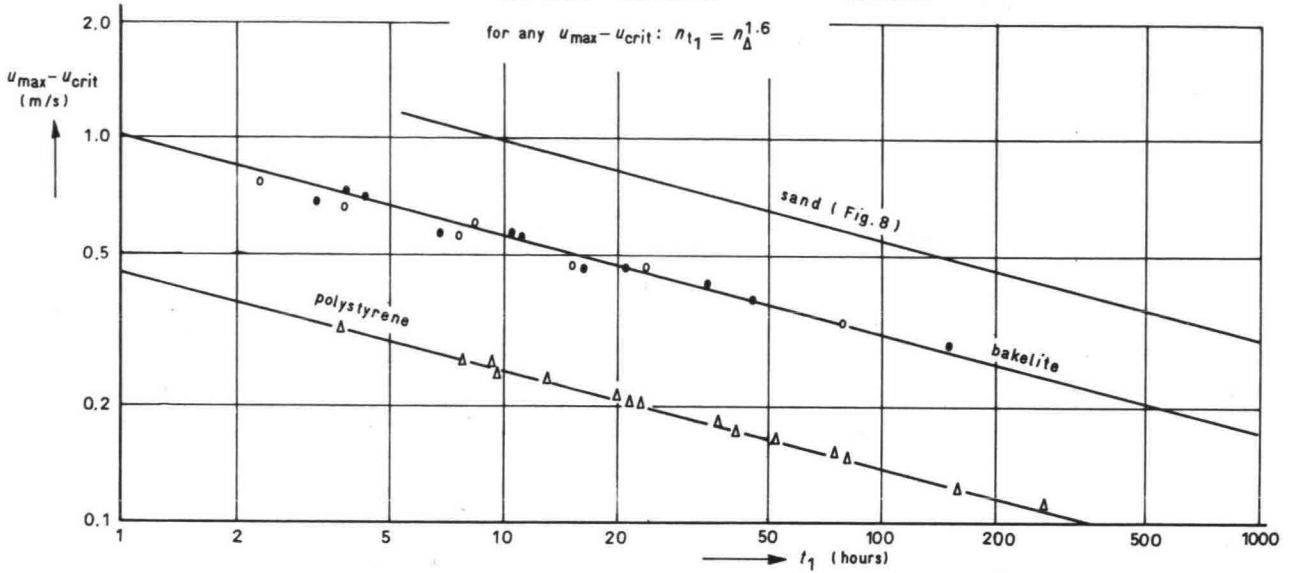
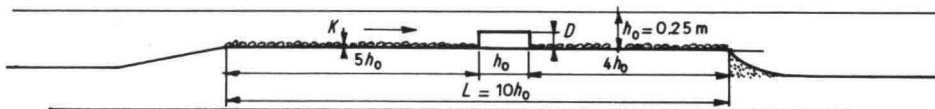


Fig. 9. Influence of material-density.

scouring tests with polystyrene $\Delta = 0.05$; $d = 1.5 \text{ mm}$



	$\frac{K}{h_0}$	$\frac{D}{h_0}$	r in %	$1 + 3r$	α_u	α_{tot}
•	0.03	0	7,3	1.22	1.0	1.22
▲	0.03	1/6	11	1.33	1.0	1.33
▼	0.03	1/3	20	1.60	1.0	1.60
+	0.03	1/2	30	1.90	1.18	2.25
o	0	0	3.6	1.11	1.31	1.45
Δ	0.006	0	5.0	1.15	1.16	1.33
∇	0.08	0	8.0	1.24	1.0	1.24
*x	0	0	2.7	1.08	1.82	1.97

* (scouring directly after contraction $L = 0$
 $r =$ mean relative turbulence intensity

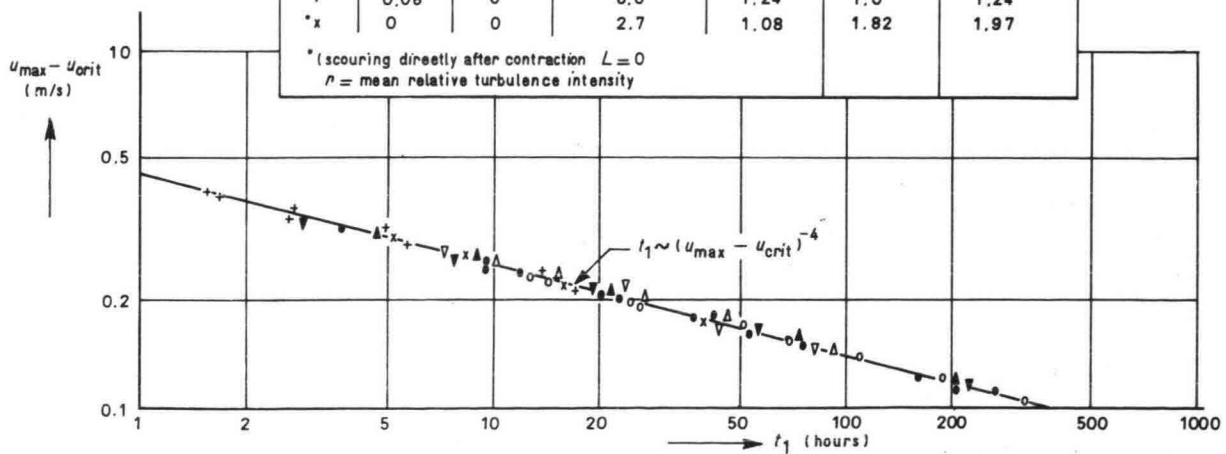


Fig. 10. Influence of flow conditions.

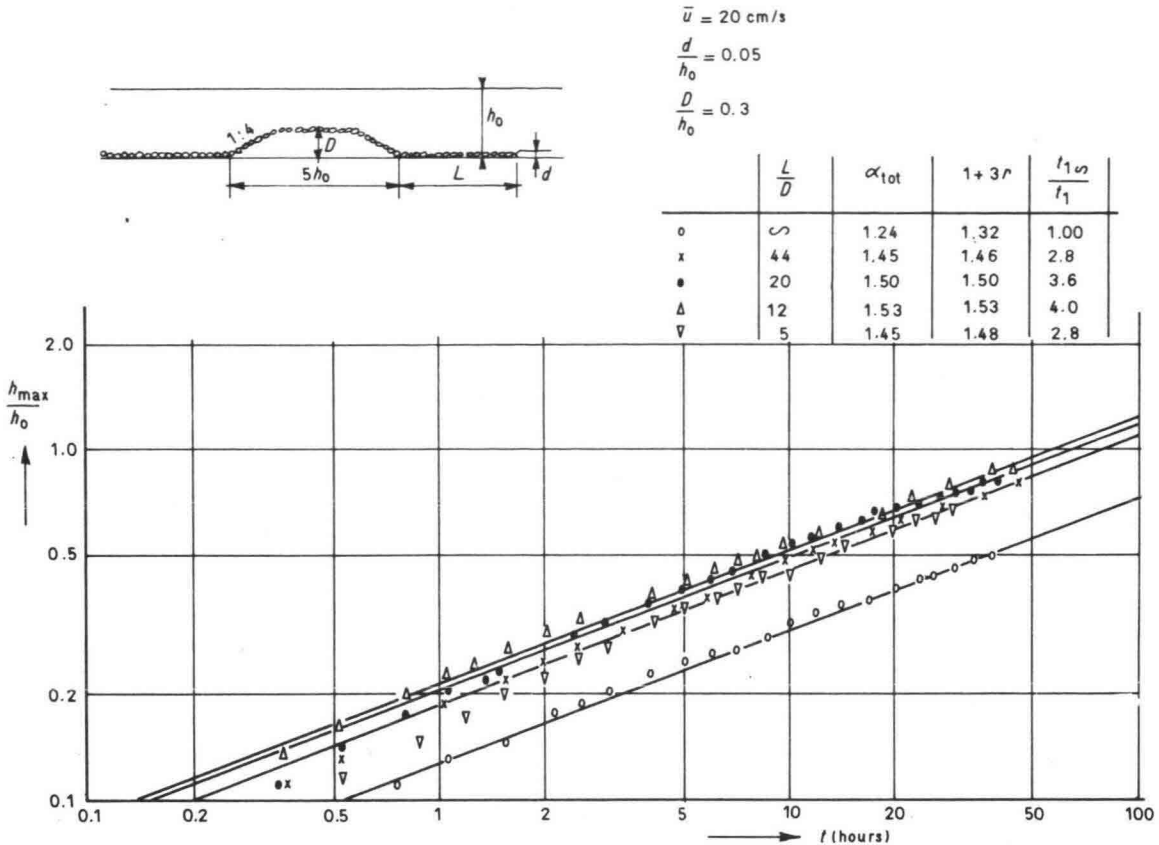


Fig. 11. Influence of turbulence.

$$U_{max} = \alpha_u (1 + 3r) \times \bar{U} \quad (\text{see fig. 10})$$

The final results of all experiments was the relation:

$$n_t = (n_{h_0})^{2.05} \times (n_1)^{1.6} \times (n_{(t_{max}-t_{crit})})^4 \quad (9)$$

The influence of Δ is in accordance with the factor 1.5 obtained by assuming a fourth power relation between Φ and Ψ^2 , the influence of the sediment diameter was less than predicted. Other factors, as cohesion, may be very important in practical cases [3].

The value of $\alpha_u(1+3r)$ is not important for the determination of the time scale if $n_u = n_{u_{crit}}$, which is also the condition for reproduction of the equilibrium scouring depth. In this case relation (9) may be simplified to:

$$n_t = (n_{h_0})^{2.05} \times (n_1)^{1.6} \times (n_{\bar{v}})^{-4} \quad (10)$$

6. Influence of flow conditions on the scouring process

From the experiments it has become evident that the velocity profile and the turbulence intensity are very important. The influence of the turbulence could be represented in many cases by the factor $(1+3r)$, from which the strong influence of peak velocities appears. This is shown in fig. 11 where the scouring downstream of a dam is given for different lengths of the bottom-protection. Even with a relatively great length the scouring is more severe than in the case without a dam, due to the persistency of the large-scale turbulence.

Besides the turbulence, the form of the velocity profile is also

of importance. A blunt profile causes rapid spreading of the flow and a relatively short and deep scouring hole with a small value of t_1 . A profile with a large velocity gradient also causes more scouring. This may be seen in fig. 12 where 5 velocity profiles are given from 5 tests with exactly the same scour/time-relationship but with different mean velocities. The smooth bottom (S 39-2) and the large gradient (S 39-5) gave values for α_u of 1.3 and 1.1 respectively.

The value of α_u varied from 1.0 to 1.4 in normal cases. For a conservative estimate of the time scale a measurement of the turbulence intensity is sufficient if α_u is assumed to be 1.0.

7. Practical application

Besides the relation for the time scale a formula for the absolute value of the maximal scour may be derived. From the experiments with sand it followed that:

$$t_1 (\text{hours}) = 180 h^2 \cdot (U_{max} - U_{crit})^{-4} \quad (11)$$

With:

$$h_{max}/h_0 = (t/t_1)^{0.38}$$

this reduces to:

$$h_{max} \approx 0.14 (h_0)^{0.25} \cdot (U_{max} - U_{crit})^{1.5} t^{0.38}$$

In case of $U_{max} \gg U_{crit}$ and $U_{max} \approx 1.6 \bar{U}$ form. (11) gives:

$$h_{max} = 0.3 (h_0)^{0.25} \bar{U}^{1.5} t^{0.38}$$

or

$$h_{max} = 0.3 q^{1.5} h_0^{-1.25} t^{0.38}$$

● ——— ●	S 39 - 1	24	rough horizontal bottom	} scouring with equal t_1
○ - - - ○	S 39 - 2	20,8	smooth horizontal bottom	
△ - - - △	S 39 - 3	18	S 39 - 1 with grid to produce extra turbulence	
∇ ——— ∇	S 39 - 4	22.5	Dam $D = 0.3 h_0$ Bottomprotection $L = 8.5 h_0$	
x ——— x	S 39 - 5	20	Dam $D = 0.5 h_0$ Slopes 1 : 20	

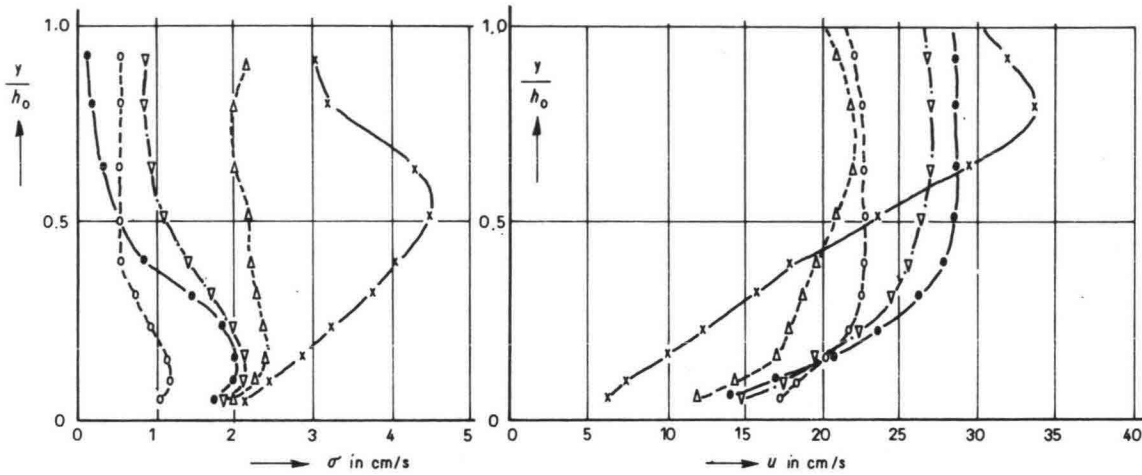


Fig. 12. Influence of velocity profile.

(q in $m^3/(s \cdot m)$), h_0 and h_{max} in m, t in hours).

For the Haringvliet sluices the practical question arises: which value of h_0 gives a minimum for the sum of h_0 and h_{max} , the total depth, for a given value of q ?

For a discharge of $15000 m^3/s$ and $t = 2000$ hours (equivalent to one year with fully opened sluice-gates) it has been found that this value will be $h_0 = 14$ m. Hence the total depth ($h_0 + h_{max}$) will be 26 m. Comparison with the actual prototype data will be difficult, due to the occurrence of thin silt layers which will retard the scouring process.

References

- [1] SCHUIF, A.: The measurement of turbulent velocity fluctuations with a propeller-type current meter. *J. Hydr. Res.* **4** (1966) no. 2 p. 37 ... 54.
- [2] PRINS, J. E.: Echelle de temps dans la reproduction d'un affouillement. *La Houille Blanche* **18** (1963) no. 2 p. 183 ... 188.
- [3] ZELLER, J.: Versuche der VAWE über die Erosion in kohärenten Gerinnen. *Schweiz. Bauzeitung* **83** (1965) no. 42 p. 733 ... 738.
- [4] BREUSERS, H. N. C.: Time scale of local scour. *Proc. XIth IAHR Congress, Ft. Collins 1967*, paper C32.

Closure of estuarine channels in tidal regions ¹⁾

III. Local scour caused by vortex streets

by ir. J. J. Vinjé, Engineer - Department Head, Delft Hydraulics Laboratory



Summary: In this article considerations are given about three-dimensional local scour caused by vortices, in non-cohesive bed-material. After a general characterization of the scour-patterns for different closing-methods and a description of the flow-pattern, the process of local scour is described more in detail.

As the development of the scouring process with time is very important for practical purposes, estimates of the time-scale are given based on reproduction in models and on a systematic research program as well.

I. Introduction

The occurrence of fine sand in the Netherlands tidal estuarine areas is the reason that one has to contend with scouring action on either downstream side of the applied bottom-protection, irrespective of the method used such as caissons or gradual closure.

In addition to the more or less important area governed by scouring which can be considered two-dimensional, there is also the area where the currents and consequently the scouring actions produce a three-dimensional phenomenon.

Due to the presence of abutments – especially the vertical terminations – vortex streets are generated whose intensity may attain such values that they may seriously endanger the stability of the construction unless effective protective measures are taken.

To illustrate the fact that in particular cases three-dimensional scouring action can play the predominant role, attention is drawn to fig. 1, showing the local scour as a function of the time of flow in a model with a horizontally protected bed. Here the three-dimensional effect was obtained by protruding a vertical baffle perpendicular to the model-flume wall. For the rest, all boundary conditions (depth, length of bottom-protection, velocity and material) are identical.

In situations with a horizontal bed there is already a considerable increase of intensity of the attack on the bottom caused by a three-dimensional flow as compared to the two-dimensional variety, but this influence becomes even more apparent in the presence of dams.

From the figs. 2, 3 and 4, comparisons can be made of the resulting bed erosions caused by scouring under corresponding

flow-time conditions, for dam-height versus water-depth ratios of 0, 0.3 and 0.6.

From the foregoing it is evident that with three-dimensional scouring a state of equilibrium is reached more quickly than in case of two-dimensional scour, but for the design of temporary works like closures it is understandable that much value is attached to the course of the bed erosion as a function of time.

In order to solve this problem one has to resort to model studies. It is therefore understandable that for each closure of some importance a separate model study is carried out in which the geometry is duplicated as true to nature as possible.

In addition to the above the characteristics of the model tests for the contemporary closures require a highly systematic approach. The scope of the works and the hazards which must be accepted make it compulsory to exploit the existing possibilities to their fullest.

Both the available time for the tests and the equipment existing at present provide broader possibilities than before.

Nevertheless, the difficulties involved in the solution of three-dimensional scour problems should not be underestimated.

On account of these complexities, the more fundamental approach of this subject could be properly started only after the various relationships of the two-dimensional scouring problem were established and an insight into the time scale was obtained.

For the sake of completeness it is pointed out that the vortex streets not only play an important part in the erosion of fine bed material, but that, under certain conditions, the heavy-rubble bottom-protection may even be affected.

This for instance is the motivation for the decision that those parts of the apron which touch the Haringvliet discharge sluices have been built as a closed concrete structure, inasmuch

¹⁾ De voorafgaande delen I en II zijn verschenen in *De Ingenieur* 1968, nr. 44, blz. B 127 resp. B 133.

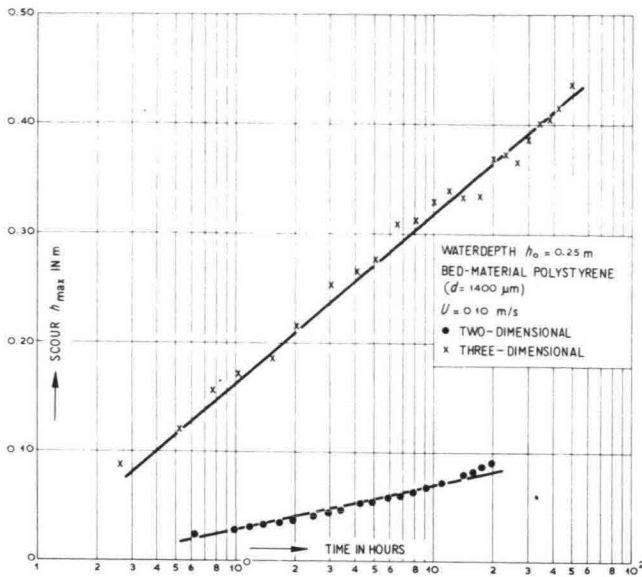


Fig. 1. Maximum scouring-depth as a function of time (horizontal bed).

as model tests indicated that even very heavy rubble was not equal to the negative pressures prevailing in vortex streets. These negative pressures might appear in unfavourable conditions, for instance when ice conditions prevent one of the gates from being lifted.

Preventive measures were necessary for those parts of the apron (situated further at a distance from the gates) where heavy rubble 300 ... 1000 kg could be utilized, but the danger existed that the underlying lighter stones would be sucked through the space left between the heavy rubble; consequently a layer of heavy rubble with a diameter $1\frac{1}{2}$ times the underlying was deemed necessary.

The attack on the rubble stone situated at a caisson-sill, should be recognized especially under conditions where all caissons but one, are placed in position on the sill.

As has been established during the model study for the closure of the Volkerak, under extreme conditions, the bottom-protection can be attacked at the upstream side in the vicinity of the edges of the caissons, as a result of vortices leaving the walls of the caissons.

2. General characterization of the scour patterns for different closing methods

The stability of the structure is of prime importance with gap-closures.

It is therefore advantageous to design the gap profile in such a manner, that the least possible scour can be expected.

The length of the bottom-protection on either side of the sill is important amongst other factors.

Characteristic differences will occur relative to the chosen closing method; they shall be briefly discussed hereafter.

Next to the financial and constructional aspects, the hydraulic aspect is often a decisive factor for the choice of the closing equipment.

Regarding the method of execution of the closure, it is evident that with caissons a leveled sill is essential whilst with a gradual closure a certain freedom as to the shaping exists.

With caisson closures certain unexpected settling movements can cause serious if not insurmountable stagnation to the work's progress, while a gradual closure affords a better opportunity to take easy and quick remedial action. The influence of the weather conditions is of less importance with a gradual closure, but with caisson closures the influence of the weather is an important factor.

Considering the two-dimensional flow pattern, the erosion may be expressed as a function of the rate of flow and turbulence intensity. By heightening the sill, the rate of flow decreases but the intensity of turbulence increases. The rate of change is conditional on the situation.

Consequently, maximum erosion is observed when the ratio of sill height to channel depth is 0.7.

Generally speaking, closures by means of caissons are unadvisable for deep estuarine channels, inasmuch as the limited construction height of the caissons necessitates a relatively high sill. In consequence of the required leveled position of the sill, it is impossible to adapt the shape of the sill to the expected erosion.

With gradual closures the stage of maximum scour, seen from a two-dimensional viewpoint (ratio of sill-height/depth 0.65 ... 0.75) should always be passed. This entails that during this stage of the closure-activities, no stagnation can be allowed.

With such a type of closure it will be possible to influence the location and quantity of the erosion by determining the most favourable ratio of sill height/channel depth. As a rule, the best contour of the closure gap is obtained (when viewed over the

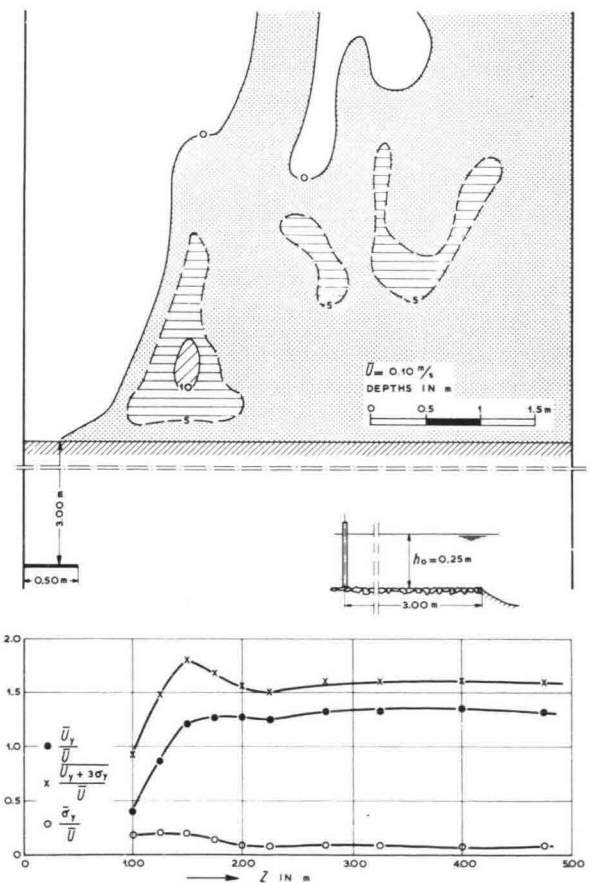


Fig. 2. Scouring-pattern after 10 hours model. Dam-height/water-depth = 0.

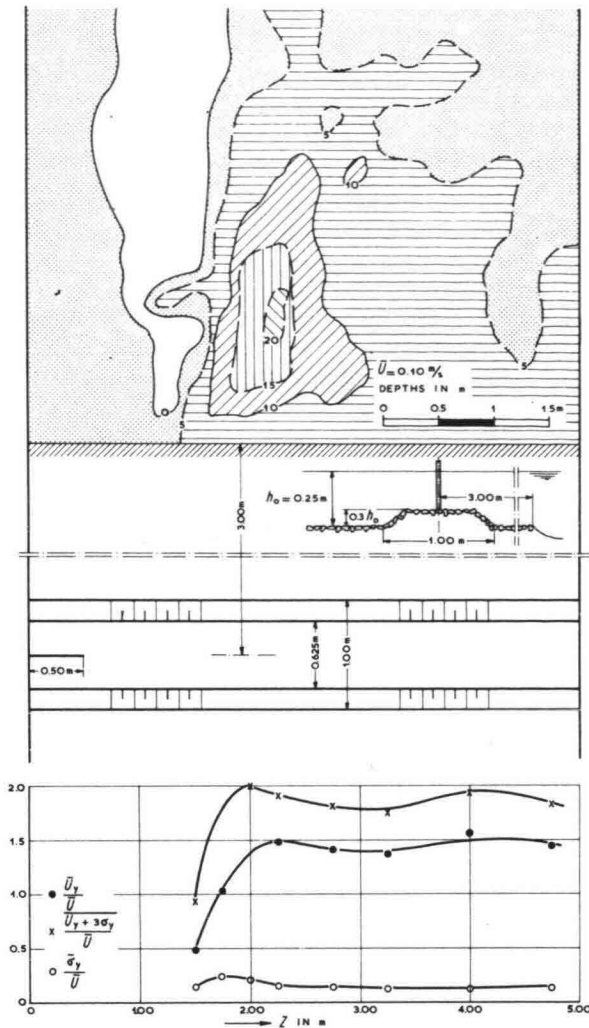


Fig. 3. Scouring-pattern after 10 hours model. Dam-height/water-depth = 0.3.

cross-section of the channel) if the ratio sill-height/channel-depth achieves a fairly constant value.

The three-dimensional flow pattern shows in connection with the various closure methods, that generally speaking vertical terminations exist with caissons, which consequently cause strong vortex streets and considerable scour. (Veersche Gat, Southern Grevelingen channel.)

In diminishing this effect, experience will be gained with the closure of the Volkerak by utilizing oblique abutment-caissons with a sloping sill (slope 1:5).

With gradual closures, terminations in the centre line of the gap can be realized with a very gentle slope which may lead to a reduction of the intensity of the vortex streets.

It is incorrect to assume that the lack of vertical terminations implies the absence of vortex streets.

With the detachment from talus, vortices with a vertical axis can also be generated; it is only with very gentle slopes that it is operative to suppress the vortex-street effect entirely.

With caisson closures there is the tendency of shaping the 'winter-gap' as narrow as possible, causing a strong contraction and consequently severe local scour.

With gradual closing however, a narrow 'winter-gap' is not compulsory, thus avoiding in this phase the contraction and

resulting in a diminished erosion-effect. With caisson closures the contraction increases in the course of the execution phase.

By utilizing 'sluice-caissons', which can only be used for closing the main estuarine channels on account of the maximum allowable velocities, this effect is only observed present to a lesser degree. Moreover, these phases are ordinarily rapidly passed through. Nevertheless, increased intensity of vortex streets and local erosions should be anticipated, but a favourable aspect is that head-effects (caused by vertical terminations) continually occur at different places. With gradual closures the different closing-phases can be scheduled in such a manner that the contraction hardly increases, thus avoiding continual erosion at one and the same location. For this reason the phases during closing should be arranged in such a way that a vertical narrowing of the closure gap occurs simultaneously with a horizontal narrowing.

From the foregoing it will be clear that with the design of the shape and size of a closing gap, it is of primary importance that a well-considered choice is made regarding the closing method on which the so essential scouring effects are dependent. For the aforementioned reasons model tests are indispensable.

3. Definition of the problem

The general purpose of the program established for fundamental research of three-dimensional scour can be summarized as follows:

1. Determination of relationships between flow-conditions, material properties and the sediment transport. In order to obtain a complete insight in the overall flow-conditions, it is not sufficient to work with mean values of the velocities but the turbulence of the water should also be taken into account. In view of the complexity of the boundary conditions, the need for model tests in solving practical problems shall remain.
2. Verification of the similitude of scour in a model by means of systematic tests and the determination of the 'time-scale' of the model.

The model tests can, to a certain extent, be divided into two fields of research, viz.: the field directed towards solving practical design-problems and the part which aims at interpreting the model results like the influence of the properties of the bed-materials, the velocity-scale and length-scale on the time-scale of three-dimensional scour.

It is impossible to draw a strict dividing line between the two fields of research inasmuch as the designer is also very much interested in the development of scour as a function of time, which entails that for a proper evaluation the time-scale of the model has to be determined.

Hence, the schedule of tests has been established in such a manner that the tests required for the design criteria can also be used for the model-scale research.

In the test-schedules various important design variables were included like sill-height, the length of the bottom-protection, the degree of roughness of dam and bottom-protection and the shape of the protrusion.

Before going into further detail on the subject of these tests, the flow-pattern will be briefly discussed.

4. Flow-pattern

The horizontal constriction of the flow profile, usually occurring in a closure gap, is the cause of a flow-concentration within a narrower path on the downstream side of the gap

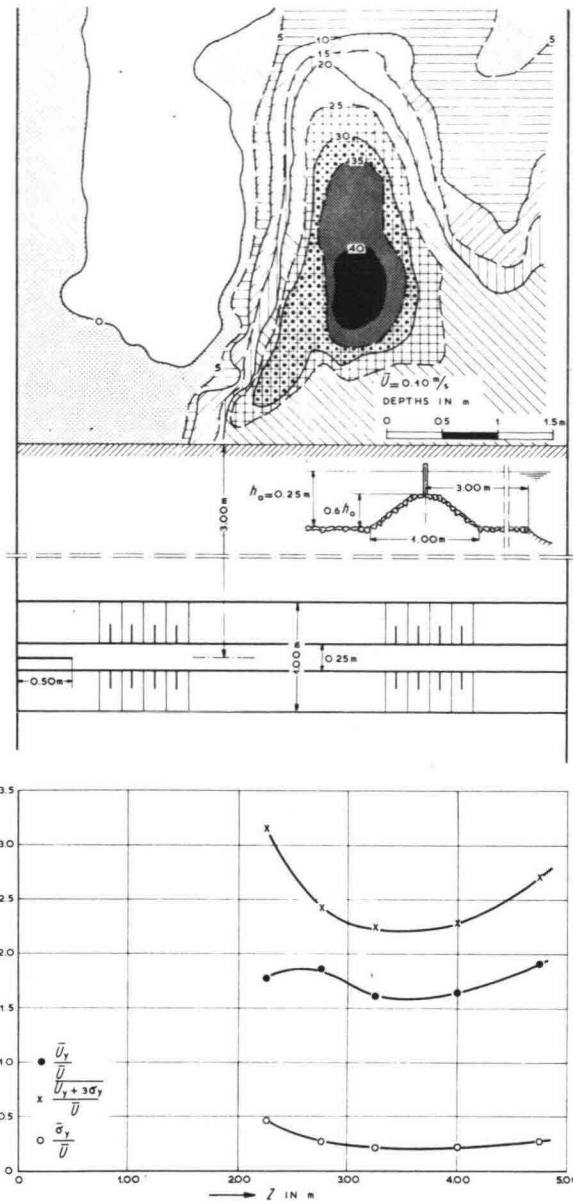


Fig. 4. Scouring-pattern after 10 hours model. Dam-height/water-depth = 0.6.

(contraction). This contraction will increase with increasing depth of the downstream bottom profile.

In view of this it is deemed unadvisable to increase the depth of the bottom profile on either side of the gap beforehand. On the other hand, the spread of the flow will increase with increasing flow-resistance downstream of the closing gap.

This means for instance that in general with models of closing gaps in which the horizontal and vertical scale ratios between model and prototype differ so that we can speak of a geometric distortion, the depth in the model is relatively too great. The resulting deviation of the flow pattern can be corrected by increasing the bottom resistance downstream of the gap.

A proper reproduction of the downstream flow-pattern of a gap, of such great importance for obtaining a correct reproduction of the scouring action, can be satisfactorily achieved, provided the bottom-resistance scale is correctly applied.

With a profile enlargement for instance just behind a closure gap in a distorted model the vertical flow-pattern however is not correctly reproduced. The eventual existing bottom eddies will be reproduced relatively too long in the model.

For a detailed research of closing gaps for which the two-dimensional part is important and the scour has to be studied quantitatively, the tests are mainly conducted with non-distorted models having a small scale factor.

The flow pattern and the velocity distribution in both the vertical and the horizontal sense, are the main governing factors for the scour that will occur. Particularly the vortices with vertical axis play an important part. These vortices are characterized by the proportional decrease in velocity with the radius ($U = C/r$). This relationship does not hold good near the centre of the vortex, since the velocity should reach infinite values there.

In reviewing the horizontal velocity distribution on the downstream side of the gap (with vortex streets) it proves that maximum velocities occur immediately adjacent to the vortex street on the side of the main current. When leaving the main current in a horizontal direction, the velocity decreases almost linearly, so that the term 'velocity gradient' may be applied to a vortex street. The intensity of the vortex street is related to the velocity gradient. The relative turbulence, however, when pursuing in the same direction, strongly increases. The latter can reach very high values (30%).

From the pressure distribution in curved flow-lines which appear in connection with closing gaps, it can be derived on mathematical grounds, based on the comparison of the flow patterns at surface and bottom, that on the upstream side of the closing gap an upwardly directed water current is generated, having its major velocity component in the direction of the main current (Tison).

At the location of the point of separation of the vortices, for instance at the abutments, it can be inferred that an ascending current must be present in the vortex. The bottom material, stirred up under the influence of currents and turbulence, can be picked up by the rotating ascending current in the vortex and be thrown out sideways.

Indicative for the vortex pattern are the slow velocity-fluctuations in the vortex street.

The frequency of these fluctuations is small in comparison with the turbulent velocity-fluctuations. The slow velocity-variations can be expressed in a Strouhal number.

In order to ascertain whether the vortex-flow thus can be characterized, the relationship between the Strouhal number

$$\frac{Z}{U_0 T_{50}} \quad \text{and other characteristic quantities, such as the Rey-$$

nolds number (Re) and the Froude number (Fr), were examined in a model with fixed bottom with a vertical protrusion in the flume profile. In this study the water-depth, velocity, roughness, dam-height and width of the protrusion could be varied at will.

The apparent reasonable correlation between the quantities mentioned before is shown in figs. 5 and 6. It shall be investigated whether and to which extent the correlation does change during the scouring process and whether it will be possible to establish a link with the scour-pattern.

Thus it may be concluded that within a vortex street a very complicated three-dimensional flow pattern exists, and consequently it has been impossible to provide even a simple characterization of the flow mechanics up till the present.

This is not so surprising, because in the two-dimensional

domain it also appears impossible to characterize the velocity profile in a simple way.

Similar to the two-dimensional scour, the empirical relationships between flow pattern and three-dimensional scouring action are based on the observations of the flow and turbulence characteristics at the end of the bottom-protection.

This is also based on practical considerations because it may be expected that here the flow conditions will hardly vary.

As the significant value of the current velocity the maximum value in horizontal sense of $\bar{U} (1 + 3 \bar{r})$ is used.

5. Process of local scour

The diameter of the fine-grained material found in the estuarine channels of the Netherlands cannot be further reduced for the purpose of the model studies, without changing the characteristics of this material.

The frictional forces are already of such importance as compared to the inertial forces that the reproduction of the bed-material becomes unacceptable on the length scale.

For this reason the sand of the model and also of the prototype have the same grain diameter, or lighter materials like polystyrene or bakelite are used. In the latter case the velocity

scale is exaggerated as compared with Froude's velocity scale, for obtaining sufficient transport.

The length of the model must then be limited in order to avoid deviations in the flow pattern. Like with two-dimensional scour, the scour-process caused by vortex streets is characterized by the geometry of the scour hole, the maximum scouring depth and the scour development as a function of the time. The upstream slope of the hole deserves special attention.

It may safely be assumed that the flow pattern can be reproduced correctly, in which case no deviations of the turbulence characteristics are expected on account of the fact that the viscosity-influence is small: usually $Re < 10^5$.

Assuming similitude in flow-pattern and in turbulence characteristics, the correct initial conditions will occur at the end of the bottom-protection at the time $t = 0$, so that it may be assumed that the transport-distribution along the bottom in the model is equal to that in prototype, provided the occurring velocities in the model are much greater than the critical one.

The configuration of the scour hole, under the influence of vortex street and certain conditions of flow and geometry, indeed appears to be identical for different materials and a given scour-depth, provided that the adjusted flow-velocities have nearly the same ratio versus the critical velocity for the material with a parallel flow.

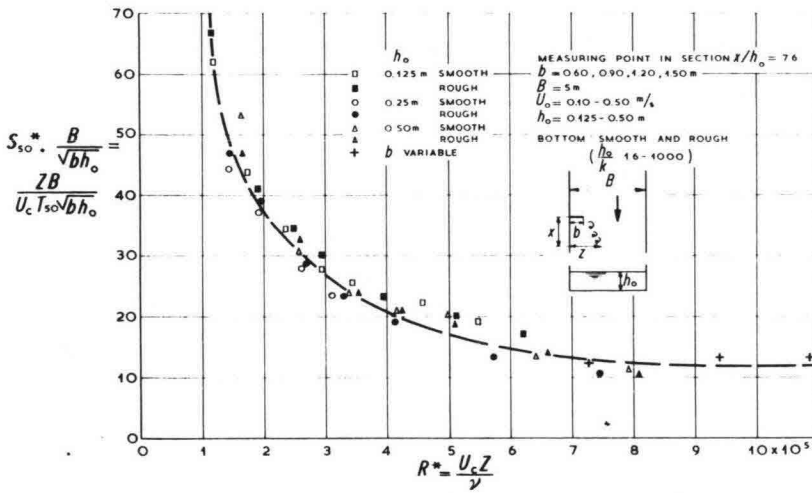


Fig. 5. Relationship between Strouhal number and Reynolds number.

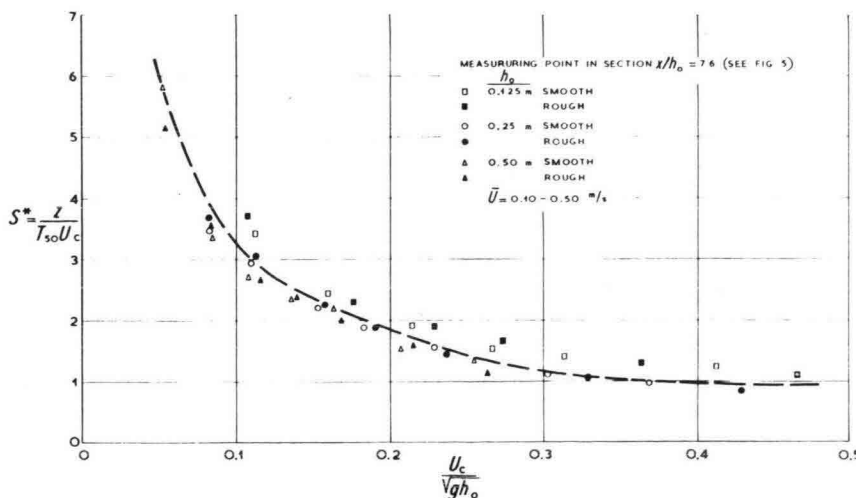


Fig. 6. Relationship between Strouhal number and Froude number.

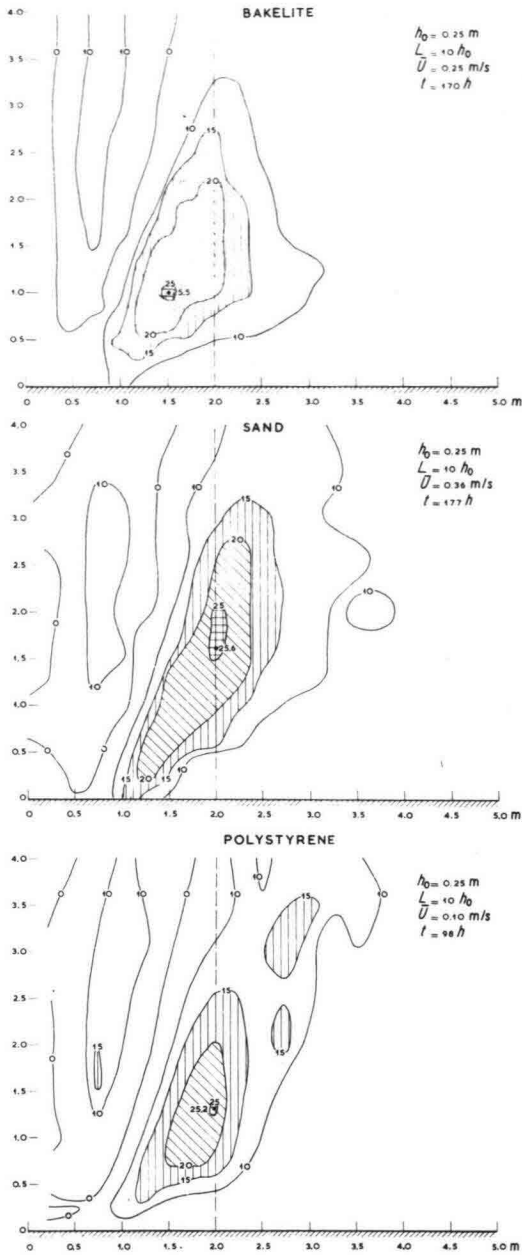


Fig. 7. Similarity of scour-pattern for bakelite, sand and polystyrene grains respectively.

It appears therefore that during the progress of the scouring action the similitude remains.

The scour-pattern at the time t_1 (for $t = t_1$ we have $h_{\max} = h_0$) is shown for bakelite, sand and polystyrene in fig. 7. The similitude is apparent. The unproportionally larger shape of the scour-hole, when sand was used, is attributable to the fact that in this case the adjusted model flow-velocity ratio was too high as compared to those used for the tests with bakelite and polystyrene.

Although the similitude in erosion with the various materials remains the same during the scouring process, the flow-pattern is observed to change.

The increasing depth causes further contraction and the flow is still more concentrated towards the central part of the channel.

This is clearly shown in fig. 8 giving the initial flow-pattern and the condition after 14 hours streaming. Hence, the mutual

influence on either flow-pattern and scouring action is apparent.

Scour-holes caused by vortex streets are characterized by steep side-talus (up to 1:2). The bulk of the material removed from the vortex street scour-hole, is deposited sideways along the hole, outside the influence of either vortex street and main current.

Experience has taught this phenomenon generally to be represented in an exaggerated way due to the too high settling velocities of the material in the model. In order to investigate whether the depth of the vortex street scour-hole is influenced by the presence of this deposit, the test was repeated under the same test-conditions, but with the careful removal of the accumulated deposit at regular intervals of time. This test clearly showed that the erosion depth is not influenced by the material deposited alongside the scour-hole (see fig. 9). From the above it may be concluded that this phenomenon during the scouring process does not contribute to the occurrence of scale-effects.

In observing the scouring action caused by vortex streets, similarity is recognized with the two-dimensional action, viz. that the erosion is clearly influenced by the height of the dam, the length of the bottom-protection and the roughness of dam and bottom-protection.

With regard to the above-mentioned criteria which are important for the design, consequently the general conclusion can be drawn: that the degree of scour will decrease when the height of the dam (D) is decreased and also when the length of the bottom-protection is increased. Further it can be concluded that a rough protection will give less scour than a smooth protection.

When it is defined that the time required to attain a depth of erosion equal to the original water depth (h_0) is t_1 , then the influence on the scour of the above-mentioned variables is clearly demonstrated in table 1. In this table the values of the time t_1 are expressed in hours for a vertical protrusion (0.5 m protrusion in a flume of 5 m width).

Table 1.

D/h_0	0	0.3	0.6	L/h_0	5	10
	t_1 (in hours)				t_1 (in hours)	
$L/h_0 = 5$, smooth	25	3.8	0.19	$D/h_0 = 0$, smooth	25	52
$L/h_0 = 5$, rough	57	8.6	0.38	$D/h_0 = 0$, rough	57	110

Material: polystyrene

The scouring capacity of vortex streets is furthermore dependent on the water-depth at the location of the vortex street and the immediate vicinity. Increasing depth causes greater flow which in turn facilitates the vortex-street development. This was clearly established during the model studies when searching for the optimum apron depth near the abutments of the discharge sluices of the Haringvliet and the Lauwerszee respectively.

It was impossible to establish relationships for the three-dimensional scour during the model studies for determining the design criteria, on account of the fact that the velocity-scale had not been changed. However, an important contribution in this respect was supplied by tests series in which, for a constant geometrical situation, only the velocity of the flow was varied. As has been mentioned in the preceding article, ²⁾ the

²⁾ Cf. *De Ingenieur* 1968, nr. 44, p. B 133.

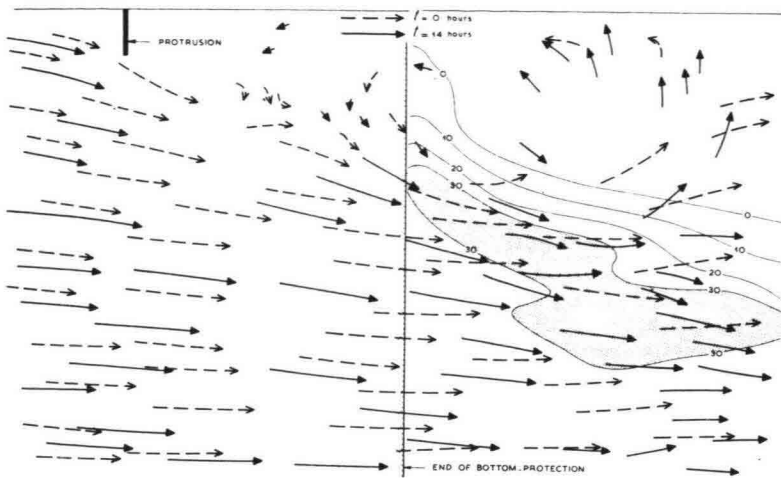


Fig. 8. Comparison between initial flow-pattern and that after 14 hours.

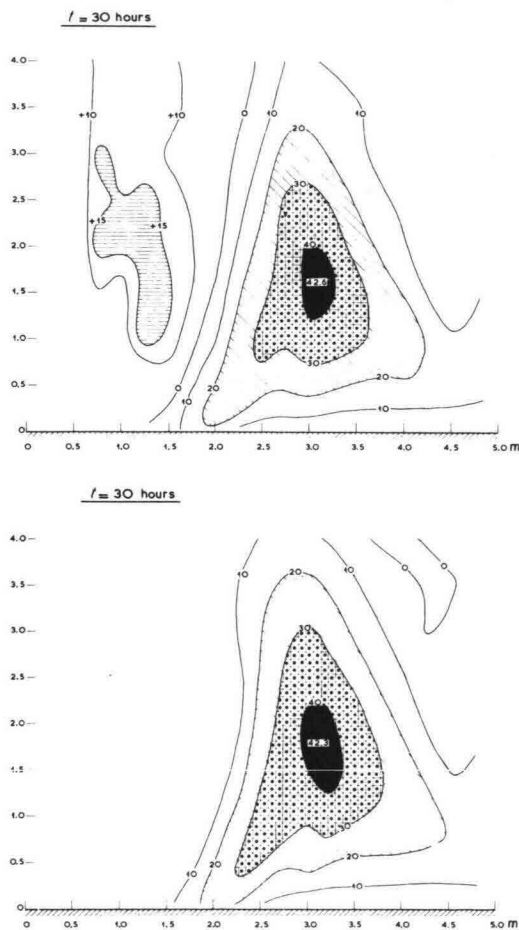


Fig. 9. Comparison of vortex-street scouring effects. Upper: with normally generated side-deposit. Lower: material of side-deposit regularly removed.

momentary maximum scouring-depth, in the case of two-dimensional scour, can be described as a power-function of time. During the investigation carried out on the erosion by vortex streets, it appeared from a large number of systematical tests with different materials (sand, coarse bakelite, polystyrene), in which the flow-velocities were varied, that the

time/erosion-curves for the deepest points can be represented by the relationship:

$$\frac{h_{\max}}{h_0} = 1 + A \log \frac{t}{t_1}$$

where:

- h_{\max} = maximum scouring-depth at the deepest point
- h_0 = original water-depth
- t = time corresponding to h_{\max}
- t_1 = time corresponding to $h_{\max} = h_0$
- A = a constant.

It must be emphasized that neither the beginning of the scouring-process (starting phenomenon) nor the termination of the process are covered by this equation. From the test-results it appears that the value of the coefficient A depends on the height of the dam. For values of D/h_0 of 0, 0.3 and 0.6, respectively, the following values for A are found: 0.54, 0.75 and 0.88. The coefficient A is independent of the velocity, the roughness (smooth to $d/h_0 = 0.07$). And the length of the bottom-protection ($L/h_0 = 5$ and 10). The shapes of the erosion/time curves are represented in figs. 10 and 11 for different velocities and for dam-heights of 0 and $0.3h_0$ respectively.

With increasing erosion, the deepest point of the scour-hole moves in a downstream direction, as well as in a direction at right angles to the latter, away from the protrusion. The latter phenomenon is clearly demonstrated in fig. 12, where the cross-sections are shown over the deepest point for different times. Although for practical cases it is of minor interest, still worth mentioning is the phenomenon that under severe scouring conditions with a low dam-height, and where the scouring depth exceeds the value h_0 , the deepest point of the scour-hole again moves closer to the bottom-protection. Simultaneously a second hole with intensive scouring action is formed at a greater distance from both bottom-protection and protrusion (see fig. 13). No conclusive explanation for this phenomenon has yet been found. It is however convenient to observe that also for this second hole the erosion/time-relation function

$$\frac{h_{\max}}{h_0} = 1 + A \log \frac{t}{t_1}$$

applies (see fig. 14), and that the horizontal distance between the time/erosion-curves for the first and for the second hole remains constant.

Further research reveals that for a depth $< 0.6h_0$ the scouring

process is better expressed as a power-function between h and t , viz.:

$$\frac{h_{max}}{h_0} = \left(\frac{t}{t_1}\right)^p$$

The value of p is again dependent on the height of the dam.

6. Estimation of the time-scale based on observed scouring actions in the prototype and reproduction in models

The acceptability of the chosen length of a bottom-protection derived from model-studies is dependent on the expected erosions in the prototype. This involves the necessity to give an estimation as to the time-scale of the erosion. Until recently one was compelled to base the closest estimation of the time-scale for vortex streets on the studies of the two-dimensional scour, supplemented by direct comparisons of the erosions caused by vortex streets, observed in model and prototype.

Needless to say, with the execution of closures every effort was made to reduce the erosive action to a minimum, in which endeavour one has very well succeeded but for a few exceptions. This implies on the other hand that very few prototype data became available which are suitable for comparison purposes.

However, an important experience was gained at the time of the Veersche Gat closure, where at the North-Beveland side of the closing gap, SW of the 'winter-gap', a considerable scour occurred under the influence of a flood-tide vortex street. This erosion also was observed in the distorted general model of the Veersche Gat (scales $n_1 = 150$ and $n_h = 50$) used preparatory to the closure.

In order to increase the insight in the problem, and also to obtain as reliable as possible an estimate of the time-scale for the erosions at both sides of the northern closing gap in the Grevelingendam, measured in a model, the development of the erosion in the Veersche Gat was again reproduced in a model, but this time in a non-distorted model to scale 1:50. These

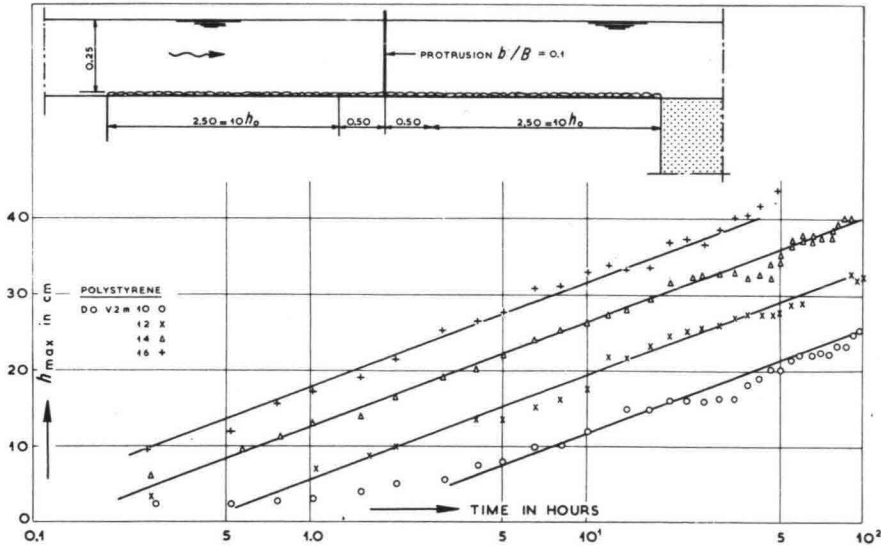


Fig. 10. Erosion/time-curves for polystyrene for different velocities; dam-height = 0.

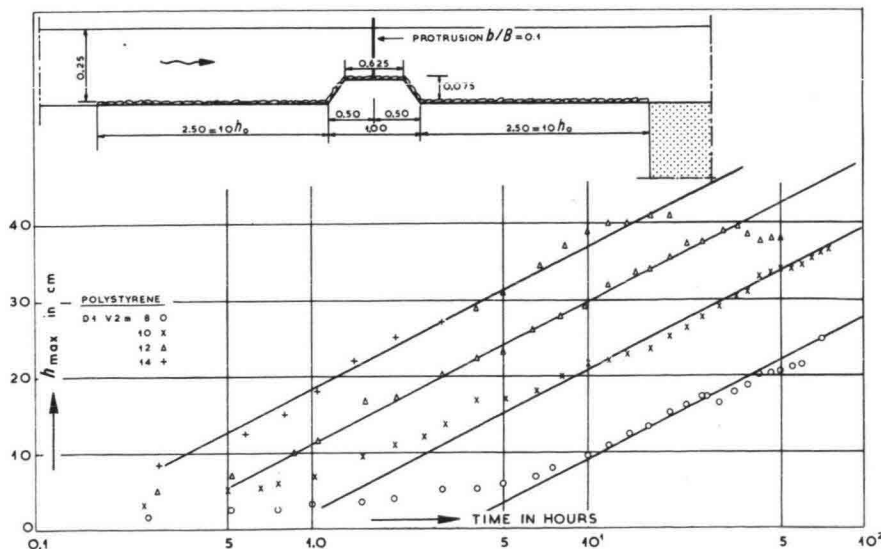


Fig. 11. Erosion/time-curves for polystyrene for different velocities; dam-height = $0.3 h_0$.

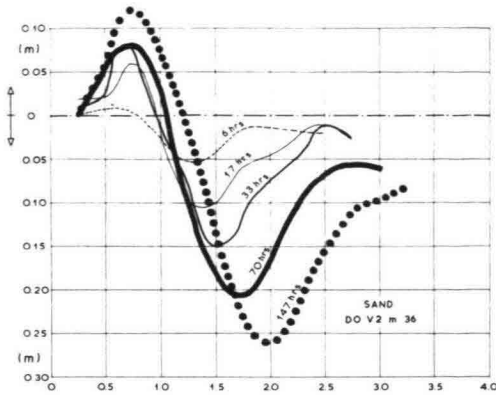


Fig. 12. Cross sections over deepest point of scour-hole for different times of flow.

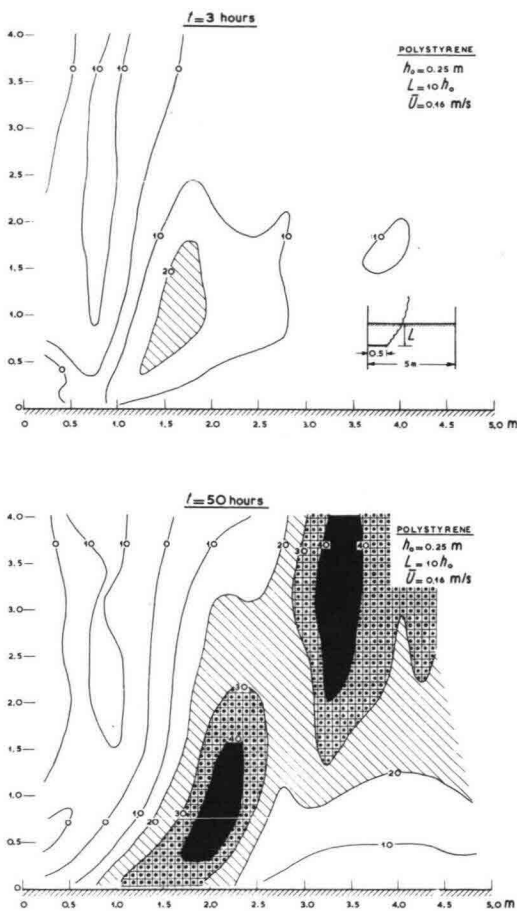


Fig. 13. Scouring effects after short and prolonged time of flow respectively.

tests were carried out with fine bakelite ($d_{50} = 600 \mu\text{m}$) as bed-material, using 5 different velocity-scales, after verification of the initial conditions in the model.

A fair agreement appeared to consist between the scour-patterns in the model and those in the prototype (see fig. 15), the only difference being that in the model the scour-hole is located somewhat more to the east than in the prototype.

As has been mentioned before, the deepest point of erosion with two-dimensional scouring action can be described as a power-function of time, viz.: $h_{\text{max}} :: t^\beta$. With geometrical

similarity of models, the value of the power δ is constant and independent on the length-scale (n_l), the velocity-scale (n_v) and the scale of the bed-material (n_Δ). Based upon this experimentally established relationship, it was possible to define a time-scale for the scour (n_t), which as a first approximation can be expressed by the equation:

$$n_t = n_l^\alpha \cdot n_v^{-\beta} \cdot n_\Delta^\gamma$$

Test results showed decreasing values of the exponents α and β with increasing turbulence intensity.

In observing the maximal erosion in the Veersche Gat as a function of time, it appears that the vortex-street hole has twice collapsed due to instability of the talus (see fig. 16). If the sections of the erosion/time-curve occurring after the collapse of the hole are reversed in time, so that the starting point coincides with the erosion-depth reached prior to the collapse, the curve attains a constant inclination (plotted double-logarithmically).

This means that also in this case the deepest point of the erosion develops as a power-function of time ($h_{\text{max}} :: t^{0.8}$). In this connection it should be added that the value of the exponent is dependent on the choice of the system of co-ordinates, or in other words from the initial conditions of the bottom-profile; translation of the system of co-ordinates changes the exponent's value.

All erosion/time-curves for the deepest point of the vortex-street hole, determined for different velocity scales, run parallel for model and prototype (plotted double-logarithmically), from which follows that the scouring action for different velocities adheres to the same relationship as the prototype. Hence, for a given velocity-scale there exists a constant time-scale.

It was also possible, in an analogous way, to develop a time-scale for the volume of the scour-hole for the various velocity-scales. These however appeared to be smaller than the corresponding time-scales for the deepest point, which meant that the scour-hole in the model was less extensively reproduced as compared to the prototype for a corresponding depth of the hole. In the distorted model of the Veersche Gat (scales 150/50), however, an opposite tendency was found as a result of the incorrect reproduction of the talus and the damping of the vortices.

Due to the fact that the tests in the erosion-models are performed under permanent flow conditions, the flood- or ebb-current periods in the prototype necessarily have to be reduced to a

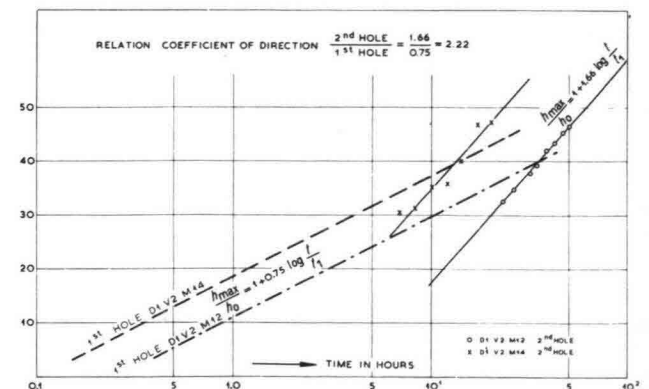


Fig. 14. Erosion/time-curves for first and second scour-hole.

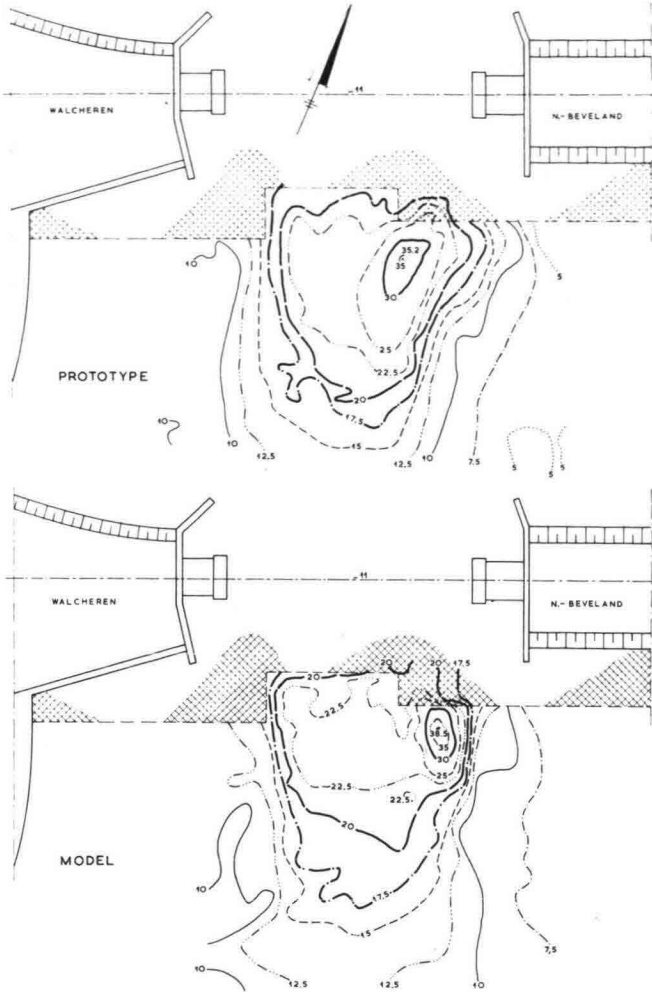


Fig. 15. Veersche Gat. Agreement between scour-patterns in prototype and model respectively.

number of flow hours (t_e) with the maximum observed velocity

$$U_{\max} \text{ in accordance with the relationship } \int \left(\frac{U}{U_{\max}} \right)^\beta dt$$

Hence, the time t_e is dependent on the shape of the velocity-curve. For the above-mentioned reduction the relationship between the time-scale and the velocity-scale must be known. The power β in the time-scale equation:

$$n_{t_e} = n_l^\alpha \cdot n_u^{-\beta} \cdot n_A^\gamma$$

could be determined in the Veersche Gat model by an analysis of the scour action caused by the vortex street after applying various velocity-scales. It appeared that the value of this power decreases with a decreasing velocity-scale. By means of these data it could be established that for the Veersche Gat the flood-flow period could be represented by a period of 1.2 hours effective flowing with the maximal flow (for the northern closing gap of the Grevelingen the ebb-flow period appeared to be 1.5 hours).

Based upon an assumption regarding the material-scale (sand in the prototype and fine bakelite in the model), derived from the two-dimensional studies, it was possible to determine the value of the power α in the time-scale equation, from the scour measured in the model and in the prototype, or in other words: the influence of the length-scale (see fig. 17). The value

of α appeared to vary between 1.7 and 2.2, dependent on the velocity-scale. The values of both α and β appeared to be dependent on the nature of the transport; i.e. decreasing with increasing turbulence-intensity.

Hence, for the determination of the time-scale in a particular case, it will be possible to find the value of β in the time-scale equation by carrying out a number of model tests with a given geometry and applying different velocity-scales.

In the past it has been assumed that, for obtaining a rough estimate of the time-scale for three-dimensional scour, it would be possible to use for the value of α in the time-scale equation the value of α corresponding to the value of β , as found in the model-studies of the Veersche Gat.

7. Recent approximation of the time-scale

In this chapter an approximation of the time-scale for scouring action by vortex streets shall be endeavoured, based upon the present knowledge obtained from the fundamental research mentioned previously. In order to define a time-scale, it is necessary that the erosion/time-curves are parallel to each other, in other words, that for a certain scouring-depth, the distance measured horizontally between two erosion/time-curves should be constant. From the fact that the erosion of the deepest point can be expressed as:

$$h_{\max}/h_0 = 1 + A \log t/t_1$$

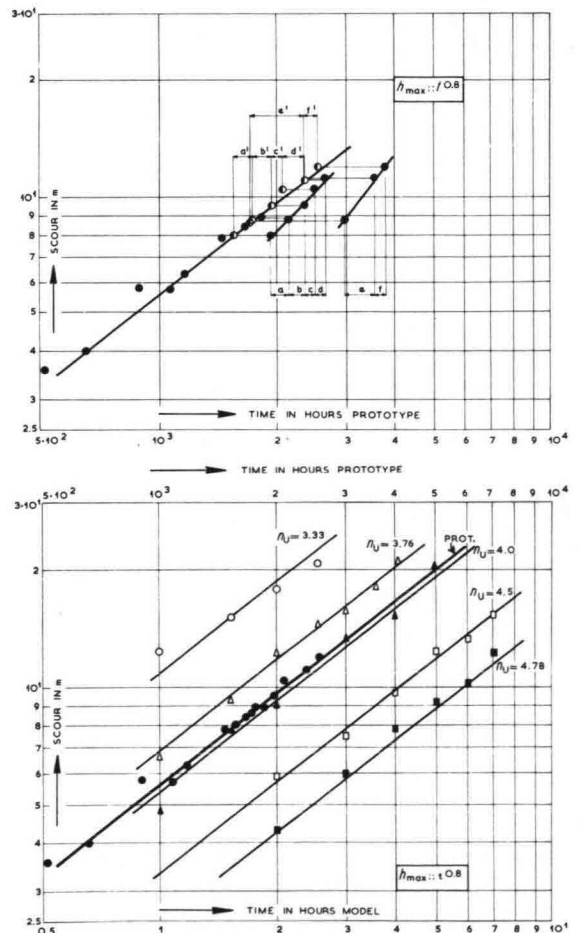


Fig. 16. Veersche Gat. Erosion/time-curves for prototype and model respectively.

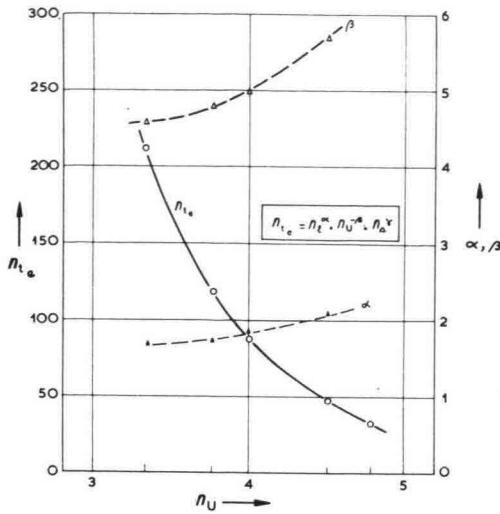


Fig. 17. Relationship of velocity-scale and time-scale, α and β respectively.

and that the coefficient A is independent on the velocity, it may be concluded that there exists a constant time-scale for different materials during the scouring-process for a given geometry (see fig. 10, 11 and 14). Characterization of model-tests with different t_1 -values offers a solution as to a time-scale.

Provided that the significant velocities used are equal to the maximum values (considered in a horizontal plane) of the equation $U_{\max} = \bar{U}(1 + 3\bar{r})$ at the end of the bottom-protection, and furthermore that for the critical velocities the same values are used as for a parallel flow, then the results of the tests can be summarized in the relationship:

$$t_1 = (U_{\max} - U_{\text{crit}})^p = c_p$$

in which the values of p and c_p are dependent on the height of the dam. However, for a given geometry and a given material p and c_p are constants.

Also, when in an analogous way as was done with the two-dimensional scour, a correction-factor α_U is introduced for deviating distribution of velocities, the following relationship is established covering all tests (see fig. 18):

$$t_1 = (\alpha_U U_{\max} - U_{\text{crit}})^4 = \text{constant.}$$

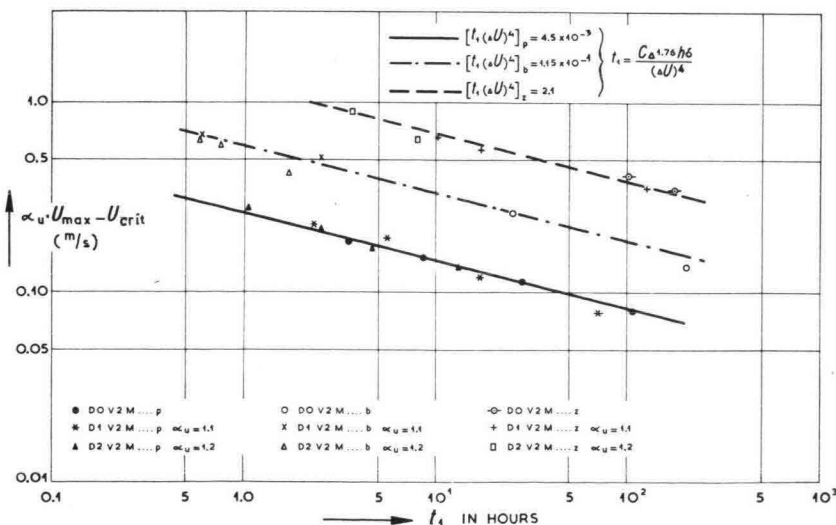


Fig. 18. Relationship between scouring-time t_1 and the value of $(\alpha_U U_{\max} - U_{\text{crit}})$.

For a length of the bottom-protection of $10 h_0$, a fair roughness ($k/h_0 = 0.02$) and a vertical protrusion, the magnitude of the correction-factor, for a dam-height $D/h_0 = 0; 0.3$ and 0.6 , will be equal to $\alpha_U = 1.0, 1.1$ and 1.2 respectively. The above-mentioned relationship applies to all of the materials used (sand, bakelite and polystyrene). The value of α_U is strongly dependent on the geometry.

The general equation for the time-scale (characterized by the time t_1) becomes then:

$$t_1 = \frac{c \Delta^\gamma h^\delta}{(\alpha_U U_{\max} - U_{\text{crit}})^4}$$

The value of γ can be determined by comparing the test-results obtained with the different materials. For the aforementioned tests, this value appeared to be approximately: $\gamma = 1.8$. The value of the power δ could be determined by means of a number of length-scale tests. This value found is $\delta = 1.8$. However the number of tests on which this value is based is still too small for using this value with full confidence. When the values of γ and δ are established, it will also be possible for any particular case to determine the value of α_U by carrying out scouring-tests with a number of different velocity-scales in a small-scale model. The time-scale will then also be fixed.

A program for future research has been drawn up to pay further attention to the influence of the length-scale and of the distortion of models.

8. Conclusions

1. Systematic three-dimensional erosion-tests in models in which different bed-materials were used have indicated a similarity in scour-development both for different materials as well as for different velocity-scales. Consequently it is possible to define a time-scale which remains constant during the scouring-process.
2. It will be possible for any particular case, to determine the value for the time-scale of three-dimensional scour, provided that the value of α_U has been determined by means of a model-study.

INTERNATIONAL ASSOCIATION FOR HYDRAULIC RESEARCH

THREE- DIMENSIONAL LOCAL SCOUR IN
NON-COHESIVE SEDIMENTS. (SUBJECT B. a.)

by

T. VAN DER MEULEN

Head Closure Works Branch, Delft Hydraulics Laboratory, Delft, the Netherlands.

and

J. J. VINJÉ

Head Laboratory De Voorst, Delft Hydraulics Laboratory, Delft, the Netherlands.

Summary

The results are described of systematic research for three-dimensional local scour in loose sediments. Relationships were determined between time-scale and scales for velocity, length and material density. As for two-dimensional flow the shape and the extent of the scour-hole due to vortices are in a high degree time dependent; originally the development as a function of time is very fast, but in a later phase the progress is slower until eventually an equilibrium situation is reached. In many practical cases the equilibrium will not be attained.

Geometry, dam-height, length and roughness of bottom protection, flow velocity and density of sediments were varied.

A relationship for the time-scale was derived, somewhat similar to that for two-dimensional scour.

For practical cases the scour has to be determined for a number of longitudinal sections which have each a different time-scale. Restrictions of the results like permanent flow and neglect of upstream material supply can be tackled with additional computation methods.

Résumé

Les résultats sont décrits d'une recherche systématique pour des érosions locales trois-dimensionnelles à fond mobile. Des relations ont été dérivées entre l'échelle de temps et les échelles pour la vitesse, la longueur et la densité du matériau.

Comme pour les écoulements bi-dimensionnels la configuration et l'étendue de l'affouillement causées par des chapelets de tourbillons sont grandement dépendant du temps; dans l'origine le développement comme fonction du temps est très vite, mais dans une phase plus tard le progrès est plus lentement jusqu'une situation d'équilibre est atteinte finalement. Pour beaucoup de cas pratiques l'équilibre ne sera pas atteint.

La géométrie, la hauteur de la digue, la longueur et la rugosité de la protection du fond, la vitesse du courant et la densité des sédiments ont été variés.

Une équation pour l'échelle du temps a été dérivée, quelque peu identique à laquelle pour des érosions bi-dimensionnelles.

Pour des cas pratiques l'affouillement sera déterminé pour un nombre des profils longitudinaux, qui possèdent une échelle de temps différente.

C'est possible de résoudre les limitations des résultats, comme l'écoulement permanent et la négligence de l'influence du transport en amont de l'obstacle par des méthodes de calcul supplémentaires.

1 Introduction

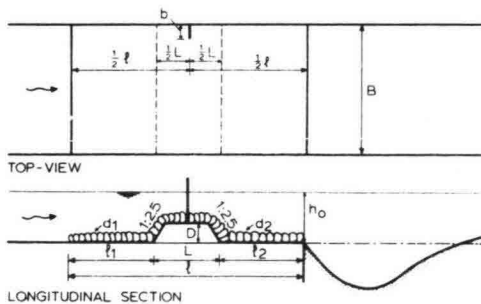
With the aid of systematic research on two-dimensional local scour in loose sediments relationships have been derived between time scale and scales for velocity, length and material density. [1].

In many practical cases, however, the local scour will be determined by three-dimensional effects - e.g. vortices during closing operations of estuaries. [2]. In order to determine the above mentioned relationships also for three-dimensional local scour the research programme, carried out at the Delft Hydraulics Laboratory and commissioned by the Netherlands Department of Public Works, was continued. Physical scale models were used as local scour in estuaries due to constructions of dams etc. can not yet be approached by means of computing techniques. Dependent on the shape and the extent of the scour-hole and the soil mechanical properties, the stability of structures can be endangered. Originally the development of scour as a function of time is very fast, but later on an equilibrium situation will be reached. During closing operations of a dam in an estuary which require a limited time the equilibrium will not be attained and then it is strictly necessary to know the development of the local scour as a function of time.

2 Programme of three dimensional scouring tests

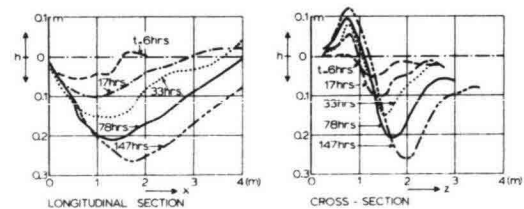
The tests have been carried out in flumes with different geometrics (10 m, 5 m and 2,5 m wide) and many variations of dam-height, length of bottom protection, roughness of bottom protection, flow velocity, sand: 0.24 till 0.64 m/s; bakelite 0.11 till 0.40 m/s; polystyrene 0.09 till 0.20 m/s, material diameters and density of sediments (2,650, 1,350 and 1,050 kg/m³). A comprehensive summary of the most important tests is given in figure 1 and the table below.

b/B	D/h ₀	d/h ₀	l/h ₀	L/h ₀	B (m)	h ₀ (m)	material density		
							2.650	1.350	1.050 kg/m ³
0.1	0	0.02	24	-	10	0.50	x		
0.1	0	0.02	24	-	5	0.25	x	x	x
0.1	0	0.02	24	-	2.5	0.125	x	x	x
0.1	0.3	0.02	24	4	10	0.50	x		
0.1	0.3	0.02	24	4	5	0.25	x	x	x
0.1	0.3	0.02	24	4	2.5	0.125	x	x	x
0.1	0.6	0.02	24	4	10	0.50	x		
0.1	0.6	0.02	24	4	5	0.25	x	x	x
0.1	0.6	0.02	24	4	2.5	0.125	x	x	x



1 Summary of situations

Sommaire de recherches



2 Sections through deepest point of scour-hole after different times

Profils a travers par la pointe la plus profonde après des temps différents

- [1] Breusers, H. N. C. Two dimensional local scour in loose sediments, Symposium Closure of estuarine channels in tidal regions, De Ingenieur 1968, no. 44, Delft Hydraulics Laboratory Publication no. 64
- [2] Vinjé, J. J. Local scour caused by vortex streets, Symposium Closure of estuarine channels in tidal regions, De Ingenieur 1968, no. 47, Delft Hydraulics Laboratory, Publication no. 64

3 Relationship between maximum scouring depth and time

The scour-hole caused by vortices is the most significant factor for three-dimensional scour. In figure 2 the development of the scour-hole due to vortices is given as a function of time by presenting the cross-sections and longitudinal sections at different time-steps of the process for a specific situation.

The deepest point of the hole moves both in longitudinal direction and laterally. As for two-dimensional scour the increase in scouring depth decreases with time.

The results of two-dimensional scour for the relationship between maximum scouring depth and time could be summarized in:

$$h_{\max}/h_o = (t/t_1)^p \quad (1)$$

in which: h_{\max} = maximum scouring depth

h_o = original waterdepth

t_1 = time at the moment $h_{\max} = h_o$

For two dimensional flow the factor p proved to be 0.38, but for three-dimensional flow this factor is dependent on the geometry. This means that p has to be derived from scouring tests. In general for three-dimensional scour the results can be written as:

$$h_{\max}/h_o = f(t/t_1), \quad (2)$$

in which the function for each geometry has to be determined experimentally.

In figure 3 the results of all tests have been summarized for one geometry ($D/h_o = 0.3$).

The scatter in the results is generally within reasonable limits so that the function f in (2) can be considered consistent for one geometry. For values of $h_{\max} > h_o$ the conformity decreases for different conditions.

In order to verify whether no scale effects or effects due to material have been blurred the results have also been specified according to used bottom materials only and to length scale (see figure 3). The conclusion is that no scale effects occur.

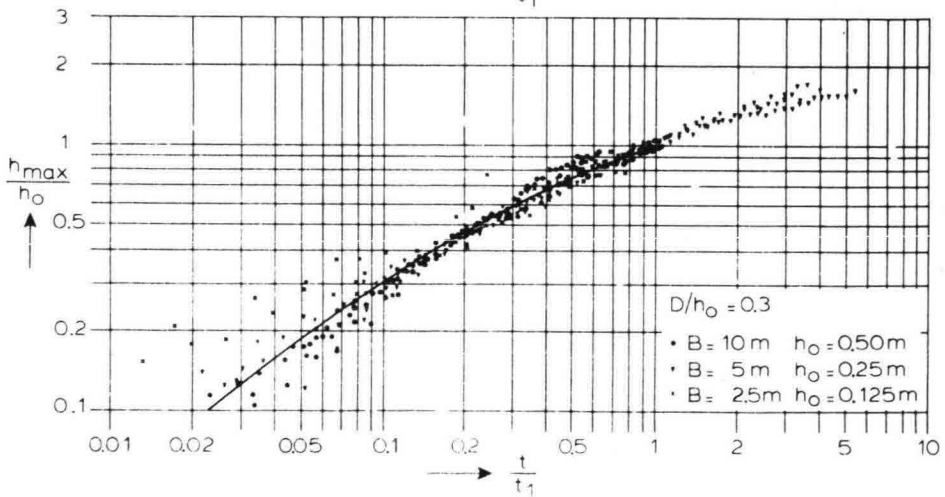
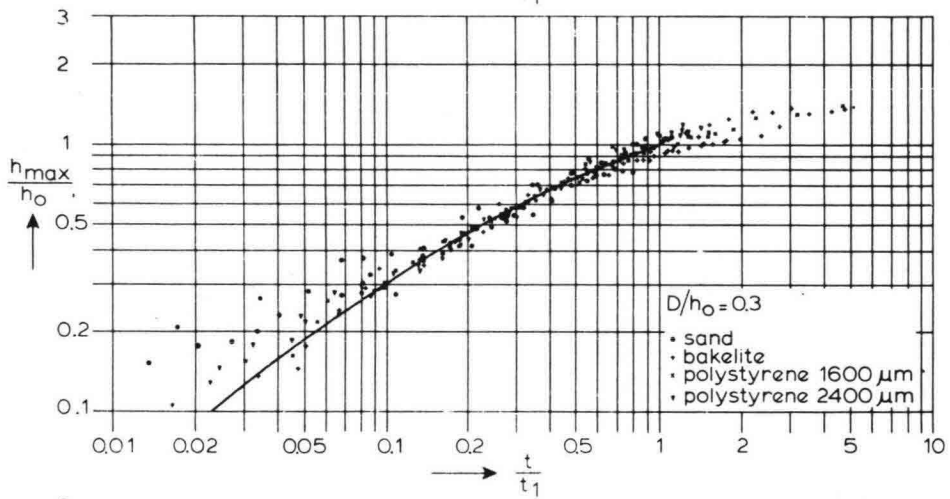
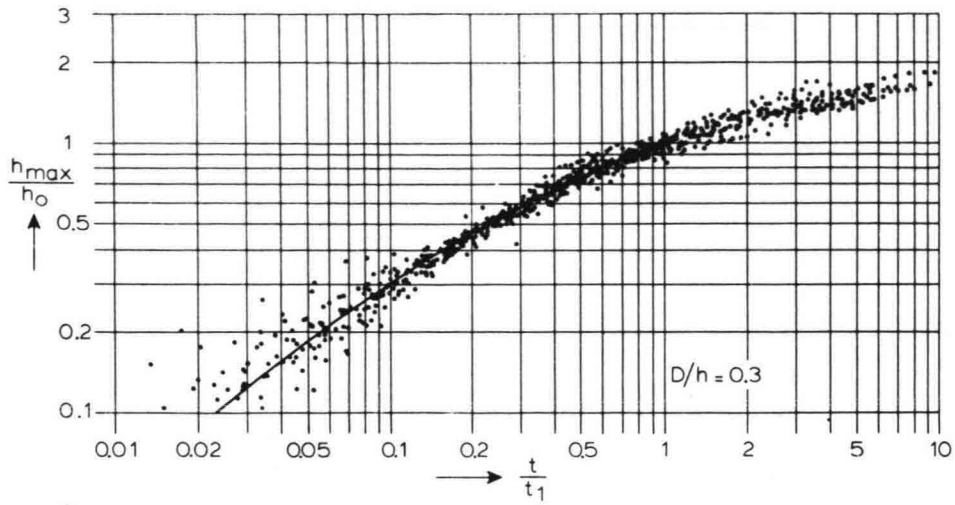
4 Influence of magnitude of the velocities, density of sediments, water depth and geometry on the scouring time

The dependence of the characteristic scouring time t_1 on the conditions of flow etc. or in other words the relationship between time scale on the one side and the velocity scale, material scale, length scale and geometric situation on the other side have been further investigated. It could be finally concluded that the influence of the various factors on the rate of the scouring process can be described with the same general relationship both for two- and three-dimensional local scour.

For two-dimensional scour the relationship is:

$$t_1 = 250 \Delta^{1.7} h_o^2 (\alpha \bar{u} - u_{cr})^{-4.3} \quad (3)$$

The influence of the waterdepth appears in the quantity h_o ; the influence of the velocity is represented in the factor $\alpha \bar{u} - u_{cr}$ and the influence of the material is expressed both in $(\alpha \bar{u} - u_{cr})$ and the quantity $\Delta = \rho_s - \rho$, in which ρ_s = density of material and ρ = density of water. In the quantity $\alpha \bar{u} - u_{cr}$ moreover the influence of the geometry has been taken into account in the coefficient α .



3 Time-scour relationships
 Relations entre temps et affouillement

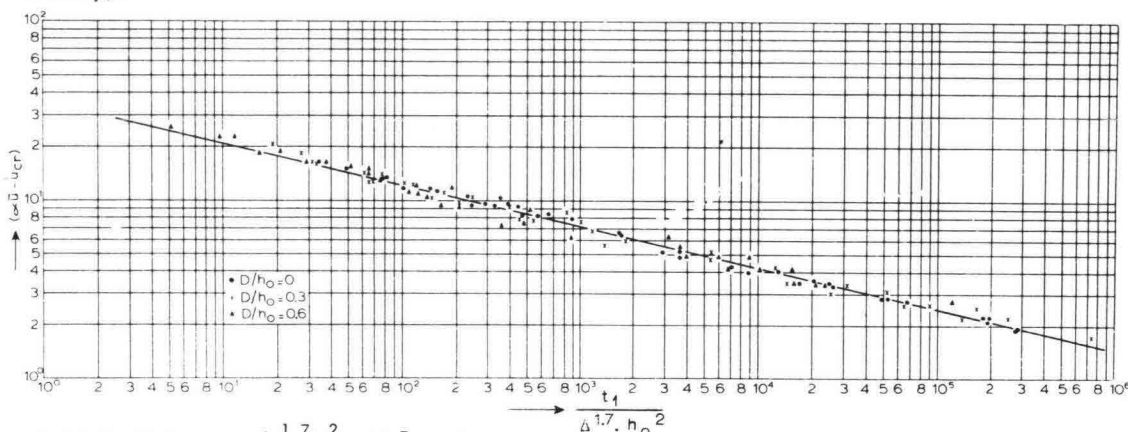
Equation (3) can be converted in a dimensionless form:

$$n_t = n \Delta^{1.7} n_h^2 n (\alpha \bar{u} - u_{cr})^{-4.3} \quad (4)$$

For each test the value of α in (3) was determined. In this factor α as well the component for turbulence-intensity (α_t), the component for vertical velocity distribution (α_v) and the component for horizontal velocity distribution are involved.

There is a significant difference in α values for various geometries. For $D/h_o = 0$ α is about 3.0; for $D/h_o = 0.3$ α varies from 4.0 till 4.7 and for $D/h_o = 0.6$ α varies from 6.5 till 8.2. The scatter in the results is greater than for two-dimensional scour. This is conceivable due to the complicated situation for three-dimensional scour for which the chance of measuring inaccuracies and the effect of casual disturbances is greater than for two-dimensional scour.

The results of the three-dimensional tests satisfy equation (4). In figure 4 the results are summarized. Plotted are the values of $\alpha \bar{u} - u_{cr}$ and $t_1/\Delta^{1.7} h_o^2$. In this figure for each geometry a constant value of α has been assumed (the average of the computed values for each geometry).



4 Relationship between $t_1/\Delta^{1.7} h_o^2$ and $(\alpha \bar{u} - u_{cr})$

Rélation entre $t_1/\Delta^{1.7} h_o^2$ et $(\alpha \bar{u} - u_{cr})$

5 Development of scour and shape of scour-hole at different locations in the cross-section

For scouring tests the length scale and the depth scale have to be the same. Moreover the chosen bottom material will be the same for the whole model.

From the relationship $n_t = n \Delta^{1.7} n_h^2 n (\alpha \bar{u} - u_{cr})^{-4.3}$, it follows that the time scale (n_t) is proportional to $n (\alpha \bar{u} - u_{cr})^{-4.3}$.

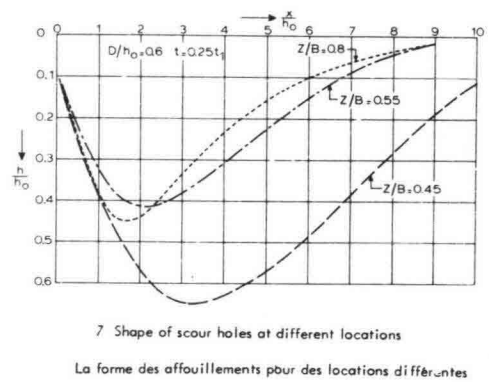
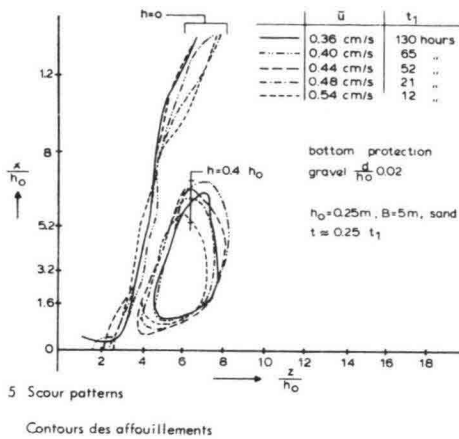
The scale factor $n (\alpha \bar{u} - u_{cr})$ has a value which is independent on the location if $\alpha \bar{u}$ and u_{cr} are constant values in the entire cross-section both in model and prototype ($\alpha \bar{u}/u_{cr} = \text{constant}$; two-dimensional scour)

For three-dimensional scour the factor $\alpha \bar{u}/u_{cr}$ will be practically never constant as u_{cr} is determined by the bottom material and the waterdepth and possible variations of u_{cr} do not show variations of $\alpha \bar{u}$.

For the test series with constant water depth u_{cr} does not vary in the cross-section and the scale factor $n (\alpha \bar{u} - u_{cr})$ is independent on the location if $n_{\bar{u}} = n_{u_{cr}}$. Mostly the value of $n_{\bar{u}}$ is small so that - in order to satisfy the just mentioned condition - the value of $n_{\bar{u}}$ and $n_{u_{cr}}$ will also be small which means large scour models.

In the test series in which the velocity was varied the condition $n_{\bar{u}} = n_{u_{cr}}$ was not satisfied, which means that the time scale is not constant in the cross-section. It is then questionable whether the basic condition is met viz. conformity of the scour-hole in model and prototype at corresponding times during the scour process. To verify this the scour patterns were compared for tests with various velocities, bottom materials and length scales.

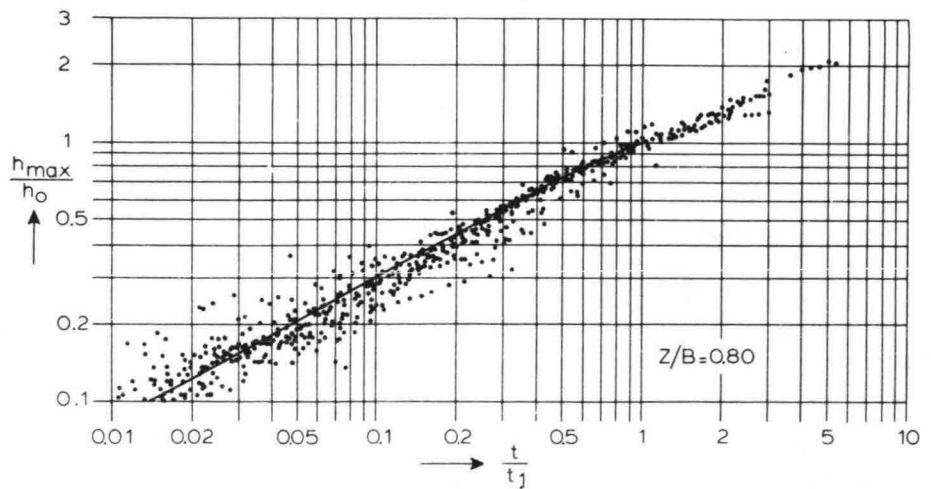
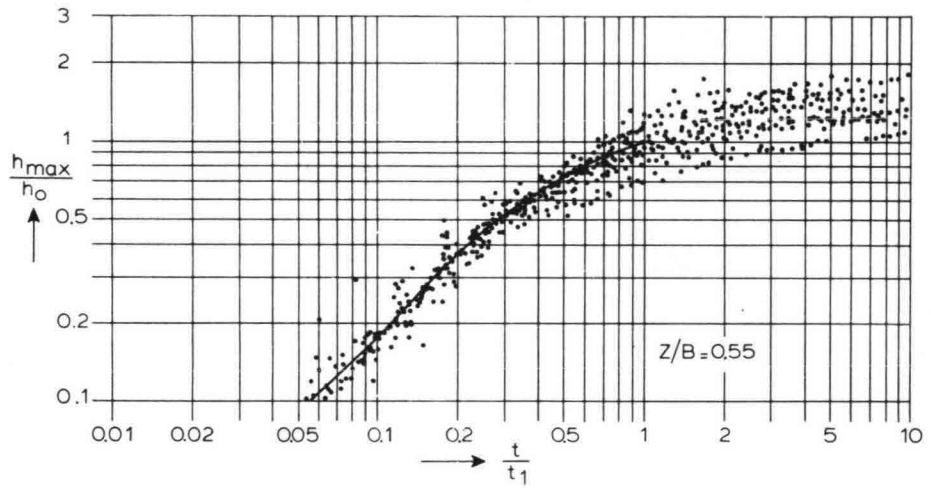
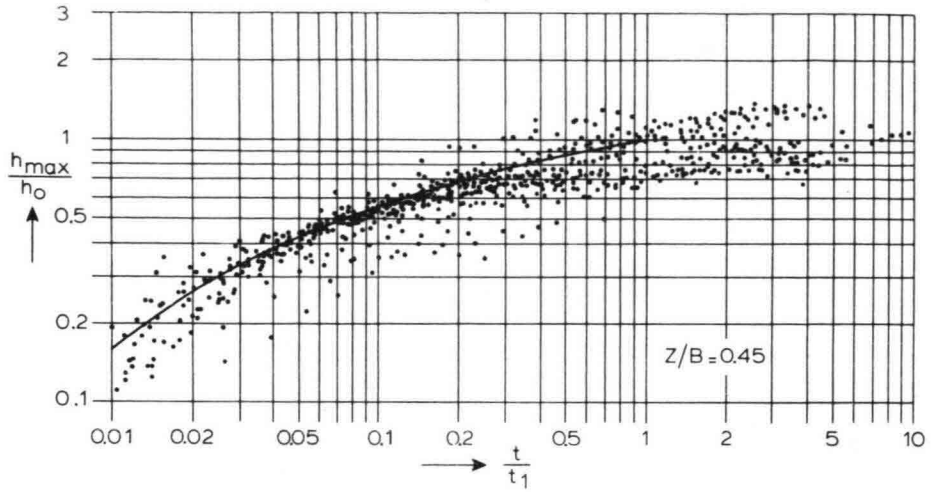
An example of the results of tests with various velocities is given in figure 5. In general it could be concluded that the differences are small and show no systematic coherence with the variables, so there are no considerable scale effects for the tested scale variations. Due to the fact that the time scale is not constant the determination of the time scale can not be made for one single point in the cross-section (in order to translate the scour pattern from the model into the prototype). It is, therefore, necessary to determine the development of scour in many longitudinal sections separately. In figure 6 the relationship is given between h_{\max}/h_0 and t/t_1 for D/h_0 in three longitudinal sections. In these figures variations in velocity, length scale and bottom material have been used. For different longitudinal sections $h_{\max}/h_0 = f(t/t_1)$, in which the function is different for each longitudinal section. For a three-dimensional case the geometric situation is not only determined by the qualities of sill and bottom protection, but also by the distance till the banks, so by the location in the cross-section. In figure 7 some longitudinal sections of the scour-hole are given for $D/h_0 = 0.6$.



6 Influence of unsteady flow

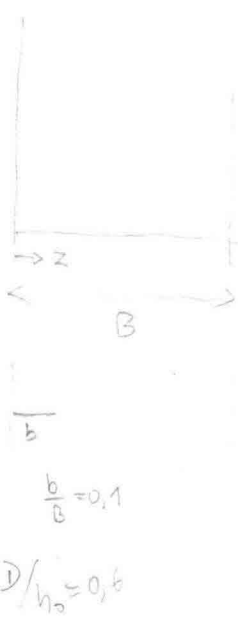
The tests which have been described were carried out with steady flow. In practice - e.g. closing of an estuary with tides - the scour pattern is caused by unsteady flow. The relationships which are valid for steady flow can not simply be used in practice because a number of significant factors are now a function of time, such as the mean velocity \bar{u} and the water depth h_0 . Mostly the variation of u_{cr} as a function of time can be neglected. The variation of α and of the function connected with the varying geometry due to variation of water depth are small and can be left out of consideration. The equations (3) and (4) can be adapted to equations for unsteady flow, taking into account that \bar{u} and h_0 are time-dependent and assuming that the unsteady flow can be considered as a succession of an infinite number of short lasting steady situations. If the unsteady flow is cyclic (tidal movement) with cycle duration T , then the value for the erosion time t_1 becomes:

$$t_1 (\text{tide}) = \frac{250 \Delta^{1.7} h_0^2 (0)}{\frac{1}{T} \int_0^T \frac{\{\alpha \bar{u}(t) - u_{cr}\}}{h_0(t)} dt} 4.3 \quad (5)$$



6 Scour as function of time for three different locations in cross-section

Affouillement comme fonction du temps pour trois locations différentes dans le profil en travers



and further:

$$\frac{h_{\max}(t)}{h_o(o)} = f \left\{ \frac{t}{t_1(\text{tide})} \right\} \quad (6)$$

7 Influence of neglection of upstream material supply

The tests have been carried out in such a way that transport of bottom material could only take place downstream of the bottom protection. Especially for fine sediments in nature there will be a certain amount of material in suspension. In this case a part of the transport capacity of the current is already occupied, so that for discharge of material thrown up from the scour-hole not the full transport capacity will be available. This means that less material will be taken away from the scour-hole and the scour-holes will be smaller than in the model tests where no upstream material supply was present. This involves a reduction of the results of the model tests, by means of computations of the capacity of the scour-hole. The contents of the scour-hole per m. width can be approached by

$$I_t = b h_{\max}^2(t) \quad (7)$$

in which b = shape factor.

I_t = quantity of material discharged from the scour-hole during time t from the beginning of erosion, if no upstream material transport is present.

If the upstream material supply is T^1 per m width, the quantity of material which has been discharged from the scour-hole will be:

$$I_{t \text{ reduced}} = I_t - T^1 t \quad (8)$$

The reduced scouring depth follows then from:

$$h_{\max}(t)_{\text{reduced}} = \sqrt{\frac{I_t - T^1 t}{b}} \quad (9)$$

For the application of this method of reduction it will be necessary to determine the magnitude of T^1 for various longitudinal sections. Measurements in prototype are for this method indispensable.

Moreover it has to be established whether all upstream material supply will be effective for reduction of the dimensions of the scour hole.

The required insight can also be obtained with the aid of a small scale model. In prototype there will hardly be any erosion after the bottom protections - the first step during closing of estuaries - have been put in place. In the model without upstream material supply there will, however, be some erosion.

In order to obtain the results in nature ($h_{\max} = o$) it can then be determined which value of

T^1 has to be used for reduction of the model results.

8 Conclusions

- There is a similarity in scour development for three dimensional local scour both for different material as for different velocity scales. This involves that it is possible to define a time scale which remains constant during the scouring process.
The time scale for three dimensional scour is given by:

$$n_t = n \Delta^{1.7} n_h^2 (\alpha \bar{u} - u_{cr})^{-4.3}$$

- It is possible to take into account factors like unsteady flow and upstream material supply by means of computations.

